



HAL
open science

Ordonnancement opportuniste dans les réseaux mobiles de nouvelle génération

Kinda Khawam

► **To cite this version:**

Kinda Khawam. Ordonnancement opportuniste dans les réseaux mobiles de nouvelle génération. domain_other. Télécom ParisTech, 2006. English. NNT: . pastel-00002059

HAL Id: pastel-00002059

<https://pastel.hal.science/pastel-00002059>

Submitted on 17 Jan 2007

HAL is a multi-disciplinary open access archive for the deposit and dissemination of scientific research documents, whether they are published or not. The documents may come from teaching and research institutions in France or abroad, or from public or private research centers.

L'archive ouverte pluridisciplinaire **HAL**, est destinée au dépôt et à la diffusion de documents scientifiques de niveau recherche, publiés ou non, émanant des établissements d'enseignement et de recherche français ou étrangers, des laboratoires publics ou privés.

THÈSE

Présentée à

**l'ÉCOLE NATIONALE SUPÉRIEURE DES TELECOMMUNICATIONS
DE PARIS**

pour obtenir le grade de

DOCTEUR de l'ENST Paris

Mention "**Informatique**"

par

Kinda KHAWAM

ORDONNANCEMENT OPPORTUNISTE DANS LES RESEAUX MOBILES DE NOUVELLE GENERATION

Soutenue le 14 Novembre 2006 devant la Commission d'Examen :

Directeur de Thèse:

Daniel Kofman, Professeur,

GET/ENST Télécom Paris.

Rapporteurs:

Eitan Altman, Directeur de Recherche,

Annie Gravey, Directeur d'études,

SOPHIA ANTIPOLIS/INRIA.

GET/ENST Bretagne.

Examineurs:

Sarah Oueslati, Chercheur,

Cathernie Rosenberg, Professeur, Directeur de Recherche,

France Télécom R&D,
Issy-les-Moulineaux.

Université de Waterloo/Canada.

Invité:

Jean-Marc Kelif, Ingénieur de recherche,

France Télécom R&D,
Issy-les-Moulineaux.

Aux enfants de Cana.

A Khaled.

Le Royaume des cieux est comparable à un trésor caché dans un champ; l'homme qui l'a découvert le cache de nouveau. Dans sa joie, il va vendre tout ce qu'il possède, et il achète ce champ.

Matthieu 13,44-46.

Remerciements

Je commence par le commencement. Je remercie mon Seigneur et mon Dieu Jésus Christ pour l'enfant qu'il a su garder en moi. Grâce à Lui, je n'ai jamais remplacé le rêve par l'ambition, la révolte par la susceptibilité et les jardins secrets par la pression sociale. Je remercie ma famille que j'aime infiniment: mon père pour l'être exceptionnel qu'il est et ma mère, la dame de mon coeur. Je remercie mon frère Georges, la prune de mes yeux, pour l'amour que j'ai pour lui, pour l'éclat de ses rires qui n'ont de cesse de réchauffer mon coeur. Je remercie ma petite soeur Hala qui n'a pas lâché ma main pendant ces trois années de thèse. Je remercie mon chéri Khaled pour tous les jours, pendant ces trois ans, où il était mal car j'étais mal. Je sais que j'ai obtenu cette thèse grâce à lui, grâce à son support sans relâche pour moi. Lui dire que je l'aime, que c'est lui qui vivifie le rêve et fait perdurer le jour, c'est peu lui dire.. Je veux remercier mes amis, mes perles rares, Marc et Michel. Je sais que tout homme passe sa vie durant à chercher ne serait-ce qu'un ami comme l'un d'eux et est si rarement comblé. Moi qui ai à mes côtés non pas un mais deux amis uniques, je suis confondue par la générosité de la vie. Je veux remercier mes compagnons de cellule et amis Samer, Artur, Maryna, Mohammad et Sassan, qui ont adouci ce séjour. Je pense en particulier à Sassan qui a rendu ces longues heures passées au bureau presque agréables, à Artur qui est venu maintes fois à mon secours pour régler mes problèmes informatiques et à Samer qui m'a énormément soutenu.

Je remercie mon directeur de thèse Daniel Kofman auprès de qui j'ai beaucoup appris pendant ces trois ans. Je remercie profondément le chef de département Infres, Michel Riguidel, pour l'accueil agréable qu'il m'a assuré dans son laboratoire. Je remercie chaleureusement Eitan Altman et Annie Gravey d'avoir accepté de rapporter ma thèse et j'exprime ma profonde gratitude envers les membres du jury Catherine Rosenberg et Sara Oueslati, ainsi qu'envers mon invité Jean-Marc Kelif. Je tiens à remercier en particulier Eitan Altman; ce fut un honneur et un grand plaisir pour moi d'avoir fait sa connaissance et travaillé avec lui, non seulement sur le plan scientifique puisqu'il est un chercheur de grande renommée mais surtout sur le plan humain. Je tiens à remercier du fond du coeur un autre grand homme, Samir Tohmé, pour l'incroyable soutien qu'il m'a fourni. Je veux remercier également les deux gentlemen, Jean-Claude Belfiore et Joseph Boutros, pour le temps qu'ils

m'ont accordé. Je remercie finalement toute personne que j'ai croisée pendant cette thèse et qui par sa douceur et sa grandeur d'âme m'a marquée, je pense en particulier à Myriam, Sophie, Claude, Quynh et Gwendal.

Résumé

Introduction

L'Internet a connu un essor remarquable ces dernières années. Cet essor n'a pas été restreint aux réseaux fixes mais a gagné récemment les réseaux mobiles. Les réseaux sans fil, initialement conçus pour véhiculer exclusivement des services voix, s'adaptent progressivement à ces changements pour transporter des services data. Avec un besoin grandissant pour accéder à ces nouveaux services, proposer des méthodes performantes pour gérer la ressource radio et fournir des garanties de performance aux services data mobiles est désormais d'une importance capitale. Dans le domaine des réseaux fixes, augmenter la capacité revient à rajouter câbles et fibres optiques. Les communications mobiles, elles, sont contraintes de se partager une ressource naturelle restreinte, fluctuante à cause des évanouissements du canal radio et entachée d'erreurs. Des efforts significatifs ont été déployés pour augmenter l'efficacité du spectre mobile faisant ainsi face aux caractéristiques uniques du canal mobile et à une demande croissante pour un accès haut débit à l'Internet mobile.

Elaborer des mécanismes efficaces de gestion d'une ressource radio rare et variable est loin d'être évident. Cependant, plusieurs méthodes ont été proposées dans la littérature et ont fait preuve dans la pratique de leur efficacité, à savoir, les politiques d'ordonnancement, le contrôle d'admission, la gestion d'interférence, la détection Multi-Utilisateurs [Ver98], l'utilisation d'antennes dites intelligentes ([LP99, BH00, Fos96]), le codage du canal (le Turbo code [BGT93]), le contrôle de puissance [Yat95], les algorithmes d'adaptation [NBK00] etc. Notre travail s'est concentré sur les politiques d'ordonnancement dites opportunistes mais a aussi abordé d'autres techniques telles que le contrôle d'admission et la gestion de l'interférence. Les ordonnanceurs opportunistes donnent une sorte de priorité aux utilisateurs expérimentant un état de canal relativement favorable dans le but d'optimiser l'allocation des ressources.

L'ordonnancement dans les réseaux mobiles est d'autant plus efficace que si les décisions d'allocation des ressources sont faites en fonction de l'état du canal des mobiles actifs. En effet, servir un mobile qui souffre momentanément d'un très mauvais canal revient à gaspiller des ressources radio trop précieuses. Une stratégie opportuniste simple et directe

visant à profiter de la connaissance de l'état du canal est de toujours servir l'utilisateur qui jouit du meilleur canal. Cette approche adoptée par l'algorithme MaxRate [Hol01] est optimale du point de vue système puisqu'elle maximise la capacité totale de la cellule. Cependant quoique efficace, une telle approche est loin d'être équitable puisqu'elle prive de ressources les mobiles qui endurent constamment de mauvaises conditions de canal. Ainsi, il existe toujours, dans la conception d'une politique d'ordonnancement opportuniste pour les réseaux mobiles, un compromis entre efficacité et équité. Il en résulte un réel besoin d'ordonnanceurs opportunistes qui servent les mobiles de sorte à être efficace en termes de performance globale du système et de satisfaction individuelle de chaque mobile. Ces politiques doivent s'adapter aux variations du canal tout en allouant aux mobiles des ressources satisfaisant une définition d'équité parmi une panoplie de critères existants: l'équité GPS (General Processor Sharing), l'équité proportionnelle (Proportional Fairness) [Kel97] et l'équité Max-Min. Nous avons exploré dans le cadre de cette thèse les deux grandes branches de l'ordonnancement sensible à l'état du canal: l'ordonnancement équitable qui approxime la politique du GPS au niveau paquet dans les réseaux mobiles (Wireless Packet Fair Queueing) et l'ordonnancement opportuniste, en particulier celui qui satisfait l'équité proportionnelle (Proportional Fair Scheduling).

Wireless Packet Fair Queueing

Dans le domaine des réseaux fixes, les garanties de performance sont octroyées aux services data par le biais de réservation de ressources et d'ordonnancement de paquets fournissant une allocation équitable des ressources du système. La politique GPS [PG93] est un ordonnancement idéal non implémentable où les flux sont vus comme des fluides. L'objet de ce modèle est de garantir une bande passante minimum à chaque flux. Pour ce faire, les flux sont servis en parallèle avec une portion du débit total proportionnelle à des poids prédéfinis. Plusieurs algorithmes ont été proposés pour simuler le modèle GPS, dont les plus connus sont l'algorithme WFQ (Weighted Fair Queueing) [DKS89], l'algorithme SQFQ (Self-Clocked Fair Queueing) [Gol94], et l'algorithme STFQ (Start-Time Fair Queueing) [GVC97].

Malheureusement, ces algorithmes-là ne peuvent pas être directement appliqués aux réseaux mobiles à cause des caractéristiques uniques du canal radio. En effet, la communication entre le serveur et les utilisateurs sans fil peut-être interrompue de façon asynchrone à cause d'une brusque rafale de paquets erronés. Ainsi, de telles rafales d'erreurs, principalement liées à la position du mobile dans la cellule, rendent certains mobiles inopinément inaccessibles alors que d'autres continuent à percevoir un bon canal et par suite, communiquent normalement avec le serveur. Les algorithmes qui émulent la politique GPS pour les réseaux fixes ne sont pas conçus pour prendre en compte des communications discontinues et par suite fonctionnent mal dans les réseaux sans fil. Cependant, des versions

modifiées de ces algorithmes ont été proposées et ont prouvé leur efficacité. Ces dernières, tout en couplant l'utilisation de l'information relative à l'état du canal et un mécanisme de compensation, réussissent à approximer la politique GPS en présence d'un canal variable. Ces solutions émulent l'ordonnancement équitable (Fair Queueing) quand le canal de tous les utilisateurs n'est pas entaché d'erreurs. Toutefois, quand un mobile donné ne peut pas transmettre, sa part est redistribuée aux mobiles pouvant le faire. Ils reçoivent ainsi un excès de service qu'ils devront restituer au mobile en question dès qu'il percevra un bon canal. De ce fait, même si une parfaite garantie d'équité à court terme ne peut-être obtenue, une garantie d'équité à long terme est tout à fait possible. Néanmoins, ces algorithmes utilisent un modèle de canal binaire simpliste: un mobile est soit capable d'émettre et de transmettre soit incapable de le faire. Ce modèle restrictif empêche ces algorithmes d'utiliser au mieux les ressources disponibles. Pour cette raison, on a jugé nécessaire de proposer un algorithme émulant la politique GPS tout en utilisant un modèle de canal à débits multiples. En particulier, nous avons proposé une version **opportuniste** de l'illustre algorithme WFQ qui réalise des débits nettement plus élevés que la version originale se basant sur un modèle de canal binaire.

Proportional Fair Scheduling

Les algorithmes d'ordonnancement opportunistes proposés dans la littérature adoptent un modèle de canal à débits multiples correspondant à l'état réel du canal variant aléatoirement et de manière asynchrone. De plus, ces algorithmes vérifient différents critères d'équité. Nous nous focalisons sur un ordonnanceur opportuniste largement déployé dans les réseaux mobiles de nouvelle génération et qui vérifie l'équité proportionnelle: l'algorithme Proportional Fair (PF). L'algorithme PF est la méthode phare adoptée par les nouvelles technologies comme HDR (High Data Rate) [BBG⁺00] et son équivalent dans 3GPP HSDPA (High Speed Data Packet Access) [LGNJ01] et qui permet, entre autres mécanismes, d'offrir désormais de très hauts débits aux usagers (HDR offre 2.4 Mbit/s pour une bande de 1.2 MHz, alors que HSDPA offre un débit maximal de 10 Mbit/s pour une bande de 5 MHz). Dans ces systèmes, l'architecture se base sur un accès TDMA sur la voie descendante. Cette dernière est partagée en slots de temps très courts (1.67 ms pour HDR et 0.67 ms pour HSDPA) et durant chaque slot, la station de base sert un groupe donné de mobiles. La station de base compte sur une sorte de feedback de la part des mobiles pour obtenir des estimations du débit que peut supporter chaque mobile. La station de base connaît ainsi, à chaque slot de temps, l'état de canal de chaque mobile et utilise cette information pour sélectionner les utilisateurs dont le service permettra d'atteindre les objectifs du système en terme de performance. En pratique, la station de base émet à puissance maximale vers **un seul** utilisateur à chaque slot de temps dans le but d'annihiler les interférences intracellulaire.

La politique opportuniste Proportional Fair est souvent préconisée du fait que, sous certaines hypothèses, elle induit un bon compromis entre équité et efficacité. Quand ces hypothèses sont vérifiées, tous les mobiles ont la même probabilité d'accéder au canal et bénéficient de la même puissance indépendamment de leur distance à la station de base. Le système est donc du type **Processor Sharing** (PS). Cela présente deux intérêts, d'une part, le mécanisme assure une équité dans la distribution des slots et, d'autre part, les performances du système sont insensibles aux caractéristiques de la distribution de la taille des flux, ce qui facilite significativement le dimensionnement.

Ces hypothèses sont les suivantes:

- La distribution des évanouissements doit être homogène et indépendante parmi les mobiles.
- Le débit réalisable instantané par utilisateur doit être linéaire en fonction du rapport signal sur bruit SNR instantané ou bien tous les utilisateurs doivent avoir un même SNR moyen.
- Les flux servis doivent rester dans le système assez longtemps pour que l'algorithme derrière l'ordonnanceur PF puisse converger. En effet, l'algorithme PF est biaisé envers les flux qui ne durent que quelques slots de temps.

Mais en pratique, ces hypothèses ne sont pas vérifiées:

- Les utilisateurs ne font pas l'expérience d'un même type d'évanouissement; ce dernier étant un phénomène très complexe résultant de l'interaction entre l'environnement de propagation et la mobilité de l'utilisateur. A titre d'exemple, il est courant d'admettre que des évanouissements du type *Rayleigh* résultent des réflexions multi chemins alors qu'une communication en visibilité directe souffre des évanouissements du type *Rician*. Le principal impact de cette absence d'homogénéité lors de l'utilisation d'une politique PF est un partage inéquitable des slots entre les utilisateurs: ceux qui ont les distributions les plus variables (donc typiquement ceux qui sont les plus éloignés de la station de base) reçoivent le moins de slots [[Hol01](#)].
- Le débit de transmission n'est pas linéaire en fonction du SNR, sauf pour les faibles débits donc typiquement pour les utilisateurs éloignés [[BP03](#)], ni un même SNR moyen ne peut être réalisé par tous les occupants de la cellule.
- Les flux élastiques, comme l'ont montré de nombreuses études du trafic Internet [[CB97](#)], sont constitués d'une minorité de flux longs alors que la majorité des flux sont courts. Il en résulte que l'algorithme PF reste en deçà de ses possibilités pour la plupart des flux servis.

Il nous a paru donc nécessaire de proposer des solutions qui contournent chacune des déficiences dont souffre PF dans un milieu réel.

Plan détaillé de la thèse et contributions

Dans le chapitre 1, nous introduisons le contexte général de cette thèse. Nous présentons le problème de gestion des ressources radio et d'ordonnancement dans les réseaux mobiles. Nous mettons en exergue les écueils, liés à la nature propre du canal radio, qui entravent la mise au point de politiques d'ordonnancement efficaces. Nous expliquons pourquoi la définition de l'équité dans les réseaux mobiles est multiple et qu'elle est loin d'être limitée à fournir aux utilisateurs mobiles la même chance d'accès aux ressources radio. Nous mettons en avance principalement la grande difficulté de proposer des algorithmes qui soient à la fois efficaces et équitables. Nous expliquons en détails le sujet axial de notre thèse à savoir l'ordonnancement sensible à l'état du canal. Nous en présentons les deux branches principales à la lumière d'un état de l'art exhaustif. Nous montrons certains défauts dont souffrent ces différents mécanismes d'ordonnancement, défauts auxquels nous apportons des solutions appropriées dans le cadre de notre thèse. De plus, nous expliquons en détails le mécanisme derrière l'ordonnanceur opportuniste le plus en vogue dans les systèmes de troisième génération: l'algorithme PF. En particulier, nous exposons le problème d'optimisation à la base de l'algorithme PF. En outre, nous passons en revue d'autres techniques de gestion de ressources radio également adoptées dans notre thèse. Dans le chapitre 2, nous présentons l'architecture des deux réseaux sans fil pour lesquels nos deux principales politiques d'ordonnancement ont été développées.

Opportunistic Weighted Fair Queueing

Dans le chapitre 3, nous abordons le premier volet de l'ordonnancement sensible à l'état du canal dans les réseaux mobiles: le *Wireless Packet Fair Queueing*. Puisque les algorithmes proposés dans la littérature réussissent à émuler le système GPS mais manquent d'efficacité, nous proposons une politique d'ordonnancement pour pallier ce problème. En effet, les algorithmes existants supposent que la capacité du canal est constante et proposent chacun un mécanisme de compensation plus ou moins efficace pour remédier au problème de communications discontinues par suite d'une rafale d'erreurs. Dans le cadre de notre travail, au lieu de supposer à tort que la capacité du canal est constante et de dissimuler ses variations aux flots servis, nous mettons à profit ces variations. Dans [KK06c], notre algorithme intitulé OWFQ (Opportunistic Weighted Fair Queueing) est une version opportuniste de l'illustre algorithme WFQ (ou Attente Equitable Proportionnée) qui donne une sorte de priorité aux paquets en-têtes jouissant d'un bon canal tout en

appliquant la définition d'équité du GPS. L'algorithme OWFQ introduit l'opportunisme au mécanisme de WFQ en prenant en compte les fluctuations de l'état du canal, ce qui lui permet d'allouer efficacement les ressources tout en offrant aux utilisateurs des garanties en terme de débit minimal.

PF dans un environnement réel

Le reste de la thèse est dédié à la politique d'ordonnancement opportuniste Proportional Fair. Le chapitre 4 rappelle les propriétés de PF dans un environnement idéal, à savoir son efficacité et sa parfaite équité. Il met ensuite en avance les défauts dont souffre PF dans un environnement réel. Les chapitres 5 à 7 proposent des politiques d'ordonnancement basées sur PF mais qui comblent ses failles.

L'algorithme WPF

Dans le chapitre 5, nous proposons une alternative à la politique PF puisque cette dernière souffre de plusieurs défauts. En effet, dans un environnement idéal, l'algorithme PF permet aux mobiles d'avoir la même probabilité d'accès aux ressources, autrement dit, il leur fournit une équité temporelle. Cependant, dans les réseaux mobiles, fournir la même fréquence d'accès aux mobiles est loin de leur garantir un même débit, autrement dit, une équité utilitaire. De plus, dans un environnement réel, PF offre une équité temporelle biaisée où les utilisateurs proches de la station de base sont servis plus fréquemment que ceux qui en sont éloignés. Ajoutons à cela que l'algorithme PF manque de flexibilité et ne permet pas au système de choisir entre efficacité et équité temporelle (qu'il a du mal à garantir). Dans [KKA06, Kha06], l'algorithme que nous proposons, intitulé WPF (Weighted Proportional Fair), engendre dans un environnement réel le comportement de PF dans un environnement idéal. En outre, notre approche permet d'introduire une flexibilité significative dans l'attribution des ressources aux mobiles. En effet, WPF permet de choisir entre équité temporelle, équité utilitaire et efficacité. Pour ce faire, la cellule est divisée en trois zones concentriques telle que dans chaque zone l'évanouissement perçu par les mobiles est quasi-homogène et la linéarité entre le débit de chaque mobile et son SNR est vérifiée. Notre WPF est une approche d'ordonnancement hiérarchique du PF qui répartit les slots de temps suivant une politique de WRR (Weighted Round Robin) entre les zones, chaque zone étant servie suivant l'algorithme de PF. Notre politique d'ordonnancement permettra, en première étape, de rétablir l'équité perdue dans un environnement réel, et en deuxième étape, donnera une flexibilité dans le partage de slots entre les utilisateurs. Ainsi, en choisissant de donner plus de slots aux mobiles éloignés (défavorisés par leur petit débit), on leur garantit une équité utilitaire. Alors qu'en choisissant de donner plus de slots aux mobiles proches de la station de base, on augmente la capacité totale du système et on gagne ainsi en efficacité.

De plus, nous proposons de contrôler les ressources du système en combinant ordonnancement selon la politique de PF et mécanisme de contrôle de puissance intercellulaire. Ainsi, en réduisant l'interférence subit par les utilisateurs proches de la station de base, nous augmentons la capacité totale de la cellule (efficacité); et en réduisant l'interférence subit par les utilisateurs éloignés de la station de base, nous augmentons leur débit individuel (équité utilitaire). Finalement, notre algorithme WPF nous a permis de servir différemment les différentes catégories d'utilisateurs (les zones), choisissant ainsi l'ordonnancement le plus adapté à chaque catégorie dans le but d'augmenter le débit global de la cellule.

L'algorithme HPF

Dans le chapitre 6, nous proposons une deuxième alternative à la politique PF puisqu'elle n'utilise pas les ressources au mieux quand le rapport signal sur bruit SNR de chaque utilisateur n'est pas proportionnel à son débit. Dans les systèmes HDR/HSDPA, il est recommandé de servir un seul utilisateur à la fois parce qu'une telle approche est optimale quand le SNR varie linéairement avec le débit réalisé. Cependant, en pratique, cette linéarité entre SNR et débit n'est pas vérifiée pour tous les utilisateurs dans la cellule et par suite une politique d'ordonnancement TDMA pure n'aboutira pas à une utilisation efficace du canal radio. En effet, quand un modèle de canal réel est adopté où, selon la théorie de Shannon, le SNR et le débit vérifie une relation logarithmique, l'hypothèse de linéarité n'est valide que pour les utilisateurs ayant de faibles rapports signal sur bruit et qui sont donc typiquement situés loin de la station de base. Pour cela, on propose dans [KK06a] un ordonnanceur hybride, intitulé HPF (Hierarchical Proportional Fair), qui alterne ordonnancement CDMA et TDMA. En effet, dans HPF, les utilisateurs éloignés de la station de base sont servis selon la politique de PF puisque leur débit est quasi proportionnel à leur SNR et en raison de leur moyenne voire mauvaise qualité de canal (nécessitant un ordonnancement TDMA pour éliminer les interférences intracellulaires). Quant aux utilisateurs proches de la station de base, ils sont servis selon un ordonnancement CDMA puisque leur débit est logarithmique par rapport à leur SNR et parce qu'ils perçoivent de bonnes conditions de canal. Ainsi, grâce à une meilleure allocation des ressources, notre algorithme HPF augmentera la capacité globale de la cellule par rapport à PF.

Les algorithmes opportunistes sensibles à la taille des flots

Dans les chapitres 7 et 8, nous nous attaquons au dernier défaut de l'algorithme PF, à savoir ses performances sous optimales obtenues lors du traitement des flots courts. Les flots courts formant la majorité des flux élastiques, un tel comportement remet sérieusement en question l'efficacité de l'ordonnanceur PF. Pour surmonter ce défaut, nous proposons dans [KK06b] trois ordonnanceurs basés sur l'algorithme PF et sensibles à la taille des flots servis.

Dans le premier algorithme – intitulé SB-HPF (Size-Based Hierarchical PF) – on sépare flots longs et flots courts en deux classes cherchant à protéger les flots courts. Dans un premier temps, les slots de temps sont distribués entre les deux classes de flots suivant une politique de WRR, et dans un deuxième temps, à l'intérieur de chaque classe, les flots sont servis selon la politique de PF. Le deuxième algorithme – intitulé SB-APF (Size-Based Adapted PF) – on modifie l'algorithme PF de sorte à augmenter la probabilité des flots courts à accéder au canal, réduisant ainsi leur temps de séjour dans le système. Le dernier algorithme – intitulé PF-LAS – est une version unifiée de deux algorithmes: PF et LAS (Least Attained Service) [RUK03]. Les trois algorithmes proposés réduisent sensiblement le temps de séjour des flots courts tout en mettant à profit la diversité Multi-Utilisateurs, utilisant ainsi le mieux possible les ressources du canal mobile. Ce qui fait l'intérêt et la robustesse des algorithmes proposés est que le gain qu'ils octroient aux flots courts est obtenu au prix d'une légère dégradation des performances des flots longs.

Finalement, le chapitre 9 contient les conclusions générales de la thèse. Nous portons le point sur les grandes contributions de ce travail, ainsi que sur les questions ouvertes soulevées et les directions de recherche future envisagées.

Conclusion et Perspectives

La présente évolution vers une généralisation de l'accès mobile aux réseaux multi services porte l'accent sur le besoin urgent d'optimiser l'utilisation des ressources radio. En particulier, des politiques d'ordonnancement qui allouent de façon optimale les rares ressources disponibles sont désormais d'une importance primordiale. Les ordonnanceurs sensibles à l'état du canal sont essentiels pour fournir de hauts débits aux utilisateurs et pour satisfaire une panoplie d'exigences en terme de qualité de service. Pour ce faire, ces ordonnanceurs, dits opportunistes, profitent de la tolérance du trafic vis-à-vis du délai pour fournir les moyens de partage optimal de ressources limitées et variables en temps. Notre travail s'est limité à l'étude de l'ordonnancement opportuniste des flots élastiques et une éventuelle poursuite de notre recherche peut se porter sur l'ordonnancement opportuniste d'un trafic mixte formé de flots à temps réel et de flots plus ou moins insensibles au facteur temps. Le cadre futur de nos investigations pourrait être la 3G LTE (3G Long Term Evolution), une architecture nouvelle et prometteuse. Alors que dans les réseaux 3G, HSDPA offre un débit théorique allant jusqu'à 14.4Mbps, le débit effectif offert aux utilisateurs est autour de 800Kbps. Dans 3G LTE, une architecture tout IP simple et optimisée promet une capacité globale allant jusqu'à 100Mbps. De plus, l'avènement de la 3G LTE offre, pour la première fois, un service VoIP (Voice over IP) cellulaire doté de performances acceptables pour les utilisateurs. Un service VoIP efficace peut donner aux opérateurs mobiles la pos-

sibilité d'intégrer services voix et services multimédia. Par conséquent, grâce aux hauts débits et aux temps de transfert réduits qu'elle promet, la 3G LTE offre l'opportunité de mettre au point des politiques d'ordonnancement opportunistes hautement performantes pourvoyant des services avec une QoS élevée aux flots temps réels et élastiques.

Abstract

The scarce resources in wireless systems compounded with their highly variable and error-prone propagation characteristics stress the need for efficient resource management.

Scheduling is a key tool to allocate efficiently the radio resource. While fading effects have long been combated in wireless networks, primarily devoted to voice calls, they are now seen as an opportunity to increase the capacity of novel wireless networks that incorporate data traffic. For data applications, there is a service flexibility afforded by the delay tolerance of elastic traffic and by their ability to adapt their rate to the variable channel quality. Opportunistic scheduling exploits these characteristics by making use of channel state information to ensure that transmission occurs when radio conditions are most favourable. When user applications have heterogeneous characteristics and quality of service requirements, opportunistic scheduling becomes a challenging task. In this thesis, opportunistic scheduling transmission schemes for supporting downlink non-real time services are proposed and analyzed for novel cellular and wireless broadband systems. The proposed schemes are designed for covering various QoS requirements for users while increasing the system utilization. We investigated the two main approaches adopted in the literature to devise efficient channel-aware policies for elastic traffic: **Wireless Fair Queueing** and **Proportional Fair Scheduling**:

- Wireless fair queueing makes use of channel state information to avoid allocating resources to users that cannot emit as they are in rather bad channel state while striving to fulfil fairness properties as defined by the GPS model. Existing wireless fair queueing algorithms use information relative to the channel state in a rather simplistic way. A given user is in a binary state: in a **good channel state** and can consequently exchange data; or in a **bad channel state** and cannot therefore exchange data. Opportunistic scheduling goes a step further and makes use of channel state information to give priority to users experiencing relatively better channel quality and thus increases system efficiency. In our work, we propose a new opportunistic wireless fair queueing scheduler for 802.16 systems. Our scheduler notably enhances the overall system performance through opportunistic scheduling as compared to existing approaches while fulfilling users' QoS needs in terms of minimum

realized throughput.

- The Proportional Fair (PF) scheduler allocates resources opportunistically according to the proportional fairness definition. It is widely adopted in HSDPA/HDR systems because it strikes a good balance between two conflicting objectives: temporal fairness and efficiency. Yet, the PF scheduler suffers from some important drawbacks in real environments. In our work, we propose three sets of performing schedulers that overcome the main shortcomings of the PF scheduler.

List of Abbreviations

2G	Second Generation
3G	Third Generation
3G LTE	Third Generation Long Term Evolution
3GPP	Third Generation Partnership Project
ACK	Acknowledgement
APF	Adapted PF
BP	Bounded Pareto
BS	Base Station
BWA	Broadband Wireless Access
CSDPS	Channel State Dependent Packet Scheduling
CIQ	Channel Indication Quality
CIFQ	Channel Independent Packet Fair Queueing
CBQ	Class-Based Queueing
CDMA	Code Division Multiple Access
DL	Downlink
DRC	Data Rate Control
DHR	Decreasing Hazard Rate
FDMA	Frequency-Division Multiple Access
GPS	General Processor Sharing
HARQ	Hybrid ARQ
HOL	Head Of Line
HDR	High Data Rate
HSDPA	High Speed Data Packet Access
IWFQ	Idealize Wireless Fair Queueing
i.i.d.	independent and identically distributed

ITO	Initial TimeOut
IP	Internet Protocol
LAN	Local area network
LAS	Least Attained Service
LOS	Line-Of-Sight
LSM	Link Status Monitor
MAN	metropolitan area network
MBAC	Measurement-Based Admission Control
NLOS	None Line-Of-Sight
OFDM	Orthogonal Frequency Division Multiplex
OFDMA	Orthogonal Frequency Division Multiplex Access
OWFQ	Opportunistic Weighted Fair Queueing
PWGPS	Packetized Wireless General Processor Sharing
PS	Processor Sharing
PF	Proportional Fair
QoS	Quality of Service
RRM	Radio Resource Management
RICQ	Relative Instantaneous Channel Quality
RTO	Retransmission TimeOut
RR	Round Robin
SQFQ	Self-Clocked Fair Queueing
SNR	Signal-to-Noise Ratio
SB-HPF	Size-Based Hierarchical PF
SPF	Standard PF
STFQ	Start-Time Fair Queueing
TDMA	Time Division Multiple Access
TCP	Transport Control Protocol
UL	Uplink
VoIP	Voice over IP
WFQ	Weighted Fair Queueing
WPF	Weighted Proportional Fair
WRR	Weighted Round Robin
WGPS	Wireless General Processor Sharing
WLAS	Wireless Least Attained Service

Contents

Résumé	ix
1 Introduction	1
2 Architectural Context: the 802.16 system and the HDR/HSDPA systems	19
2.1 General System Model	19
2.1.1 The 802.16 system	20
2.1.2 The HDR/HSDPA systems	22
2.2 Proposed Schedulers and Corresponding Technologies	23
3 Opportunistic Weighted Fair Queueing	25
3.1 Introduction	25
3.2 Opportunistic Weighted Fair Queueing	26
3.2.1 The Radio Model	26
3.2.2 Reminder on Weighted Fair Queueing	27
3.2.3 Opportunistic WFQ	27
3.3 Fairness Guarantee	28
3.4 Numerical Experiments	29
3.5 Concluding Remarks	33
3.6 Appendix	34
3.6.1 Proof of Lemma 1:	34
3.6.2 Proof of Lemma 2:	36
4 The PF scheduler: False assumptions and Drawbacks	37
4.1 Introduction	37
4.2 PF in an Ideal Environment	37

4.2.1	The Radio Resource	38
4.2.2	The Three Assumptions	39
4.2.3	The PF Algorithm	40
4.3	PF in a Real Environment	41
4.4	Concluding Remarks	42
5	The Weighted Proportional Fair Scheduler	43
5.1	Introduction	43
5.2	The Cell Partitioning	44
5.2.1	The Radio Model	45
5.2.2	Delimiting the Cell into Zones	46
5.3	Analytical Study of PF vs. WPF	48
5.3.1	The WPF Scheduler	49
5.3.2	The PF Scheduler	50
5.3.3	Numerical Results	51
5.4	Dynamic Model of WPF	53
5.4.1	Analytical Model	54
5.4.2	Simulation Results	55
5.5	Intercell Scheduling	56
5.6	The WPF+CDMA Scheduler	58
5.6.1	Average Rate per Slot	58
5.7	Concluding Remarks	59
5.8	Appendix	60
5.8.1	Computing $g_z(n_z)$:	60
5.8.2	Computing the scheduling gains $G_z(n_0, n_1, n_2)$:	61
5.8.3	Computing the probabilities a, b & c :	61
6	A Hierarchical Proportional Fair Scheduler	63
6.1	Introduction	63
6.2	A Hierarchical Scheduling Approach	64
6.2.1	The Radio Resource	64
6.2.2	CDMA vs. TDMA	65
6.2.3	Delimiting the Cell into Zones	67
6.3	Analytical Study of HPF vs. Standard PF	69

6.3.1	The Average Peak Rate in HPF	70
6.3.2	The Average Peak Rate in Standard PF	71
6.3.3	Average Gain	72
6.4	Dynamic Model of HPF	74
6.4.1	The Processor Sharing Model	76
6.4.2	Simulation Results	78
6.5	Concluding Remarks	79
7	Flow Size-Aware Proportional Fair Schedulers	81
7.1	Introduction	81
7.2	Radio Model and Traffic Characteristics	82
7.2.1	Traffic Characteristics	83
7.3	Proportional Fair Algorithm	83
7.3.1	The Analytical Study of PF	84
7.3.2	Numerical Experiments	84
7.4	The SB-HPF Scheduler	86
7.4.1	The Analytical Study of SB-HPF	86
7.5	The SB-APF Scheduler	91
7.5.1	The SB-APF-a Scheduler	91
7.5.2	The SB-APF-b Scheduler	94
7.6	The PF-LAS Scheduler	95
7.6.1	The Wireless LAS Scheduler	97
7.6.2	The PF-LAS Scheduler	97
7.6.3	Numerical Experiments	97
7.7	Concluding Remarks	98
8	The impact of TCP on Flow Size-Aware Proportional Fair Scheduling	101
8.1	Introduction	101
8.2	Radio Propagation and Traffic Models	103
8.2.1	System Model	103
8.2.2	Traffic Characteristics	104
8.3	Simulation results of the PF scheduler	105
8.4	Simulation results of the SB-HPF scheduler	106
8.5	Simulation results of the SB-APF scheduler	108

8.6	Simulation results of the PF-LAS scheduler	109
8.7	Conclusion	110
9	General Conclusion	111
9.1	Summary of Contribution	111
9.1.1	Wireless Fair Queueing	112
9.1.2	Opportunistic Scheduling: The Proportional Fair Scheduler	112
9.2	Future Directions	114

List of Figures

1.1	Wireless Transmission Scheduling: Mobile 2 perceives an error-free channel while Mobile 1 perceives an erroneous channel.	4
1.2	Channel-Aware Scheduling	6
3.1	Mean throughput per flow as a function of load	30
3.2	dT as a function of load	31
3.3	Total throughput as a function of load	32
5.1	Mean Rate per Zone and Total Mean Capacity	53
5.2	Average Throughput for Zone 0	55
5.3	Average Throughput for Zone 1	55
5.4	Average Throughput for Zone 2	56
5.5	Intercell Scheduling	57
6.1	Ratio ς_k for $f=0$	66
6.2	Ratio ς_k for $h=0.03$	67
6.3	Ratio ς_k for $f=0.3$	67
6.4	Ratio ψ_k for $f=0.1, h=0.03$	72
6.5	Average Rate for Zone 1	74
6.6	Average Rate for Zone 2	74
6.7	$F_{k,2}(n_2)$ as function of r	76
6.8	Throughput as a function of $\frac{1}{\lambda_T}$ in Zone 1	79
6.9	Throughput as a function of $\frac{1}{\lambda_T}$ in Zone 2	79
7.1	Mean Sojourn Time of short flows	85
7.2	Mean Throughput of long flows	85
7.3	Blocking Rates for long flows	87

7.4	Mean Sojourn Time of short flows for SB-HPF(1,1)	88
7.5	Mean Throughput of long flows for SB-HPF(1,1)	88
7.6	Mean Sojourn Time of short flows for SB-HPF(2,1)	88
7.7	Mean Throughput of long flows for SB-HPF(2,1)	88
7.8	Mean Sojourn Time of short flows for SB-HPF(1,2)	88
7.9	Mean Throughput of long flows for SB-HPF(1,2)	88
7.10	Mean Sojourn Time of short flows	89
7.11	Mean Throughput of long flows	89
7.12	Mean Sojourn Time of short flows (with MBAC)	90
7.13	Mean Throughput of long flows (with MBAC)	90
7.14	Mean Sojourn Time of short flows	93
7.15	Mean Throughput of long flows	94
7.16	Mean Sojourn Time of short flows	96
7.17	Mean Throughput of long flows	96
7.18	Mean Sojourn Time for $\lambda = 20.0$	98
7.19	Mean Sojourn Time for $\lambda = 15.0$	98
7.20	Mean Throughput for $\lambda = 15.0$ and $\lambda = 20.0$	99
8.1	Mean Throughput of long and short flows in PF	105
8.2	Mean Sojourn Time of short flows	107
8.3	Mean Throughput of long flows	107
8.4	Mean Sojourn Time of short flows for SB-HPF(2,1)	108
8.5	Mean Throughput of long flows for SB-HPF(2,1)	108
8.6	Mean Sojourn Time of short flows for SB-HPF(4,1)	108
8.7	Mean Throughput of long flows for SB-HPF(4,1)	108
8.8	Mean Sojourn Time of short flows	109
8.9	Mean Throughput of long flows	109
8.10	Mean Sojourn Time of short flows	110
8.11	Mean Throughput of long flows	110

List of Tables

3.1	Throughput in OWFQ	33
3.2	Throughput in WFQ	33
5.1	Average Rate per user	53
6.1	Total Average Peak Rate	73
8.1	Simulation parameters	104

Chapter 1

Introduction

Fuelled by the growth of Internet use, a great deal of research has focused on making the data access wireless. With an increasing request for wireless data services, methods for managing the scarce radio resources become vital. For wireline communications, extended capacity can be obtained by adding more wires or fibres, whereas wireless communications are compelled to share a limited natural resource. Furthermore, in comparison with a wireline channel, the radio channel is time-variant and subject to asynchronous bursts of errors making the radio resource allocation a challenging task. Significant efforts have been invested in increasing the wireless spectrum efficiency to cope with the unique characteristics of the radio channel and the ever-growing demand for high-data-rate wireless communication. This chapter recaptures some key components of Radio Resource Management and highlights some of the most relevant previous work. The plan of the thesis is given at the end of the chapter.

1.1 Radio Resource Management

Efficient Radio Resource Management (RRM) is of dominant importance due to the rapid size-increase of the wireless mobile community, its demand for high-data rates communications and the limited available resources. Allocating resources efficiently is not straightforward basic when it comes to serving users with heterogeneous characteristics and heterogeneous QoS requirements. Nevertheless, suitable RRM tools have been proposed in the literature and proven to be efficient, such as transmission scheduling, admission control, interference management, multi-user detection [Ver98], smart antennas ([LP99, BH00, Fos96]), channel error control coding (Turbo coding/decoding [BGT93]), power control [Yat95], adaptation techniques [NBK00] (variable spreading, coding, and code aggregation in Code Division Multiple Access (CDMA) systems; adaptive coding, adaptive modulation, and incremental redundancy in Time-Division Multiple Access (TDMA) systems), etc. Our work

centers on **transmission scheduling** but also uses other techniques such as **admission control** and **interference management**.

1.1.1 Transmission Scheduling in Wireless Networks

The number of devices accessing the network through wireless interfaces is growing fast and will overtake, in the coming years, the number of wireline connected devices. This evolution exacerbates the difficulties raised by the scarce and highly variable radio resources and increases the need for optimal utilization of the latter. Scheduling is a key tool for optimizing resource allocation while providing fairness guarantees to mobile users. In our thesis, we worked on **Opportunistic Scheduling** that makes use of channel state information to further increase the efficiency of resource allocation.

1.1.1.1 Variable Channel

In wireline networks, resource allocation schemes and scheduling policies play important roles in providing service performance guarantees, such as throughput, delay, fairness, and loss rate. Scheduling disciplines and associated performance problems have been widely studied in packet-switched networks [PG93, DKS89]. Unfortunately, resource allocation schemes from the wireline domain cannot be directly applied to wireless systems because of the unique characteristics of wireless channels. The key characteristics of the wireless medium can be summarized as follows:

- Dynamic variations of wireless channel capacity.
- Location-dependent and bursty channel errors.
- Dependence of network performance on channel conditions and signal processing techniques.
- If the same resource is given to different users, the resulting network performance (e.g., throughput) can be different from user to user (this notion is related to fairness and will be explained in the corresponding section 1.1.1.2).

These characteristics are discussed next in more detail and the reason why they are important to the design of wireless scheduling policies is given.

The signal transmitted from the sender may reach the receiver directly (line-of-sight) or through multiple reflections on local obstacles. As a result, the received signal is affected by multiple random attenuations and delays. Moreover, the mobility of either the sender/receiver or the obstacles may cause these random fluctuations to vary over time. Furthermore, in a shared wireless environment, the transmitted signal incurs interference – due to concurrent transmissions – that is also time-varying. This interference is of two

types: intracell interference from other users in the cell and intercell interference from adjacent cells.

The attenuation incurred in wireless propagation can be divided up into three main elements:

- **Path-loss** responsible for signal attenuation due to the distance between communicating nodes.
- **Shadowing** responsible for attenuation effects due to absorption in local structures.
- **Multi-path Fading** responsible for rapid signal fluctuations due to constructive and destructive interference of multiple reflected radio wave paths.

The channel characteristics depend on the combination of all three propagation effects and can also be affected by sender/receiver filters. We conclude that the achievable rate for a sender/receiver pair depends, in a complex manner, not only on the way resources are shared among all sender/receiver pairs, but also on the highly variable channel.

There are basically two approaches to handle the channel variability depending on the considered application:

- The system can adapt the used radio resources to compensate for the varying channel quality and to maintain a fixed rate.
- The system can dynamically adapt the rate so as to match the variations in channel quality.

The first approach is appropriate for voice services, while the second is suitable for data services that do not have a stringent rate requirement. In the second approach, the system can profit from the delay tolerance of data services to adaptively exploit the time-varying channel conditions of users to achieve higher utilization of wireless resources. This is called **opportunistic** scheduling where the wireless channel variations are continuously tracked by the server and used to schedule transmissions to users with relatively better instantaneous channel quality. Intuitively, the opportunistic scheduler wishes to serve users experiencing good channel conditions so that resources can be used efficiently. At the same time, it wants to provide some form of fairness guarantees to all users. For instance, allowing only users close to the Base Station (BS) to transmit with high transmission power may result in very high system throughput, yet it may starve other users located far from the BS. Hence, in opportunistic scheduling, there always exists a trade-off between global *efficiency*¹ and *fairness*.

¹efficiency in terms of overall cell capacity.

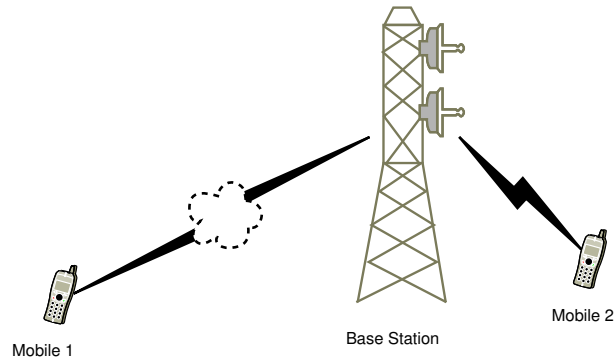


Figure 1.1: Wireless Transmission Scheduling: Mobile 2 perceives an error-free channel while Mobile 1 perceives an erroneous channel.

1.1.1.2 Fairness

The fairness issue arises whenever a given amount of *resource* is to be shared by a number of *users*. In a wireless environment, due to random channel variations, we must distinguish between **Temporal** fairness (which means that each user gets a fair share of system resources) and **Utilitarian** fairness (which means that each user gets a certain share of the overall system capacity). While **Temporal** fairness equals **Utilitarian** fairness in a wireline environment, they can be substantially different in a wireless environment. Indeed, the performance (e.g., throughput) of a user depends on the channel condition it experiences, thus, different performance is obtained when the same resource (e.g., radio frequency) is assigned to different users. For example, if we consider a cell with two users: the first user is close to the BS and thus enjoys good channel conditions and the second user is at the edge of the cell and therefore endures bad channel conditions due to significant path-loss and high interference from neighbouring cells. If the same amount of resource (power, time-slots, etc.) is assigned to both users, it is likely that the throughput of the first user will be much larger than that of the second user.

Further, we consider another type of fairness related to the inherent nature of elastic traffic. Measurement studies have shown that elastic traffic exhibits the mass disparity phenomenon: nearly 80% of flows are short with 10-20 packets on average and about 20% of flows are large, containing a large fraction of the mass (bytes) [CB97]. Many factors like the conservative congestion control mechanisms of TCP and the lack of coordination between the latter and opportunistic scheduling, have an adverse impact on short flows performances. This is critical as short flows represent the large majority of elastic traffic. Since the basic idea of opportunistic scheduling is to let users transmit in good channel conditions, they are expected to wait until they are in favourable channel conditions before receiving service. But how long a short flow is willing to wait for good channel conditions when its performance goal is to minimize transfer latency, contrary to long flows

whose performance goal is to maximize throughput. Hence, there always exists a compromise between two conflicting objectives when opportunistic schedulers serve elastic traffic: guaranteeing efficiency for long flows and providing short-term temporal fairness for short flows. Therefore, devising opportunistic scheduling policies which provide a prompt service to short flows while only incurring a slight penalty to long flows in terms of realized throughput is of paramount importance.

1.1.2 Multiple Access

Multiple access techniques allow a communication medium to be shared among different users. The three basic multiple access techniques are FDMA (Frequency-Division Multiple Access), TDMA and CDMA. Various hybrid schemes which consist of the aforementioned fundamental techniques also exist. First generation analog cellular systems use FDMA. Second and third generation digital cellular systems use both TDMA and CDMA techniques. In 3.5G networks, TDMA scheduling is advocated because it has been shown that, assuming the feasible transmission rate is linear in the Signal-to-Noise Ratio (SNR), one-by-one scheduling maximizes overall throughput [BBR99, HR98, Pot95]. However, this optimality principle is not valid when a more realistic model is adopted, where the feasible rate and the SNR follow a logarithmic relation according to Shannon's law. In that case, scheduling one user at a time does not result in maximum channel utilization for all users in the cell.

1.1.3 Interference Management

Interference management is a decisive component of efficient radio resource utilization because interference eventually limits the system capacity. Interference management is traditionally implemented via Power Control. It has been extensively studied and used in wireless systems to maintain desired link quality, minimize power consumption, and reduce interference suffered by users [Yat95]. Moreover, joint scheduling and power-allocation schemes are used to further improve the spectrum efficiency and enable the system to control its resource allocations.

1.1.4 Admission Control

The purpose of admission control is to preserve the quality of ongoing connections while admitting new ones. A good admission scheme would grant access to as many users as possible without jeopardizing the performances of ongoing users. However, admission control becomes more challenging in a wireless environment because serviced users have heterogeneous characteristics and different QoS requirements. There are two major approaches to the admission control problem:

- Admitting a user based on whether the network can satisfy the QoS requirements of all users at the time of admission.
- Admitting a user based on whether the network can satisfy the QoS requirements of all users while taking into consideration the variation in the channel performance.

The first solution is used in our thesis because it has the appeal of being simple but obviously results in conservative decisions. The second approach has the advantage of more intelligent decision-making at the cost of increased complexity [LAN97].

1.2 Related Work

The work in this thesis addresses the two main areas in Channel-Aware Scheduling: **Wireless Fair Queueing** and **Opportunistic Scheduling**. We give a description of the most representative work in the respective direction. In particular, we explain in details the mechanism behind the most extensively used opportunistic scheduler in novel cellular networks: the Proportional Fair Scheduler. We also explain briefly the concept of intercell scheduling as it was used in our thesis.

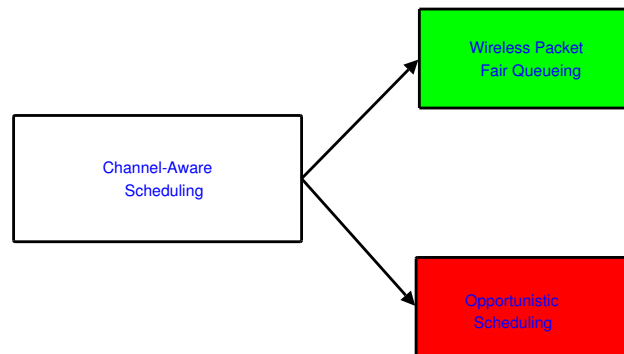


Figure 1.2: Channel-Aware Scheduling

1.2.0.0.1 Introduction: The major concern of this thesis is opportunistic scheduling of elastic traffic. A direct and simple strategy for taking advantage of opportunistic scheduling is to serve the user at any scheduling decision with the best channel quality. This approach is adopted in [KH95] where it is shown that the optimal scheduling policy aiming to maximize the total information-theoretic capacity consists in selecting, at any time, the user with the highest transmission rate. The same approach is adopted in the MaxRate algorithm [Hol01]. Such an approach, although optimal from an overall system point of view, is far from being fair because it over-allocates resources to good-channel state users while depriving consistently bad channel-state users from accessing resources. As

already mentioned, there always exists a trade-off in wireless scheduling policies between achieving system efficiency and achieving fairness. Hence, schedulers that can conjugate overall system performance and individual user satisfaction are highly desirable. These policies are expected to deal with time-varying channel conditions while allocating resources so as to provide several fairness definitions such as: the General Processor Sharing (GPS) [PG93], the proportional-fairness [Kel97], and the max-min fairness [BG87].

1.2.1 Wireless Packet Fair Queueing

In wireline domain, performance guarantees are supplied to data users by means of resource reservation and packet scheduling that provide a fair allocation of system resources. The GPS policy [PG93] is a well-known fluid fair queueing discipline for scheduling flows over a shared link where each of the competing flows, represented as a fluid flow, obtains a part of the total bandwidth proportional to a predefined weight. There are quite many scheduling algorithms proposed in the literature for wireline networks that schedule packets in such a way that they approximate as faithfully as possible the performance of the GPS fluid fair queueing model. The most noteworthy among them are WFQ (Weighted Fair Queueing) [DKS89], SQFQ (Self-Clocked Fair Queueing) [Gol94], and STFQ (Start-Time Fair Queueing) [GVC97].

Unfortunately, packet fair queuing algorithms devised for the wireline domain cannot be simply carried out to the wireless domain and still be work-conserving and efficient due to the matchless features characterising wireless links. Indeed, the communication between the server and wireless users may be asynchronously interrupted due to a sudden burst of errors. Therefore, bursty and location-dependent errors make some mobile users unexpectedly unreachable, while others – perceiving an error-free channel – are perfectly able to send and receive packets. However, packet fair queueing algorithms were not designed to account for on-off communications because, in the wireline domain, all active flows perceive clean channels and are expected to emit at their fair rate. Hence, these disrupted communications make it impossible to directly apply wireline solutions to the wireless domain while still providing the fairness properties defined by the GPS model. Still, by combining channel state dependent scheduling and compensation, these problems can be surmounted. Several scheduling algorithms have been proposed to provide the fairness properties of wireline packet fair queueing policies that emulate the GPS model. Notable among them are CSDPS (Channel State Dependent Packet Scheduling) [BKT96], CIF-Q (Channel Independent Packet Fair Queueing) [LB99] and IWFQ (Idealize Wireless Fair Queueing) [ENSZ98] algorithms. Wireless fair queueing approximate wireline fair queueing when all users are in a good channel state and can, at all times, communicate with the server. When some users start perceiving bad channel conditions and can no longer communicate with the server, they are not scheduled and thus relinquish their slots

to good channel state users; in return, the latter will give their transmit rights back to the former category when it exits from bad channel state. The goal is to hide from users the short-term channel error bursts. Next, we explain the major wireless fair queueing schedulers proposed in the literature.

1.2.1.1 CSDPS

The work in [BKT96] is a pioneer in proposing an algorithm to address the problem of location-dependent and bursty errors faced by wireless scheduling. The CSDPS algorithm works as follows. An individual queue is maintained for each flow and is served in a FIFO order. When a flow encounters error, the server defers transmission of packets for the flow in question. The LSM (Link Status Monitor) supervises the channel state for all users. When the acknowledgment of a packet from a given flow is not received, the LSM determines that the corresponding flow is in a bad channel state and marks its queue. The server does not schedule packets from marked queues. The queue is unmarked after a time-out period corresponding to the average duration of a burst of errors for its channel. CSDPS lessens the Head Of Line (HOL) blocking problem of a FIFO queue, thus reducing the average delay of packets. However, it lacks mechanisms guaranteeing bandwidth for served flows. A bad channel state flow receives less than its fair service share and its allocated service is given to other flows although they may have already exceeded their fair service share. Furthermore, because the amount of extra service given to flows is unlimited, CSDPS does not offer any delay guarantees. In order to solve the problem of unfair bandwidth sharing in CSDPS and unbounded delay, a scheduling scheme, termed CSDP+CBQ, combining CSDPS and Class-Based Queueing (CBQ) [FJ95] is proposed in [FSS98].

1.2.1.2 IWFQ

The IWFQ [LB99] scheduling scheme is defined with reference to an error-free WFQ model. For each flow, two queues are maintained: a virtual queue in the reference system and the actual queue in the real system. In the reference system, an error-free WFQ service is provided to the virtual queue which has the same arrival sequence as the real queue. The service received by a flow in the real error-prone IWFQ system is compared with the error-free system. A flow is said to be leading, lagging, or in sync at any time instant if its queue size is respectively smaller than, larger than, or the same as the queue size in the ideal system. When all flows are in a good channel state, IWFQ operates identically to plain wireline WFQ: when a packet of a given flow arrives, it is tagged with a virtual start time and finish time, and the scheduler always picks up the packet with the smallest finish time. The difference between IWFQ and WFQ arises when channel errors occur. If the chosen packet cannot be transmitted because it belongs to a flow in bad channel state,

the packet belonging to other flows with the next smallest finish time and good channel conditions will be chosen instead. Since the time tags of packets that already arrived in the system are not changed, a flow that loses its chance to be picked by the scheduler will have packets with smaller finish times in comparison with other flows' packets. Consequently, it will have precedence in accessing resources when its channel no longer suffers from error. Therefore, the compensation is guaranteed and although perfect short-term fairness cannot be achieved, long-term fairness is quite feasible. Yet, unbounded compensation entails that good channel state flows may be deprived from accessing the channel for long periods, and hence strict delay bounds cannot be ensured. To deal with this compromise between achieving perfect fairness and realizing strict delay guarantees, only a limited amount of compensation is provided. Another downside of IWFQ is that compensation is supplied to flows in the same fashion and independently of their predefined weights which is in contrast with the fundamental property of WFQ where a larger guaranteed rate implies better quality of service. Moreover, the delay and throughput guarantees are tightly coupled which is undesirable.

1.2.1.3 CIF-Q

The chief contribution of CIF-Q [ENSZ98] is that it points out the four essential properties that any wireless fair queueing algorithm should have. These broad properties are the following:

- **Delay bound and throughput guaranteed rates.** Delay bound and throughput for error-free flows are guaranteed and are not disturbed by error-prone flows.
- **Long-term fairness.** During a large enough busy period, if an active flow exits error state, it should get back its lost service provided it remains long enough in the system.
- **Short-term fairness.** The difference between the normalized services received by any two good channel state flows that are constantly active and are in the same state (leading, lagging, or in sync) during a time interval should be bounded.
- **Graceful degradation.** During any time interval and while it perceives a clean channel, a leading active flow should necessarily receive at least a minimum fraction of its service in an error-free system.

Just like IWFQ, the real error-prone scheduling system, denoted by S , is run in reference to an error-free fair queueing system, denoted by S^r . Each flow has its own queue and when a flow is served, its HOL packet is transmitted. One of the main distinctions between CIF-Q and IWFQ is that virtual time is only kept and updated in S^r , not in S . When

channel errors occur, if a packet is picked by the scheduler in S^r , it is served in both S^r and S . Nevertheless, when a chosen packet in S^r cannot be transmitted in S because of channel error, the real packet in the queue of S is kept, but the virtual packet in the queue of S^r is still served and the corresponding flow's virtual time is updated according to SFQ (SFQ is chosen although other wireline fair queueing algorithms can also be used). A parameter lag_i is associated with flow i to keep track of the difference between the service received by a flow in S and the service it receives in S^r . To realize graceful degradation, a parameter δ is used in such way that a leading flow i will continue to receive service at an average rate of $\delta \cdot r_i$, where r_i is its predefined weight. The residual service share is given up by the leading flow to compensate lagging flows.

The key rules of CIF-Q scheduling are summarized below:

- When scheduling a packet, the HOL packet with the smallest virtual start time in S^r is chosen, and the corresponding packet in S is transmitted save in one of the subsequent circumstances:
 1. The chosen packet belongs to a flow whose channel is in error-state.
 2. The chosen packet belongs to a leading flow that has received more than a fraction δ of the normalized service it should have received based on its weight.
- Lagging flows have precedence in receiving extra service available thanks to leading flows relinquishing their lead (case 2) or chosen flows not served as they are in a bad channel state (case 1).
- Rather than giving all the extra service to the flow that has the largest lag, the compensation is shared among the lagging flows in proportion to their weights.
- If all lagging flows are in error-state and are thus unable to receive additional service, the extra available service is distributed to error free non lagging flows in proportion to their weights.

By enforcing the above rules, the four previously listed fairness properties can be satisfied. So compared to IWFQ, CIF-Q improves scheduling fairness by associating compensation rate and penalty rate with a flow's allocated service rate and guaranteeing flows, with error-free channels, a minimal service rate. However, just like IWFQ, the algorithm complexity of CIF-Q is rather high.

In order to function properly, all of the above-mentioned scheduling policies assume that all flows have the same packet size. [JMA01] proposes a wireless fair queueing algorithm, termed WGPS (Wireless General Processor Sharing), that considers unequal packet sizes. A packetized version of WGPS, termed PWGPS, is also proposed.

1.2.2 Opportunistic Scheduling in Wireless Fading Channels

In the previous section, wireless scheduling algorithms associated with error-prone wireless channels and a simple on-off channel model were considered. Their performance objective is to allocate system resources according to the GPS model. In this section, we examine scheduling strategies that provide resource allocations that satisfy various fairness criteria and are not restricted to the fairness definition of the GPS model. Moreover, these scheduling algorithms adopt more general channel models such as multi-rate channels. The multiple service rates of users depend on the randomly and asynchronously time-varying channel conditions. Their general system model consists of a BS that transmits data to a fixed number of users over a shared wireless fading channel. The downlink channel is time-slotted and in every time slot, the BS transmits to a subset of users. The BS is aware of users service rates, in a slot-by-slot fashion, and makes use of this information to schedule in every time slot the subset of users whose service will permit attaining the system performance objectives. The standard scheduling adopted in third generation systems is the well-known Proportional Fair (PF) algorithm whose performance objective is to verify the Proportional Fairness definition [Kel97].

The fairness objective for a single congested link is immediate and is defined by max-min fairness [BG87], where rates of individual flows are made as equal as possible and is realized by fair queueing. Max-min fairness is achieved by allocating available resources to as many underprivileged users as possible while avoiding to waste resources to no purpose. However, for wireless networks, a key challenge in fair resource allocation is that when a fraction of resources is allocated to a flow, it does not necessarily imply that the allocated resources will be used efficiently due to channel errors. Therefore, the appropriateness of a strict fairness as that provided by the max-min fairness is questionable when it comes to applying it in a wireless environment. Proportional fairness addresses the resource allocation problem from another perspective as it refers to maximizing an objective function that represents the overall utilization of all users while respecting the total available resource constraint. Hence, the proportionally-fair throughput vector (whose elements are the throughputs of users) is such that if another throughput vector is used to increase the throughput of a specific user by $x\%$ of what that user receives under the proportional fair allocation, the summation of all percentages of throughput decreases suffered by all other users in the new algorithm will be more than $x\%$. The proportional fairness turns out to be a special case of the Nash bargaining solution concept. Defined already in 1950 by J. Nash [Nas50], it has been applied to flow control since 1991 [MMD91]. Moreover, this concept is very appealing in the Internet context because it has been observed that the TCP protocol grabs bandwidth in a way that is compatible with this fairness notion [KMT98]. The PF scheduling algorithm was first proposed by Tse in [CBHT02, Tse]

and has been further studied in [Hol01, Hol00]. The convergence properties of PF under general assumptions have been examined in [Kus04, TG03] where it was shown that PF results in throughput allocations that converge to proportional-fair allotments assuming that all user queues are continually backlogged. We give a detailed explanation of the optimization problem behind the PF scheduler in what follows.

1.2.2.1 The PF Scheduler

We begin by providing a mathematical formulation of the scheduling algorithm given by Kelly [Kel97]. The main idea is that each user j is represented by a utility function U_j which can be understood as a quantitative description of the user satisfaction. Hence, if flow j is allocated a throughput T_j , then this has utility $U_j(T_j)$ to the flow. Although there has been no agreement on the exact form of the user utility as a function of its throughput, it is extensively recognized that -for an elastic user- the utility function $U_j(T_j)$ should be an increasing, concave and continuously differentiable function of T_j for $T_j \geq 0$ [She95]. It has been shown in [She95] that there is a general equivalence between maximizing concave utility functions and achieving fairness. The type of fairness achieved depends on the utility function used in the allocation algorithm.

We consider the following utility maximization problem given by Kelly [Kel97]:

A network with channel capacity C and k active users is considered. It is assumed that users' utilities are additive so that the aggregate utility of throughputs $\vec{T} = (T_j, j = 1..k)$ is $F(\vec{T}) = \sum_{j=1}^k U_j(T_j)$. A throughput allocation is feasible if $\sum_{j=1}^k T_j < C$ and hence to find the system's optimal throughput allocation, the following optimisation problem is considered:

$$\text{Maximize } F(\vec{T}) = \sum_{j=1}^k U_j(T_j) \quad (1.2.1)$$

$$\text{Subject to: } \sum_{j=1}^k T_j \leq C \quad (1.2.2)$$

$$\text{over: } T_j \geq 0, \quad 0 \leq j \leq k \quad (1.2.3)$$

Since it is assumed that the utility function of each user is strictly concave and differentiable, the same also holds for the objective function $F(\vec{T})$ in (1.2.1). Besides, since the feasible region in (1.2.2)-(1.2.3) is compact, an optimal unique solution exists and can be

found by Lagrangian methods. However, the optimal solution changes over time since both the channel capacity and the number of active users vary with time. As a consequence, the optimal solution is also time varying. To solve this problem, a gradient ascent method given by [Hos02] is used. Although the optimal throughputs can be computed, the system cannot be instantly moved to the optimal allocation. As we are aiming at a moving target, the best to do in each scheduling decision is to move towards, for the time being, the optimal solution. Therefore the user who results in movement along the maximum objective function F is served. To be able to make this decision, the average throughput of each user T_i must be computed. An exponentially smoothed filter is used to calculate the throughput,

$$T_i(t+1) = \left(1 - \frac{1}{\tau}\right) \cdot T_i(t) + \frac{1}{\tau} \cdot R_i(t) \cdot \mathbf{1}_{\{user(t)=i\}}, \quad (1.2.4)$$

where $\mathbf{1}_{user(t)=i}$ is the indicator function which equals 1 if user i is chosen at time slot t and 0 otherwise. $R_i(t)$ is the current feasible rate of user i at time slot t and τ is the time constant of the smoothing filter.

The optimization problem can be scaled down to finding the maximum gradient direction, i.e. maximizing $F'_j(\vec{T}(t))$, the gradient in the direction of serving user j . This could be done by parameterizing the movement along the ray corresponding to serving user j . Parameterizing by α and using 1.2.4 gives us,

$$F_j(\alpha) = \sum_{i=1}^k U_i(T_i(t) + \alpha \cdot (T_i(t+1) - T_i(t))).$$

Taking the derivative with respect to α and evaluating the derivative at $\alpha = 0$, we get,

$$\begin{aligned} F'_j &= U'_j(T_j(t)) \cdot \frac{R_j(t) - T_j(t)}{\tau} - \sum_{i=1, i \neq j}^k U'_i(T_i(t)) \frac{T_i(t)}{\tau} \\ &= U'_j(T_j(t)) \cdot \frac{R_j(t)}{\tau} - \sum_{i=1}^k U'_i(T_i(t)) \frac{T_i(t)}{\tau}. \end{aligned}$$

We want to choose user j who results in movement along the maximum gradient direction. As the summation term is common to all users, it can thus be removed. Finally, we choose the user for which,

$$j^* = \arg \max_j \{F'_j(\vec{T}(t))\} = \arg \max_j \{R_j(t) \cdot U'_j(T_j(t))\}.$$

Different scheduling algorithms can be obtained using different utility functions: for instance, the Max-min optimal throughput sharing is approximated with $U_j(T_j) = 1 - 1/T_j^m$. By using this family of functions, it is shown in [LB00] that the allocation of throughputs

converges to the max-min allocation as $m \rightarrow \infty$. The MaxRate algorithm [Hol01] uses the utility function $U_j(r) = \beta \cdot T_j$ because the user satisfaction is expressed in terms of delivered bits. Hence, the scheduling algorithm will choose the user for which,

$$j^* = \arg \max_j \{R_j(t)\},$$

which means, as mentioned earlier, that the user with the highest current rate will be picked by the scheduler. This scheduling policy will result in maximum overall throughput and hence maximum revenue. However, to maximize total throughput, the MaxRate will always serve users with good channel state at the expense of users with bad channel state leading to an unfair allocation of resources. The PF scheduler takes both fairness and efficiency into account by striving to attain proportional fairness while allotting resources efficiently. To realize proportional fairness the utility function used is logarithmic $U_j(T_j) = \log(T_j)$ and hence the resulting scheduler picks the user such that,

$$j^* = \arg \max_j \left\{ \frac{R_j(t)}{T_j(t)} \right\}.$$

This will provide some degree of fairness at the expense of reduced overall throughput in comparison with the MaxRate algorithm. Indeed, users with comparatively good channel conditions are scheduled: the momentary estimated feasible rate is compared to the average rate for each user and as a consequence, users in bad conditions must also be served. The PF scheduler will be able then to conjugate fairness and efficiency. Unfortunately, PF is optimal only under some assumptions that are not valid in real scenarios. We will see, in chapter 4, what are these assumptions and examine their impact on the performances of the PF scheduler when they are no longer maintained.

1.2.2.2 Other Scheduling Policies

In this section, we present some relevant opportunistic scheduling policies for novel generation systems. These policies control user transmissions so as to provide throughput allocations that satisfy several fairness criteria such as:

- proportional-fair throughput allocation.
- maximization of the minimum throughput allocation.
- maximization of system average throughput subject to fairness constraints on user time-fraction assignments.

1.2.2.2.1 A framework for opportunistic scheduling in wireless networks: The authors in [LCS03], using the utility-based model in [Kel97], present an optimal oppor-

tunistic transmission scheduling for shared wireless channels with time-varying channel conditions. With each channel state and each user, there is a concave utility function modelling the user level of satisfaction (e.g. the service rate). Total utility is then defined as an aggregate of the utility functions of all active users. The authors address three resource allocation problems aiming each to realize one of the following objective performances:

- Temporal fairness where each user is associated with a minimum time fraction assignment. The goal is to optimize the average system performance – the sum of the average throughputs allocated to users – subject to the minimum time fraction requirement for each user.
- Utilitarian fairness where each user is associated with a minimum fraction of the average system performance. The goal is to optimize the average system performance while guaranteeing that each user receives a portion of the overall performance at least equal to its minimum assignment.
- The optimization of the average system performance is again targeted but subject to absolute performance requests for each user (the minimum throughput obtained by each user must be at least equal to a pre-specified value).

Optimal scheduling policies for each of the three optimization problems are given assuming that the channel state process is stationary and ergodic. The proposed policies in [LCS03] are off-line since scheduling decisions are exclusively dependent upon the knowledge of channel statistics and are hence independent of the actual time the decision is made. However, the off-line scheduling policies are coupled with on-line estimation algorithms for the determination of the scheduling parameters.

1.2.2.2.2 Revenue-based Opportunistic Scheduling: In [BW01], a scheduling policy is developed aiming to maximize the minimum normalized average user throughput. A throughput target is associated with each user indicating the user QoS request. The normalized throughput of a user is the ratio of its average throughput to its associated target throughput. Under the assumption of stationary channel state process, it is shown that the objective performance targeted can be optimally attained through reward-based schemes functioning as follows:

Slot t is assigned to a user k , such that,

$$k = \arg \max_i (w_i \cdot R_i(t)),$$

where w_i is the reward of user i . The optimal strategy is proved to be associated with an optimal reward vector w^* . Yet, straight determination of the optimal reward vector

involves complex calculations and knowledge of channel statistics. As an alternative, adaptive algorithms are presented that dynamically regulate the reward vector sequence $w(t)$, based on observed throughput performance and drive the present sequence towards the optimal reward vector w^* .

1.2.2.2.3 The Score-Based opportunistic scheduler: While PF is fair and opportunistic in an ideal environment with homogeneous fading (i.e. all users experience the same fading characteristics), it may be unfair and unable to fully exploit multi-user diversity gains in the presence of heterogeneous channel statistics. The author in [Bon04] proposes an alternative scheduler to PF – termed score-based opportunistic scheduler – that overcomes this shortcoming and operates as follows:

Slot t is assigned to user k , such that,

$$k = \arg \min_i (s_i(t)),$$

where the score $s_i(t)$ corresponds to the rank of the current service rate $R_i(t)$ of flow i among the past values $\{R_i(t), R_i(t-1), \dots, R_i(t-W+1)\}$ observed in a time window of size W . Therefore, the proposed scheduler selects a user with the highest service rate in comparison with its own service rate statistics, contrary to PF which selects a user with the highest service rate in comparison with its observed average throughput. The score-based scheduler behaves like PF in the ideal case and it is shown -via simulations- that in general, its performance does not suffer from the impact of heterogeneous fading.

1.2.2.3 Flow-Level Performance

All that preceded dealt with static scenarios with a fixed number of users and continuously backlogged queues. Indeed, the evaluation of scheduling algorithms is most often performed assuming a static population of users which is necessary but not sufficient since the actual set of active users is dynamic. Besides, users perceive performance at flow level rather than at packet level. Finally, as wireless systems often apply an admission control scheme to prevent overload situations, it is necessary to take into consideration the flow-level dynamics when assessing different admission control policies. Flow-level performance has received little attention so far and was first introduced in [Bor03] where the flow-level dynamics for the PF scheduler have been characterized while assuming homogeneous fading. In that ideal case, all users get access to the channel the same asymptotic fraction of time and so the PF scheduler **fairly** shares resources among users. In [BP03], the authors develop further the previous analytical model to more general scheduling and admission control schemes and apply it to a number of practical issues such as evaluating the cell capacity. They also evaluate the gain in capacity obtained through opportunistic scheduling. In both papers [Bor03, BP03], the assumption of homogeneous fast fading is

necessary to get tractable analytical models. Indeed, this assumption yields models based on processor sharing queues.

1.2.3 Intercell Scheduling

In this section, we describe a rather different and relatively new notion of scheduling that relies on coordination of transmissions among BSs. The key principle is that the perceived channel quality is affected by the degree of interference from adjacent BSs, so that significantly higher SNRs may be seen by users when the power of interfering BSs is lowered or even completely switched off. When the increase in the SNR is sufficiently large, it may prevail over the loss in terms of realized SNR at the BSs whose power is momentarily lowered or turned off, resulting in a substantial overall gain. Indeed, the results in [BBR99, HR98] show that inter-cell scheduling realizes considerable throughput gains. Although inter-cell scheduling is not similar to opportunistic scheduling, the key idea behind the two approaches is related in the sense that coordinating the activity phases of interfering BSs can be seen as means of opportunistic scheduling operated on a network scale and generating favourable channel conditions. In our thesis, we used intercell scheduling to control resources in the cell: the proposed scheduler can choose to alleviate interference suffered by users close to the BS (i.e. good channel state users) to increase overall throughput, as it can choose to do so for users far from the BS (i.e. bad channel state users) to provide utilitarian fairness.

1.3 Radio Propagation and Traffic characteristics

The three basic propagation mechanisms which impact propagation in a mobile communication system are reflection, diffraction and scattering [Rap96]. As mentioned earlier, the propagation models that reflect the impact of these three basic propagation mechanisms are respectively the power-law propagation, the log-normal shadowing and fast multi-path fading. Throughout our thesis, we neglect the impact of slow fading (i.e. shadowing) for simplicity (except in chapter 8 where we consider a realistic environment), restricting our propagation models to power propagation and fast fading. Furthermore, we consider that path-loss remains constant during the time-scales of interest (i.e. mobility is not considered).

Data flows arrive as a Poisson process. This assumption is fairly plausible since traffic is due to the independent activity of a large population of users, each individually having a very small intensity, which can therefore be modelled by a Poisson process. Flow sizes are independent and identically distributed. All simulations, except those obtained in chapter 8 that are run in ns-2, are run in simulators coded in language C.

1.4 Plan of the Thesis

In order to present an exhaustive work on channel-aware scheduling, we explore in our thesis the **two** main trends adopted to devise efficient channel state dependent schedulers: **Wireless Fair Queueing** and the opportunistic **Proportional Fair Scheduler**. We give in chapter 2 the general system model used throughout this work and the **two** wireless network architectures suitable for our devised opportunistic schedulers.

For wireless fair queueing, we propose, in chapter 3, an **Opportunistic** wireless fair queueing scheduler that guarantees fairness according to the GPS model while allocating resources **opportunistically** by using a multi-rate channel model. Similar to opportunistic schedulers, our wireless fair queueing scheduler, termed Opportunistic WFQ, makes use of channel state information to favour packets belonging to flows that are relatively in good channel conditions while emulating the WFQ scheduler. We show how OWFQ notably increases the average system performance through opportunistic scheduling while fulfilling users QoS needs in terms of minimum realized throughput.

The rest of the thesis is built around the most noteworthy opportunistic scheduler in third generation networks: the PF scheduler. We highlight in chapter 4 the assumptions necessary so that the PF scheduler combines fairness with efficiency. We also pinpoint the shortcomings of PF that arise when these unrealistic assumptions are no longer valid. In Chapters 5, 6 and 7, we propose high-performance schedulers based on the PF scheduler that overcome its drawbacks. We propose, in chapter 5, a modified version of PF – termed Weighted Proportional Fair (WPF) – that gives, contrary to PF, flexibility in sharing resources between active users while allocating resources fairly in a realistic environment. Various opportunistic schedulers, in chapter 7, give preferential treatment to short flows while preserving performances of long flows. As mentioned earlier, it has been shown that, assuming the feasible transmission rate is proportional to the SNR, TDMA scheduling maximizes overall throughput. However, for a logarithmic relation between the channel quality and the transmission rate, scheduling one user at a time (e.g. according to PF) does not always result in maximum channel utilization for all users in the cell. For that reason, we put forward, in chapter 6, a new hybrid scheduler that alternates CDMA scheduling and PF scheduling, resulting in increased overall throughput.

Chapter 2

Architectural Context: the 802.16 system and the HDR/HSDPA systems

In this chapter, we describe briefly the two wireless network architectures suitable for our devised channel-aware schedulers. We tackled in our thesis opportunistic scheduling with different fairness criteria: the GPS fairness definition and the proportional fairness definition. Each of these scheduling policies is designed to function properly in an adequate network architecture:

- *Our GPS opportunistic scheduler proposed in chapter 3 is designed for 802.16 systems [Gos05].*
- *Our proportional fair opportunistic schedulers proposed in chapters 5, 6 and 7 are designed for HDR/HSDPA systems [BBG⁺00, LGNJ01].*

The predominance of these systems in nowadays mobile networks underline the relevance of our proposed schemes.

2.1 General System Model

The general system model consists of a BS that transmits data to a number of users (fixed or variable in time) over a shared wireless fading channel. Users share resource in terms of time, frequency and power. We consider exclusively the downlink channel as in general, downlink transmission is more important to data traffic, due to the highly asymmetric nature of data services. The access technique is mainly TDMA, however CDMA is also used. In TDMA access, the BS is aware of users service rates and makes

use of this information to schedule the user whose service will permit attaining the system performance objectives.

2.1.1 The 802.16 system

Service providers are continually striving to develop a global standard enabling them to reach non-serviced areas in a manner that supports infrastructure build outs comparable to cable, DSL, and fibre. For years, the WiFi Wireless LAN technology has been widely used in Broadband Wireless Access (BWA) applications in conjunction with many proprietary based solutions. Unfortunately, it results in limited performance in terms of bandwidth, number of served users and range for outdoor BWA applications. Therefore, while a great fit for indoor Wireless LAN, the WiFi technology is not adapted for outdoor BWA. The IEEE 802.16 standard is a wireless protocol that focuses on the **last mile** applications of wireless technology for broadband access. It offers performance – in terms of robustness and QoS – appropriate for scalable, long range and high capacity **last mile** wireless communications. Contrary to previous Wireless MAN technologies (Local Multipoint Distribution Systems (LMDS), Wireless Local Loop (WLL), Fixed Wireless Point-to-Multipoint (FWPMP) and Multi-channel Multiple Point Distribution Systems (MMDS)), the IEEE 802.16 is developed to guarantee the compatibility and inter-operability of broadband wireless access equipments.

To meet up the needs of different types of access, two versions of the 802.16 standard have been defined. The first version is based on the IEEE 802.16-2004 and is optimized for fixed and nomadic access. The second version is based on the IEEE 802.16e amendment of the standard and is intended to support portability and mobility.

2.1.1.1 The Medium Access Control (MAC)

The 802.16 standard is a Point-to-Multipoint protocol which allows numerous users to access the same radio resources using both multiplexing and queueing. Initially limited to Line-of-Sight (LOS) communications because of the originally available high band frequency (10-66Ghz), the 2-11 GHz amendment project extended the support for None Line-of-Sight (NLOS) communications. The 802.16 system is designed to operate efficiently within the spectrum allocated because of its flexibility and ability to use both TDD (Time Division Duplexing) and FDD (Frequency Division Duplexing). Access and bandwidth allocation algorithms accommodate a large number of end-users. The services required by these end-users cover a wide variety of applications (TDM voice and data, IP and VoIP connectivity) compelling the 802.16 MAC to accommodate both continuous and bursty traffic. Moreover, these diverse services expect to be assigned tailored QoS. The 802.16 standard addresses also the need for very high bit rates for both uplink and

downlink. In fact, it provides MAN connectivity at speeds up to 75 Mbps. The modulation and coding schemes are indicated in a burst profile that may be tuned adaptively for each burst to each user. The request-grant mechanism is devised to be scalable, effective, and self-correcting. Despite the fact that a wide variety of bandwidth allotment and QoS techniques are offered, the fine points of scheduling and reservation management are left unstandardized.

2.1.1.2 The Physical Layer (PHY)

2.1.1.2.1 Common Specification

Generic Framing Structure – PHY specification operates in a framed format. Each frame consists of a downlink subframe and of an uplink subframe. The frame duration may be variable from one PHY specification to another. This frame is divided into physical slots to enable bandwidth allocation and identification of PHY transitions. A physical slot is equivalent to 4 QAM symbols. The downlink subframe starts with information required for frame synchronization and control. In the TDD case, the downlink subframe precedes the uplink subframe. In the FDD case, uplink transmissions occur simultaneously with the downlink frame.

The Downlink Subframe Structure – It begins with a preamble containing DL-MAP and UL-MAP. These specify PHY transitions on the downlink in addition to bandwidth allocations and burst profiles on the uplink. The DL-MAP is always related to the present frame. In both TDD and FDD systems, the UL-MAP provides allocations relative to the next downlink frame. Yet, it can provide allocations starting in the current frame provided that processing times and round-trip delays are observed. After the DL and UL-MAP, the downlink subframe continues with TDM portions and optional TDMA portions. Downlink data is transmitted to each user relying on a negotiated burst profile.

The Uplink Subframe Structure – Unlike the downlink, the UL-MAP allocates bandwidth to precise users. Users emit in their assigned allocations using the burst profile indicated by the Uplink Interval Usage Code (UIUC) in the UL-MAP entry granting them bandwidth. The uplink subframe may also enclose contention-based allocations for initial system access and broadcast or multicast bandwidth requests.

2.1.1.2.2 Specification Variants

10-66 GHz – In this LOS propagation environment, a single-carrier modulation was selected and the corresponding air interface is designated as WirelessMAN-SC. The BS

transmits a TDM signal where particular users are granted time slots serially. Access in the uplink direction is TDMA. The details of scheduling and reservation management are left unstandardized.

2-11 GHz – In this NLOS propagation environment (with significant multipath propagation), three air interface specifications are available:

- WirelessMAN-SC2: with a single-carrier modulation format.
- WirelessMAN-OFDM: with orthogonal frequency-division multiplexing and a 256-point transform. TDMA access is adopted.
- WirelessMAN-OFDMA: with orthogonal frequency-division multiple access and a 2048-point transform. Multiple access is adopted.

2.1.2 The HDR/HSDPA systems

The well-known CDMA 1xEV-DO system relies on the HDR (High Data Rate) standard developed by Qualcomm [BBG⁺00]. HDR is designed to provide an adaptable wireless Internet solution that delivers high data rates [xxE]. The first fundamental design choice of HDR is to separate services by including two interoperable modes: **1x mode** for voice and low-rate data and **1xEV mode** for high-rate data services. In 1xEV mode, a single user is served in a given time slot, thus avoiding power sharing by allocating the entire BS power to the user being served. The main goal is to get rid of intra-cell interference, achieving very high peak rates for users situated in a good coverage area. The BS relies on some sort of feedback information from users to obtain estimates of service rates. In fact, the BS obtains knowledge of users service rates via a mixture of techniques based on channel measurements. In particular, in every slot, the BS transmits a pilot signal on the downlink channel and each user supervises the quality of this signal (i.e. the SNR). Once users estimate their feasible rates based on their perceived SNR, they transmit the corresponding information through Data Rate Control (DRC) signals to the BS over their uplink channels. The slot duration is assumed to be short enough so that user service rates remain constant within one slot. HDR systems offer a maximum data rate of 2.4 Mbit/s over a signal bandwidth of 1.2 MHz, while their 3GPP equivalent HSDPA (High Speed Data Packet Access) systems [LGNJ01] offer a maximum data rate of around 10 Mbit/s over a signal bandwidth of 5 MHz. These systems deliver high spectral efficiency by using the aforementioned TDMA-like strategy and opportunistic scheduling [BBG⁺00, LGNJ01]. The opportunistic standard scheduling adopted in HDR and HSDPA systems is the well-known Proportional Fair (PF) algorithm thoroughly explained in the previous chapter. In addition to opportunistic scheduling, two fundamental technologies that also rely on rapid adaptation of transmission parameters to the instantaneous radio conditions are used to

increase the spectrum efficiency: **Fast Link Adaptation** techniques and **Fast Hybrid Automatic Repeat Request** (HARQ) algorithms.

2.1.2.1 Fast link adaptation

Using Adaptive Modulation and Coding (AMC), the fast link adaptation technique permits providing data rates up to 10 Mbps. It enables the use of spectrally efficient higher order modulation when channel conditions are favourable, and slip back to robust Quaternary Phase Shift Keying (QPSK) modulation when less favourable channel conditions occur. The use of higher order modulation in conjunction with link adaptation permit utilizing optimally the fading radio channel. By transmitting at constant power, the modulation and coding schemes can be chosen so as to maximize the throughput of the downlink channel. Thus link adaptation replaces somehow fast power control. The BS selects the Modulation and Coding Scheme (MCS) that matches the instantaneous radio channel conditions of a given user and eventually its QoS request.

2.1.2.2 Fast HARQ

Fast Hybrid Automatic Repeat Request algorithms rapidly ask for the retransmission of missing information and combine the soft information from the original transmission and any succeeding retransmissions before decoding a message. This technique significantly improves performance and adds robustness against link adaptation errors. It also serves to adjust the effective code rate compensating for the errors made by the link adaptation mechanism. If the information is correctly decoded, an acknowledgment is sent to the BS. Otherwise, retransmission is requested immediately. Once the data has been retransmitted, the user combines the previous versions of information with the present retransmitted version. This soft combining augments the probability of successful decoding. Retransmissions are requested until the information has been decoded correctly or until the maximum predefined number of attempts has been attained.

2.2 Proposed Schedulers and Corresponding Technologies

This work examines two widely used fairness definitions in the literature: the GPS fairness and the proportional fairness. Both of these definitions are applied in the context of opportunistic scheduling. The resulting opportunistic schedulers are suitable for data traffic in new generation networks. The GPS opportunistic scheduler proposed for 802.16 networks can also be adapted for HDR/HSDPA, while the various proportional fair opportunistic schedulers proposed for HDR/HSDPA systems are well adapted for 802.16 networks. Therefore, the given mapping between the devised scheduling algorithms and

existing technologies is not strict. However, contrary to the proportional fair schedulers that are applied on a flow level, the GPS opportunistic scheduler is run on a packet level. Indeed in our GPS scheduler, we take advantage opportunisticly of the channel periodic variation by integrating it in the scheduling scheme on a packet by packet basis. To that aim, the packet duration time must be in the same order of fast fading variations. It is the case when large capacities are provided to flows as in 802.16 networks. Otherwise fragmentation of packets is necessary if the channel is not varying slowly enough so that it remains constant during a packet scheduling time. For that reason, the GPS opportunistic scheduler is best suited for 802.16 systems although it can be tailored for HSDPA/HDR systems via fragmentation of packets.

Chapter 3

Opportunistic Weighted Fair Queueing

In this chapter, we propose a scheduler whose performance objective is to allocate system resources according to the GPS model in a wireless environment. Many existing schedulers satisfying the GPS fairness definition have dealt with the case of error-prone wireless links with a binary on-off channel model. However, our proposed model, termed OWFQ (Opportunistic Weighted Fair Queueing), makes use of a more realistic model with multi-rate channels integrating channel state information into the scheduling scheme. In fact, the WFQ algorithm is modified in such way as to account for channel state when allocating resources to the various connected equipments. Simulation results show the notable gain in terms of mean throughput and delay obtained from our proposed wireless fair queueing scheduler in comparison with WFQ.

3.1 Introduction

In wireline networks, fair queueing has long been a popular paradigm for providing fairness and several algorithms have been proposed for adapting fair queueing to the wireless domain (e.g. [BLN99]). These algorithms make the assumption that the channel capacity is constant and try to make short bursts of channel errors transparent to flows by a dynamic reassignment of channel allocation over small time scales. In this chapter, we follow a different approach: rather than falsely assuming that the shared capacity is constant, we propose to enhance the radio link utilization by allowing the scheduler to make its decisions based on the knowledge of the various terminals channel state. More precisely, we propose a modified version of the WFQ algorithm [PG93] that notably increases the average system performance through opportunistic scheduling while fulfilling users' QoS needs in terms of minimum realized throughput. Our mechanism can enhance the perfor-

mance of existing and future systems, as those based on the 802.16 ([Gos05]) technology. The rest of the chapter is organized as follows. In section 3.2, we present the proposed OWFQ mechanism and in section 3.3, we prove analytically that OWFQ guarantees fairness among competing flows. section 3.4 is devoted to performance comparison between WFQ and OWFQ in a wireless environment impacted by fast fading. We conclude in section 3.5.

3.2 Opportunistic Weighted Fair Queueing

Most scheduling algorithms designed for radio access divide the flows in a simplistic and binary way into two categories: good channel-state flows that can be scheduled and bad channel-state flows that cannot be scheduled and consequently relinquish their bandwidth to the former category. The scheduler keeps track of the excess bandwidth obtained by good-channel state flows in order to restore it to bad channel-state flows. Existing algorithms differ mainly by the compensation process they propose. The main limitation of these policies is that channel condition is modelled as either *good* or *bad* which is too simple to characterize realistic wireless channels. Contrary to existing schemes, our approach profits from the channel fluctuations by way of opportunistic scheduling, seeking to augment overall throughput under user QoS requests. In this section, we present the radio resource model and then introduce our scheduling mechanism.

3.2.1 The Radio Model

We consider a wireless system where the scheduling is performed by a BS serving a multitude of flows in a downlink channel of mean capacity C .

Let x_i be the i.i.d. (independent and identically distributed) random variables (of unit mean) representing the effect of fast fading experienced by flow i , then the channel capacity of this flow at time t is,

$$C_i(t) = C \cdot x_i(t). \quad (3.2.1)$$

As we consider Rayleigh fading, the random variables x_i are exponentially distributed. However, we choose to bound the minimum value taken by x_i to $x_{min} \neq 0$ to obtain a stable system.

Indeed, let S_i be the sojourn time of a packet i of size L_i and let T_i be its service time. We know that $S_i \geq T_i$ and thus,

$$\mathbb{E}[S_i] \geq \mathbb{E}[T_i] = \mathbb{E}\left[\frac{L_i}{C \cdot x_i}\right] = \frac{1}{C} \cdot \mathbb{E}[L_i] \cdot \mathbb{E}\left[\frac{1}{x_i}\right].$$

Since $\mathbb{E}\left[\frac{1}{x_i}\right] = \infty$, the mean service time is also infinite and the system is not stable. Thus,

we replace (3.2.1) by the following,

$$C_i(t) = \max(C \cdot x_i(t), C \cdot x_{min}). \quad (3.2.2)$$

3.2.2 Reminder on Weighted Fair Queueing

WFQ is a packet scheduling technique allowing guaranteed bandwidth services. It is an approximation of the GPS scheduling which allows different flows to have different service shares according to a predefined weight. In a link of capacity C , WFQ guarantees to each flow i of weight r_i , a minimum rate \mathfrak{R}_i given by,

$$\mathfrak{R}_i = C \cdot \frac{r_i}{\sum_j r_j}.$$

The WFQ scheduler assigns a start tag and a finish tag to each arriving packet and serves packets in the increasing order of their finish tags. We denote by p_i^k the k^{th} packet of flow i , by $A(p_i^k)$ its arrival time and by $S(p_i^k)$ and $F(p_i^k)$, respectively, the start and finish tags assigned to p_i^k . The WFQ behaviour is defined by the following equations,

$$S(p_i^k) = \max(V(A(p_i^k)), F(p_i^{k-1})) \quad (3.2.3)$$

$$F(p_i^k) = S(p_i^k) + \frac{L_i^k}{r_i} \quad (3.2.4)$$

where L_i^k is the size of packet p_i^k and $V(t)$ is the virtual time at time t defined by,

$$\frac{dV(t)}{dt} = \frac{C}{\sum_{i \in B(t)} r_i}, \quad (3.2.5)$$

with $B(t)$ being the set of active flows at time t .

3.2.3 Opportunistic WFQ

In order to account for the variability of the channel capacity, we propose a new scheduler, named Opportunistic WFQ, defined as follows,

$$S(p_i^k) = \max(V(A(p_i^k)), S(p_i^{k-1}) + \frac{L_i^{k-1}}{r_i}). \quad (3.2.6)$$

Whenever the BS finishes serving a packet at time TS , in order to schedule the next packet, it computes the finish tag for HOL packets of active flows according to the following equation,

$$F(p_i^k) = S(p_i^k) + \frac{L_i^k}{r_i \cdot x_i(TS)}. \quad (3.2.7)$$

As in WFQ, HOL packets are scheduled in increasing order of their finish tags.

The rationale behind OWFQ is as follows: the better the channel quality experienced by a flow i , the greater the value taken by x_i and the lower the value taken by its finish tag. As a result, its chance to be scheduled will increase. Thus, potential candidates for accessing the channel may be compelled to pass their turn in favour of flows with better channel state which will obviously increase global throughput. Besides, flows that "missed" their turn will not wait "too long" even if they experience persisting bad channel state because we do not change the definition of the start tag and therefore the state of the channel only impacts one of the terms defining the finish tag. Indeed, the start tag is still computed as in the original model and reflects how frequently the present flow is served in respect to its weight. For that reason, the penalized flow will eventually have the smallest finish time among contending flows despite its large virtual service time.

As we consider fast fading, the approach reaches its optimal behaviour when the packet duration time $\frac{L_i}{C_i}$ is in the same or lower order of magnitude of fast fading variations. This is the case when large capacities are provided to flows. Otherwise, fragmentation of packets will enhance performances.

3.3 Fairness Guarantee

Different metrics of fairness can be defined. In this section, we use the weighted fairness concept as defined in [Gol94] and prove that, when using OWFQ, the following quantity $\left| \frac{W_i(t_1, t_2)}{r_i} - \frac{W_j(t_1, t_2)}{r_j} \right|$ is bounded for any interval $[t_1, t_2]$ in which both flows i and j are backlogged, where $W_i(t_1, t_2)$ is the aggregate service (in bits) received by flow i in the interval $[t_1, t_2]$.

The proof is obtained by establishing an upper and lower bound on $W_i(t_1, t_2)$ in Lemmas (3.1) and (3.2) respectively (for clarity, detailed proofs are found respectively in Appendix 3.6.1 and Appendix 3.6.2).

Lemma 3.1. *In an OWFQ server, if flow i is backlogged in the interval $[t_1, t_2]$, then,*

$$W_i(t_1, t_2) \geq r_i \cdot (v_2 - v_1) - L_{max} - \frac{L_{max}}{x_{min}},$$

where $v_1 = V(t_1)$ and $v_2 = V(t_2)$.

We conclude that OWFQ guarantees a minimum throughput for each flow.

Lemma 3.2. *In an OWFQ server, during any interval $[t_1, t_2]$, we have that,*

$$W_i(t_1, t_2) \leq r_i \cdot (v_2 - v_1) + L_{max}.$$

Theorem 3.1. *For any interval $[t_1, t_2]$ in which two flows i and j are backlogged during the entire interval, the difference in the service received is bounded by,*

$$\left| \frac{W_i(t_1, t_2)}{r_i} - \frac{W_j(t_1, t_2)}{r_j} \right| \leq L_{max} \left(\frac{1}{r_i} + \frac{1}{r_j} \right) + \frac{L_{max}}{x_{min}} \cdot \max \left(\frac{1}{r_i}, \frac{1}{r_j} \right).$$

The result is straightforward from Lemmas 1 and 2. We conclude that OWFQ provides fairness guarantees.

3.4 Numerical Experiments

The values chosen in the following numerical analysis are inspired by the properties of 802.16 systems. We consider a wireless channel of mean capacity equal to $C = 10Mbps$ subject to Rayleigh fading. Packet size follows the Bounded Pareto distribution $BP(p, q, \alpha)$ where p and q are respectively the minimum packet size (50 bytes) and maximum packet size (1500 bytes) and α is the exponent of the power law. Its probability density function is,

$$f_{BP}(x) = \frac{\alpha \cdot p^\alpha}{1 - \left(\frac{p}{q}\right)^\alpha} \cdot x^{-\alpha-1}, \quad p \leq x \leq q, 0 \leq \alpha \leq 2.$$

We take $\alpha = 1.16$ and therefore the mean packet size equals 155 bytes.

We consider three independent permanent Poisson processes of intensity $\lambda/3$ with the following weights $r_0 = 0.5$, $r_1 = 0.25$ and $r_2 = 0.1$. The global arrival process is therefore a Poisson process of intensity λ . In order to vary the load in the cell, we vary λ . We take $x_{min} = 0.1$ and we normalize the mean capacity to $C = 1.0$. The buffer capacity of each flow is limited to 10^6 packets. New packets generated when the buffer is full are lost.

We consider two independent models, in the first, flows are served according to the WFQ algorithm and in the second, flows are served according to our Opportunistic WFQ. The total load ρ is defined as the ratio of the total arrival rate, λ , over the average capacity C . We first analyze and compare, for both models, the impact of total load on the obtained mean throughput, the packet loss ratio and the percentage of packets served at the minimum rate for each individual flow. At last, we analyse the impact of total load on delay.

For $\rho \leq 0.2$: We can see in Figure 3.1 that OWFQ does not realize any gain in terms of throughput compared with WFQ which is natural since the probability of having more than one bottleneck flow is negligible and therefore no advantage results from taking into account the radio channel state. Indeed, any scheduling policy based on opportunism will bring no improvement in comparison with a non-opportunistic scheme if there are not at least two active users present in the system when the scheduling decision is made.

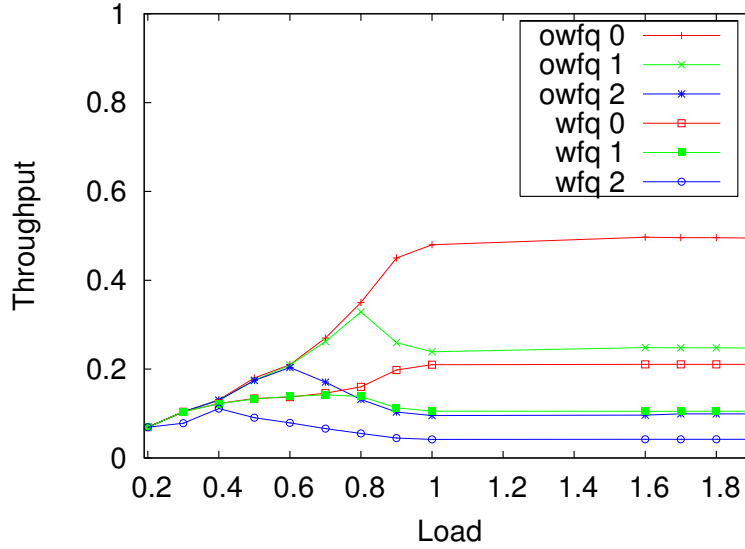


Figure 3.1: Mean throughput per flow as a function of load

For $\rho \leq 0.3$: OWFQ does not realize any gain in terms of throughput for flows 0 and 1 since only flow 2 has bottlenecked packets with non-negligible probability; according to simulation results, the mean number of packets enqueued for flows 0 and 1 is strictly inferior to 2 for this range of the total load. Nevertheless, while the number of packets served at the minimum rate in WFQ remains constant when ρ varies in the cited range (approximately equal to 9.6% of the total number of served packets), the latter decreases in OWFQ as load increases passing from 8% for $\rho = 0.2$ to 6% for $\rho = 0.3$. As for flow 2, the mean number of packets enqueued is around 2 which means that the latter is often active and served simultaneously either with flow 0 or flow 1. As a result, flow 2 realizes a gain in mean throughput of approximately 20%.

For $0.4 \leq \rho \leq 1.0$: The gain obtained from multi-user diversity is tangible: for flow 0, the gain in mean throughput as compared to WFQ varies from 6% for $\rho = 0.4$ to 128% for $\rho = 1.0$. For flow 1, the gain varies from 6% to 127% and for flow 2, the gain varies from 25% to 128%. Moreover, at $\rho = 1.0$, flow 0 and flow 1 lose respectively 30% and 70% of their packets in WFQ due to buffer overflow while no packet losses have been observed during the simulation time in the OWFQ case. Besides, 9.6% of packets are served at C_{min} in WFQ against respectively 4% and 2% in OWFQ. As for flow 2, the number of lost packets, at $\rho = 1.0$, is 85% in WFQ against 55% in OWFQ while the number of packets served at C_{min} is limited to 0.4% in OWFQ (their number remains the same in WFQ for all flows and equals 9.6% whatever the load is). Besides, the differentiation in the service received by flows 0 and 1 appears in OWFQ at $\rho > 0.8$ while it appears earlier in WFQ at $\rho = 0.7$ which highlights the efficient allocation of resources in OWFQ.

For $1.0 < \rho \leq 1.5$: The gain in mean throughput for flow 0 is around 137% while at $\rho = 1.5$, half of packets are lost in WFQ and only 10% in OWFQ. The number of packets served at C_{min} for flow 0 is around 5% in OWFQ. For flow 1, the gain is around 136% and while the number of lost packets is only lowered from 90% to 80% at $\rho = 1.5$, the number of packets served at C_{min} is around 1% in OWFQ. As for flow 2, the gain in throughput is around 129% and although the blocking probabilities are alike in both scenarios, the number of packets served at C_{min} is only 0.1%, at $\rho = 1.5$, in OWFQ. We conclude that, in addition to notably increasing performances in terms of realized throughput, our approach protects flows at much higher rates than in plain WFQ.

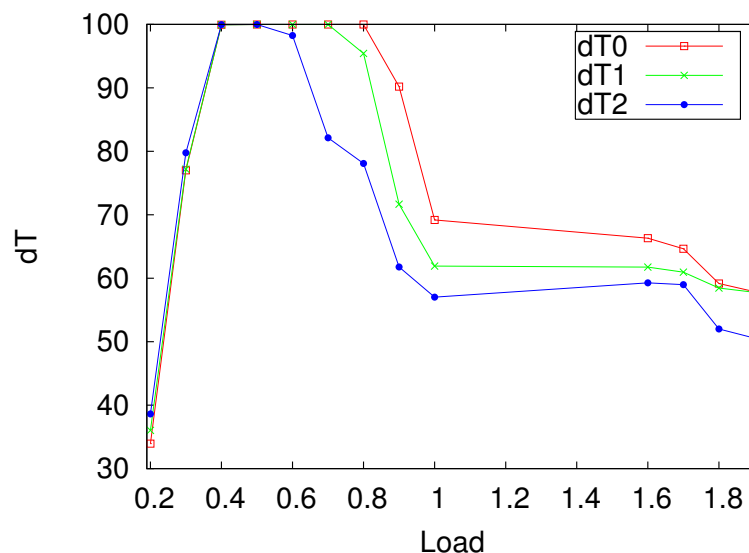


Figure 3.2: dT as a function of load

Mean delay: The last remark allows predicting that Opportunistic WFQ will lead to a reduction in average sojourn times. We analyse now the impact of the total load on the relative deviation dT of the mean sojourn time in the WFQ case, termed T_{WFQ} , from the mean sojourn time in the OWFQ case, termed T_{OWFQ} , which we define as $dT = |T_{WFQ} - T_{OWFQ}| / T_{WFQ} \times 100$. We can see from Figure 3.2 that the Mean Sojourn Time in OWFQ is dramatically reduced as compared to WFQ. Therefore, the gap in the realized mean throughput between OWFQ and WFQ will widen even more in a realistic model based on the TCP protocol where the delay experienced by packets has severe negative repercussions on the overall performances.

Total throughputs: We denote by C_{WFQ} and C_{OWFQ} the total throughput for the

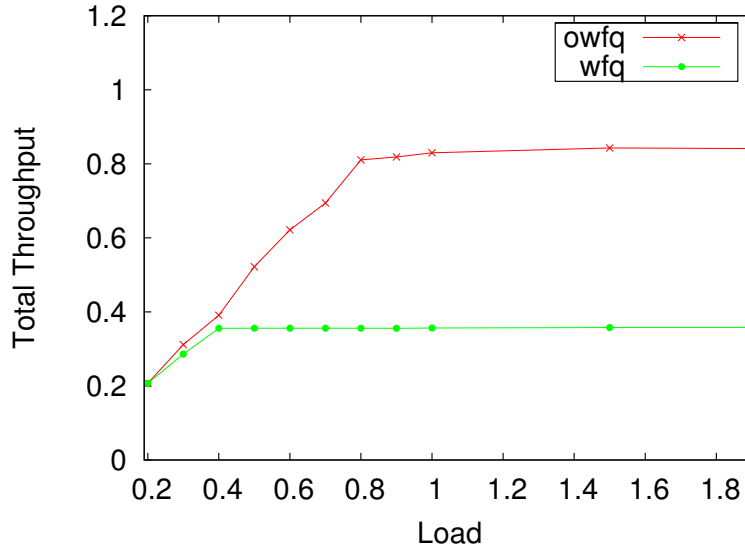


Figure 3.3: Total throughput as a function of load

WFQ and the OWFQ cases respectively. From Figure 3.3, we can see the remarkable gain realized in terms of total throughput in OWFQ in comparison with WFQ. We notice also that C_{WFQ} converges to 0.36. This value is very inferior to the mean capacity given by the following,

$$\mathbb{E}[C(t)] = C \cdot \int_0^\infty \max(x, 0.1) \cdot e^{-x} dx \approx C,$$

which in our experiments is approximately equal to 1.0 (recall that $C = 1.0$). To interpret this result, we observe that our model is equivalent to a model of constant capacity C fed by the same arrival process as in the original model but with packets of length $\frac{L_i}{x_i}$. We thus have the following stability condition,

$$\lambda \cdot \mathbb{E}\left[\frac{L_i}{x_i}\right] \leq C. \quad (3.4.1)$$

From (3.4.1), we have that,

$$\lambda \cdot \mathbb{E}[L_i] \cdot \mathbb{E}\left[\frac{1}{x_i}\right] \leq C \Rightarrow \lambda \cdot \mathbb{E}[L_i] \leq \frac{C}{\mathbb{E}\left[\frac{1}{x_i}\right]}.$$

Hence, the actual mean capacity of the system is,

$$\frac{C}{\mathbb{E}\left[\frac{1}{x_i}\right]} = \frac{C}{\int_0^\infty \frac{1}{\max(x, 0.1)} \cdot e^{-x} dx} \approx 0.36 \cdot C, \quad (3.4.2)$$

which explains the result obtained in WFQ.

OWFQ	Th_1	Th_2	C_{OWFQ}
6	0.3088	0.1544	1.39
10	0.2367	0.1184	1.78
14	0.1798	0.0896	1.89

Table 3.1: Throughput in OWFQ

WFQ	Th_1	Th_2	C_{WFQ}
6	0.0798	0.0398	0.359
10	0.0475	0.0238	0.357
14	0.0342	0.0171	0.359

Table 3.2: Throughput in WFQ

In OWFQ, the behaviour of the system is much more complex so we cannot provide a similar analytical evaluation of the capacity. The gain shown in Figure 3.3 is due to the usage of an opportunistic approach.

Multi-user diversity: To show that the gain obtained increases with the number of users (multi-user diversity), we run three sets of simulations with respectively $n = 6, 10$ and 14 flows at overload. For every value of n , flows are divided into two categories with equal number of flows ($\frac{n}{2}$). All flows of a given category have the same weight and the weight of flows of the first category is twice the weight of flows of the second category. We compute the total throughput C_{WFQ} and C_{OWFQ} for both schedulers – given by $(Th_1 + Th_2) \cdot \frac{n}{2}$ – where Th_1 and Th_2 denote, respectively, the average rate of flows in the first and second category. Results are given for OWFQ and WFQ respectively in Tables 3.1 and 3.2.

First, we notice that C_{OWFQ} increases significantly with the number of flows. We also observe that C_{WFQ} is approximately equal to 0.36 for all values of n , which was expected from formula (3.4.2). To estimate the gain obtained in terms of realized total throughput, we compute the relative deviation of C_{OWFQ} from C_{WFQ} by applying the following formula $G_n = |C_{WFQ} - C_{OWFQ}| / C_{WFQ}$. We get the subsequent results $G_6 \approx 2.87$, $G_{10} \approx 3.99$ and $G_{14} \approx 4.26$. Hence, we can see that the achieved gain is significant and that it increases with the number of served flows, which means that our scheduler takes advantage of flows diversity. Moreover, we see that for both schedulers, we have $Th_1 \approx 2 \cdot Th_2$ and thus, the differentiation in the realized throughputs is achieved.

3.5 Concluding Remarks

Emerging packet cellular networks seeks to support diverse data applications with sustained QoS requirement over dynamic and shared wireless channel. While fair queueing

has long been a popular paradigm for guaranteeing minimum throughput for users over a shared wireline link, these algorithms can not be applied directly to the wireless domain because of the dynamic nature of the wireless channel. In this chapter, we present a modified version of WFQ that couples opportunistic scheduling to fair queueing to enhance overall performances. Unlike existing approaches that assume that the wireless channel is constant and strives to hide its variations from competing flows, our proposed model take advantage from these channel variations to enhance performances. We proved analytically that our Opportunistic WFQ guarantees fairness among users and we showed through simulations that our solution provides significantly better performances than the WFQ approach.

We did not handle the case where a scheduled user cannot actually emit because it suffers from very bad channel conditions in our OWFQ as we supposed that the channel capacity is limited to a minimal value strictly greater than zero, at which the user is able to communicate with the BS. This issue is complementary to our proposed scheduler and is not at all essential to assess its performances, especially that the same radio channel model was used to compare OWFQ and WFQ. However, an exhaustive system model is desirable. As already mentioned, existing wireless fair queueing schemes propose a compensation mechanism that swaps opportunities to access the channel between users that cannot emit and users that can, when they are designated by the scheduler. One of these existing compensation models present in the literature can simply be added to our OWFQ scheduler to deal with the case where certain flows are blocked due to very bad channel quality. More importantly, we intend also to investigate the interactions of our scheduler with the dynamics of TCP.

3.6 Appendix

3.6.1 Proof of Lemma 1:

If $r_i \cdot (v_2 - v_1) - L_{max} - \frac{L_{max}}{x_{min}} \leq 0$, Lemma 1 holds trivially since $W_i(t_1, t_2) \geq 0$. Hence, we consider the case where:

$$v_2 > v_1 + \frac{L_{max}}{r_i} + \frac{L_{max}}{r_i \cdot x_{min}} \quad (3.6.1)$$

Let packet p_i^k be the first packet of flow i to receive service in (v_1, v_2) . To observe that such a packet exists, we consider the following two cases:

- Packet p_i^n such that $S(p_i^n) < v_1$ and $S(p_i^n) + \frac{L_i^n}{r_i} > v_1$ exists: since flow i is backlogged in $[t_1, t_2]$, we conclude that $V(A(p_i^{n+1})) \leq v_1$. From (3.2.6), we get $S(p_i^{n+1}) = S(p_i^n) + \frac{L_i^n}{r_i}$. Using the fact that $S(p_i^n) < v_1$, we get that $S(p_i^{n+1}) < v_1 + \frac{L_{max}}{r_i}$. Also,

using (3.6.1), we deduce:

$$S(p_i^{n+1}) < v_2 \quad (3.6.2)$$

Since $S(p_i^{n+1}) = S(p_i^n) + \frac{L_i^n}{r_i} > v_1$, using (3.6.2), we conclude that $S(p_i^{n+1}) \in (v_1, v_2)$.

- Packet p_i^n such that $S(p_i^n) = v_1$ exists: p_i^n may finish service at time $t < t_1$ or $t \geq t_1$. In either case, since flow i is backlogged in $[t_1, t_2]$, we conclude that $V(A(p_i^n)) \leq v_1$. Hence $S(p_i^{n+1}) = S(p_i^n) + \frac{L_i^n}{r_i}$. Using the fact that $S(p_i^{n+1}) < S(p_i^n) + \frac{L_{max}}{r_i}$ and $S(p_i^n) = v_1$, we get from (3.6.1) that $S(p_i^{n+1}) < v_1 + \frac{L_{max}}{r_i} < v_2$. Since $S(p_i^{n+1}) = v_1 + \frac{L_i^n}{r_i} > v_1$, we conclude that $S(p_i^{n+1}) \in (v_1, v_2)$.

Since either of the two cases always holds, we conclude that packet p_i^k such that $S(p_i^k) \in (v_1, v_2)$ exists. Furthermore, we have the additional following result:

$$S(p_i^k) < v_1 + \frac{L_{max}}{r_i} \quad (3.6.3)$$

Let p_i^{k+m} be the last packet to receive service in the virtual time interval (v_1, v_2) . Thus, $F(p_i^{k+m+1}) \geq v_2$. From (3.2.6) and (3.2.7), we know that at time TS :

$$F(p_i^{k+m+1}) = S(p_i^{k+m}) + \frac{L_i^{k+m}}{r_i} + \frac{L_i^{k+m+1}}{r_i \cdot x_i(TS)} \quad (3.6.4)$$

We deduce the following result:

$$S(p_i^{k+m}) \geq v_2 - \frac{L_i^{k+m}}{r_i} - \frac{L_{max}}{r_i \cdot x_{min}} \quad (3.6.5)$$

Using the tagging scheme in Section 3.2.2, we can derive the following:

$$S(p_i^{k+m}) = S(p_i^k) + \sum_{j=0}^{m-1} \frac{L_i^{k+j}}{r_i} \quad (3.6.6)$$

Thus, from (3.6.5) and (3.6.6), we get that:

$$S(p_i^k) + \sum_{j=0}^m \frac{L_i^{k+j}}{r_i} \geq v_2 - \frac{L_{max}}{r_i \cdot x_{min}} \quad (3.6.7)$$

From (3.6.3) and (3.6.7), we get the following result:

$$\sum_{j=0}^m \frac{L_i^{k+j}}{r_i} \geq (v_2 - v_1) - \frac{L_{max}}{r_i} - \frac{L_{max}}{r_i \cdot x_{min}}$$

Since $W_i(t_1, t_2) \geq \sum_{j=0}^m L_i^{k+j}$, Lemma 1 follows.

3.6.2 Proof of Lemma 2:

The set of flow i packets during time interval $[t_1, t_2]$ have start tags at least v_1 and at most v_2 . This set can be partitioned in two subsets:

- Set D consisting of packets that have start tags at least v_1 and strictly inferior to v_2 . Formally, $D = \{k | v_1 \leq S(p_i^k) < v_2 \wedge F(p_i^k) \leq v_2\}$. For packets in D, using (3.2.6) and (3.2.7), we get $\sum_{k \in D} l_i^k \leq r_i \cdot (v_2 - v_1)$.
- Set E consisting of packets that have start tags equal to v_2 and finish tags strictly greater than v_2 . It is obvious that at most one packet belongs to this set, because

$$S(p_i^k) = v_2 \Rightarrow S(p_i^{k+1}) = S(p_i^k) + \frac{L_i^{k+1}}{r_i} > v_2$$

Hence $\sum_{k \in E} l_i^k \leq l_{max}$.

We conclude that Lemma 2 holds.

Chapter 4

The PF scheduler: False assumptions and Drawbacks

The PF algorithm provides a good compromise between fairness and efficiency. Nevertheless, the hypotheses according to which its good performances are obtained are not valid in real environments. We show in this chapter that PF results in suboptimal performances in a real environment where realistic assumptions are adopted.

4.1 Introduction

Scheduling is a viable option in the provisioning of data services. Thanks to the delay tolerance of data traffic, there exists a freedom in adapting the transmission attempts to the channel quality of users. In this chapter, we study thoroughly the most adopted opportunistic scheduler in novel wireless networks: the PF scheduler [CBHT02, Tse, Hol01, Hol00, Kus04, TG03]. The PF scheduler is widely deployed in new wireless systems because it strikes a good balance between fairness and efficiency. However, while fair and indeed opportunistic in the ideal case, we show that the PF scheduler is unfair and unable to fully exploit multi-user diversity in a realistic environment. The performance of the classical PF scheduler is evaluated in the ideal case and some hints on its performance are given in more realistic cases. In this chapter, we stress on the drawbacks of PF as we will propose in the rest of the thesis schedulers that will overcome these shortcomings.

4.2 PF in an Ideal Environment

The PF scheduler transmits to the user with the highest data rate relative to its present realized mean data rate in order to conjugate fairness and efficiency. To be more precise, under **three** main assumptions, all users in the PF algorithm get access to the channel

the same asymptotical fraction of time and get the same average power ¹ independently of their distance to the BS. The system acts then like a Multi-class Processor Sharing queue ² [Coh78] distributing slots fairly among users while still taking advantage of instantaneous channel variations.

Next, we give the static analytical model for the PF scheduler in an ideal environment. We mean by *ideal environment*, an environment where the aforementioned three assumptions are adopted. We begin by presenting such an environment by giving its corresponding radio resource model, along with the adopted assumptions necessary so that the PF algorithm results in optimal performances. The presented radio model will be used in the remaining part of the thesis, however, it will be more or less altered throughout the chapters to account for more realistic assumptions.

4.2.1 The Radio Resource

4.2.1.1 The Propagation Model

The power received by a given user depends on the radio channel state and varies with time due to user mobility and fading effects. In our model, the mobility will not be included. Let P be the transmission power emitted by the BS, γ_k the free space path loss and x_k the fast fading (of unit mean) for user k . The power received by a user k situated at a distance r_k from the BS, at time t , is then given by,

$$P_k(r_k, t) = P \cdot \gamma_k(r_k) \cdot x_k(t). \quad (4.2.1)$$

The adopted model for the free space path loss is the following,

$$\gamma_k = 1 \quad \text{if } r_k \leq \epsilon \quad \text{and} \quad \gamma_k = \left(\frac{\epsilon}{r_k}\right)^\beta \quad \text{otherwise}, \quad (4.2.2)$$

where β is the path loss exponent (taking values between 2 and 5) and ϵ is the maximum distance at which the full power P is received.

We compute next the feasible rate of each user ensuing from the presented radio resource model.

¹The transmission power of the BS is equally time-shared between active users.

²Multi-class Processor Sharing discipline is Processor Sharing (PS) discipline where the rate at which users are served is an arbitrary positive function of the number of users.

4.2.1.2 The Feasible Rate

For user k , the Signal-to-Noise Ratio and Energy-per-bit to Noise Density Ratio [Vit95] are respectively equal to,

$$SNR_k = \frac{P_k}{(\eta + I_k)}, \quad \frac{E_b}{N_0} = \frac{W}{R_k} \cdot SNR_k, \quad (4.2.3)$$

where R_k is the feasible rate of user k , W the cell bandwidth, η the background noise and I_k the interference due to other BSs (intercell interference).

For a given target error probability, $\frac{E_b}{N_0}$ must be greater than a given threshold σ_k . Assuming the equality, the feasible data rate of a user k is then,

$$R_k = \frac{W}{\sigma_k} \cdot SNR_k. \quad (4.2.4)$$

Using (4.2.1), (4.2.1.2) and (4.2.4), we have the following,

$$R_k(r_k, t) = C_k(r) \cdot x_k(t), \quad (4.2.5)$$

where $C_k(r)$ is the mean rate of user k and is given by the following,

$$C_k(r) = \frac{W}{\sigma_k} \cdot \frac{P \cdot \gamma_k(r_k)}{(\eta + I_k)}. \quad (4.2.6)$$

To obtain the value of intercell interference I_k endured by user k situated at a distance r_k from the BS, we consider hexagonal networks where the interference suffered by a user in a given cell is almost utterly generated by the 6 neighbouring BSs. This assumption is fairly valid in an urban environment where the path loss is at least equal to 4 because interference generated by farther cells is negligible. \Re being the cell ray, an approximation of this interference is given by [BP03],

$$I_k(r_k) = P \cdot [\gamma(2\Re - r_k) + 2 \cdot \gamma(\sqrt{(\Re - r_k)^2 + 3\Re^2}) + \gamma(2\Re + r_k) + 2 \cdot \gamma(\sqrt{(\Re + r_k)^2 + 3\Re^2})]. \quad (4.2.7)$$

4.2.2 The Three Assumptions

The **three** assumptions required in order for PF to achieve optimal performances are the following:

1. *Assumption 1*: The distribution x_k representing the fading effects must be homogeneous and independent among users.
2. *Assumption 2*: Either the instantaneous rate R_k must scale linearly with the instantaneous signal-to-noise ratio SNR_k or all users must have the same average

signal-to-noise ratio.

3. *Assumption 3*: Any served flow must last long enough so that the PF algorithm attains its equilibrium state for this flow.

The first two assumptions (adopted in the ideal radio model presented in the preceding section 4.2.1) are necessary so that the relative rate fluctuations of users are i.i.d. leading to a PS (Processor Sharing) system [Coh78]. The last assumption is necessary to obtain convergence of the PF algorithm because when the served flow only lasts a few time slots, the algorithm does not have time to converge and results in bad performances.

4.2.3 The PF Algorithm

PF is thoroughly studied in [Kus04] in the case of homogeneous fading. We start by presenting some results from the cited paper that we use in our analysis:

At time slot t , PF schedules the user with the highest feasible rate relative to its current average throughput,

$$k^* = \arg \max_k \left[\frac{R_k(t)}{T_k(t)} \right], \quad (4.2.8)$$

where $R_k(t)$ is given by (4.2.5) and $T_k(t)$ is the exponentially smoothed throughput given by (1.2.4) in chapter 1. In (1.2.4), τ captures the time-scales of the PF scheduler, its value is chosen to balance the need of estimating throughput (requiring a large value of τ) with the ability to track channel characteristics (requiring a smaller value of τ).

Since we assume that fading is homogeneous, the random variables x_k representing the fading are i.i.d.. As a result and with the assumption that served flows are long enough (Assumption 3), we have that $T_k(t) = C_k \cdot U_k(t)$, where U_k are identically distributed random variables (but not independent). Furthermore, if $\frac{1}{\tau} \rightarrow 0$, then $U_1, \dots, U_n \approx V$, for some constant V , where n is the total number of active users. Thus, we have that $T_k(t) \approx C_k \cdot V$. More specifically, according to [Kus04], V is approximately equal to $\frac{g(n)}{n}$, with $g(n) = \mathbb{E}[\max(x_1, \dots, x_n)]$. Hence, the exponentially smoothed throughput is given by,

$$T_k \rightarrow C_k \cdot \frac{g(n)}{n}. \quad (4.2.9)$$

In practice, τ has large values as this offers the opportunity of waiting a long time before scheduling a user when its channel quality is maximal: the scheduler is then expected to better exploit multi-user diversity. Hence, we adopt formula (4.2.9) whenever PF services flows that are not too short in an environment with homogeneous fading. We refer to [Kus04] for rigorous justifications of the above claims.

We deduce from what preceded that, at time slot t , the scheduler picks user k such that,

$$\begin{aligned}\frac{R_k}{T_k} &= \max_{l=1..n} \frac{R_l}{T_l} \\ \frac{C_k \cdot x_k}{C_k \cdot V} &= \max_{l=1..n} \frac{C_l \cdot x_l}{C_l \cdot V} \\ x_k &= \max_{l=1..n} x_l\end{aligned}\tag{4.2.10}$$

4.2.3.1 Fairness

Assuming that the random variables x_k are i.i.d., the probability that a given user k is picked by the scheduler is,

$$P = \mathbb{P}(x_k = \max(x_1, \dots, x_n)) = \frac{1}{n},\tag{4.2.11}$$

with n being the number of active users. We deduce that all users have the same probability to access the channel when PF is run in an ideal environment and hence PF behaves like a PS system.

4.2.3.2 Efficiency

To evaluate the efficiency of PF in an ideal environment, we will compute the average feasible rate of a given user k , denoted by χ_k , served according to the PF algorithm,

$$\begin{aligned}\chi_k &= \mathbb{E}[R_k \cdot \mathbf{1}\{\frac{R_k}{T_k} = \max_{l=1..n} \frac{R_l}{T_l}\}] \\ &= C_k \cdot \mathbb{E}[x_k \cdot \mathbf{1}\{x_k = \max_{l=1..n} x_l\}] \\ &= C_k \cdot \mathbb{E}[x_k | x_k = \max_{l=1..n} x_l] \cdot \mathbb{P}\{x_k = \max_{l=1..n} x_l\} \\ &= \frac{C_k}{n} \cdot \mathbb{E}[\max(x_1, \dots, x_n)]\end{aligned}\tag{4.2.12}$$

We compute the ratio, denoted by $G(n)$, of what the user receives in PF as compared to a blind RR (Round Robin) scheduling and obtain $G(n) = \mathbb{E}[\max(x_1, \dots, x_n)]$. For Rayleigh fading, the random variable x_k are exponentially distributed and therefore $G(n) = \sum_{i=1}^n \frac{1}{i}$ [Bon04]. As $G(n) > 1$ when $n > 1$, we deduce that the PF scheduler combines fairness and efficiency.

4.3 PF in a Real Environment

Unfortunately, in practice, the three assumptions necessary so that PF is fair and efficient are not valid:

1. **First**, users do not experience the same type of fading which is a very complex phenomenon ensuing from the interaction of the propagation environment and therefore varies widely across users. As a result, while the random variables representing the fading effects are independent among users, they are not identically distributed. The principal impact of this lack of homogeneity is an unfair distribution of slots amid active users: users with the most variable distributions – typically those who are the furthest away from the BS – receive the least amount of slots [Hol01].
2. **Second**, the linearity between the feasible rate and the SNR is too optimistic except for users with low SNR (again, typically for users far from the BS) and users are unlikely to have the same mean SNR. Note that for a logarithmic relation between the channel quality and the transmission rate R_k (which is more realistic than the linear relation) where $R_k = W \cdot \log(1 + SNR_k \cdot x_k)$, we cannot obtain a relation of the form $x_k = \max_{l=1..n} x_l$ from (4.2.10), necessary to obtain a PS system.
3. **Third**, while PF behaves well for long-lived flows, it underperforms when it comes to serving short-lived flows. This is critical since, as it has been shown by various Internet traffic analyses [CB97], short flows represent the large majority of elastic traffic.

4.4 Concluding Remarks

In this chapter, we pointed out the weaknesses of PF in a realistic environment. PF fails to be fair and efficient when the assumptions according to which it behaves like a PS system are no longer valid. Each missing assumption incurs a specific deficiency in the performances of PF and for which we proposed a solution. Hence, three sets of schedulers based on the PF model are developed to prevail over the three shortcomings of PF. The three proposed opportunistic schedulers are respectively presented in the three following chapters 5, 6 and 7 and the exact performance of PF in the absence of the above cited assumptions is also given.

Chapter 5

The Weighted Proportional Fair Scheduler

In this chapter, we address and solve one of the main shortcomings of the Classical PF scheduler, i.e. its inability to share resources fairly between active users when the latter suffer from heterogeneous fading. We will propose an alternative scheduler, based on PF, that allows for a fair allocation of resources in realistic environments. More importantly, our proposed scheduler gives the system total freedom to choose between temporal fairness, utilitarian fairness and efficiency, contrary to PF which is a rigid scheduler that does not offer any flexibility in the allotment of resources.

5.1 Introduction

In HDR/HSDPA systems, opportunistic schedulers reap the benefits of multi-user diversity over short time-scales and determine how resources are allocated over longer time-scales. As already mentioned, in a wireless environment, a scheduler has usually two contradictory targets: maximizing the overall throughput and guaranteeing fairness:

- The MaxRate approach [Hol01], where the scheduler transmits at a given time slot to the user with the highest available data rate, increases the system throughput but starves users with low SNRs (typically situated far from the BS): very high **efficiency** is obtained at the expense of **fairness**.
- The Round Robin (RR) scheduler guarantees perfect **fairness** while sacrificing overall throughput: perfect **fairness** is obtained at the expense of **efficiency**.
- The well-know PF scheduler transmits to the user with the highest data rate relative to its present realized mean data rate, conjugating **fairness** and **efficiency**.

Yet, despite the attractive properties of PF, the latter is unable to control the allocation of system resources and provides only a restricted fairness. Indeed, PF is a rigid and non-adaptable scheduler as it falls short from enabling the system to define which trade-off between efficiency and fairness is targeted. Moreover, in a homogeneous environment, PF has only a *fair power* sharing but can still be considered as *unfair* as the throughput perceived by users decreases with distance. More importantly, this restricted fairness is not fulfilled with heterogeneous fading. Hence, in a realistic environment and under PF scheduling, users with the most variable channel conditions receive the least amount of slots [Hol01].

To cope with these drawbacks, we suggest in this chapter an alternative to the policy of PF, termed Weighted PF (WPF), which is a hierarchical scheduler that allows to fully control the trade-off between fairness and efficiency. To introduce the required control, we define different classes of users. At its first hierarchical level, WPF distributes the slots between the defined classes in a **Weighted** Round Robin (WRR) fashion. At its second level, users inside each class are served by means of PF, the PF scheduler taking independent decisions inside each class. We define user classes in such a way that, on the one hand, users belonging to a given class have comparable SNRs (served according to PF, they will obtain comparable feasible rates) and, on the other hand, fading is homogeneous inside each class; thus, applying PF to a given class induces a strict fairness in accessing resources for users belonging to that class. We stress on the fact that it is not possible to reach this target when applying PF to the whole cell due to heterogeneous fading. By doing so, not only will we control the resource allocation but also obtain in a real environment the behaviour that PF provides only in an idealistic environment.

The rest of the chapter is organized as follows. In section 5.2, we present the cell partitioning. In section 5.3, we analyze the performances of the WPF scheduler; in particular, we obtain analytical results for the mean rate for a fixed number of users for PF and WPF in an environment with heterogeneous fading. In section 5.4, we present an analytical study for WPF under dynamic traffic conditions. In section 5.5, we use the proposed segmentation of the cell in order to control resources through intercell scheduling. In section 5.6, we suggest to serve the nearest users in a CDMA fashion and justify how this solution will improve performances. We conclude in section 5.7.

5.2 The Cell Partitioning

To obtain different classes of users with comparable SNRs, we divide the cell into different geographical zones; each Zone z corresponding to the set of users whose distance to the

BS ranges from a minimal value r_z to a maximal value r_{z+1} . We decided to segment the cell in only three zones ($z = 0, 1, 2$) since increasing the number of zones limits the number of users per zone and therefore reduces the gain resulting from multi-user diversity. Consequently, users in Zone 0 are those whose distance to the BS ranges between $r_0 = 0$ and r_1 , users in Zone 1 are those located between r_1 and r_2 , while users in Zone 2 are those located between r_2 and $r_3 = \mathfrak{R}$, where \mathfrak{R} is the ray of the cell. To justify our choice of the values taken by r_1 , r_2 and r_3 , we give next the radio model we use.

5.2.1 The Radio Model

The radio model used in this chapter is mainly that introduced in section 4.2.1 of chapter 4: subsection 4.2.1.1 – entitled *The Radio Model* – remains the same; however, subsection 4.2.1.2 – entitled *The Feasible Rate* – is altered as some refinements are added to the proposed model.

5.2.1.1 The Feasible Rate

In the vast majority of references, σ_k – in formula (4.2.4) of chapter 4 – is taken as a constant in order to preserve the linearity between the feasible rate R_k and the Signal-to-Noise Ratio SNR_k of user k . However, this assumption is not valid when different types of modulation are used which is the case for HDR and HSDPA systems. Thus σ_k will vary with the feasible rate and hence with the distance from the BS. Therefore, we improve the existant models by considering in our model different values of σ_k per zone (σ_k is then replaced by σ_z in R_k , for $z = 0, 1, 2$). In practice, the way we define the zones induces that inside Zone 0 and Zone 2, σ_k is indeed constant and equals 6.5dB and 2.5dB respectively [BBG⁺00]. For Zone 1, we define σ_1 as the mean value of σ_k in this zone. The feasible rate of user k in Zone z is then,

$$R_{k,z} = \frac{W}{\sigma_z} \cdot SNR_k. \quad (5.2.1)$$

We denote by C_0 the maximum peak rate offered by the used coder and by r^* the maximum distance at which this peak rate is achieved in the absence of fading, i.e.,

$$r \leq r^* \Leftrightarrow R = C_0.$$

We suppose that the interference I_k is constant inside each zone (it increases with the zone index). Hence, I_k will be replaced by I_z . Using (4.2.3) of chapter 4, (5.2.1) and knowing that C_0 is the maximum peak rate that can be attained, we have the following,

$$R_{k,z}(r, t) = \min \left[C_0, \frac{W}{\sigma_z} \cdot \frac{P \cdot \gamma_k(r) \cdot x_k(t)}{(\eta + I_z)} \right]. \quad (5.2.2)$$

Assuming that C_0 can be achieved, i.e. $r^* \geq \epsilon$, we get from the path loss model in (4.2.2) the following,

$$C_0 = \frac{W \cdot P}{\sigma_0 \cdot (\eta + I_0)} \cdot \left(\frac{\epsilon}{r^*}\right)^\beta. \quad (5.2.3)$$

Using (5.2.2) and (5.2.3), the feasible rate of a user k in Zone z is therefore given by,

$$R_{k,\mathbf{z}}(r, t) = C_0 \cdot \min\left[\left(\frac{r^*}{r}\right)^\beta \cdot x_k(t) \cdot K_z, 1\right], \quad (5.2.4)$$

with $K_z = \frac{\sigma_0}{\sigma_z} \cdot \left(\frac{\eta + I_0}{\eta + I_z}\right)$.

The average feasible rate of a user k in Zone z , denoted by $C_{k,\mathbf{z}}$, is then,

$$C_{k,\mathbf{z}}(r) = C_0 \cdot \mathbb{E}[\min\left[\left(\frac{r^*}{r}\right)^\beta \cdot x_k(t) \cdot K_z, 1\right]]. \quad (5.2.5)$$

5.2.2 Delimiting the Cell into Zones

As mentioned earlier, PF falls short from realizing perfect temporal fairness in a realistic environment where users experience heterogeneous fading and where the feasible rate does not scale linearly with the SNR. In other words, when *Assumption 1* and *Assumption 2* cited in chapter 4 are no longer valid. Therefore, our target is to define the previously introduced zones in such a way that these two assumptions become fairly valid inside each zone. For that reason, we will follow the approach taken in [BP03] as it serves well our purposes (although the reasons why the zones were introduced in the cited paper are completely different). We take a path loss exponent $\beta=4$ as we consider urban environments. The random variables x_k are exponentially distributed (with unit mean) as we consider Rayleigh fading.

Zones are defined as follows:

5.2.2.0.1 Zone 0: Users in this zone are those who get the maximum peak rate C_0 with probability equal to 0.95. Hence, from (5.2.4), r_1 is given by,

$$\begin{aligned} \mathbb{P}(R_{k,\mathbf{0}}(r_1, t) = C_0) &= 0.95 \Rightarrow \\ \mathbb{P}\left(\left(\frac{r^*}{r_1}\right)^4 \cdot x_k \cdot K_0 > 1\right) &= 0.95 \Rightarrow \\ e^{-\left(\frac{r_1}{r^*}\right)^4} &= 0.95 \Rightarrow r_1 = (-\ln(0.95))^{1/4} r^* \end{aligned}$$

The mean rate of a user k in Zone 0 is then $C_{k,\mathbf{0}}(r) \approx C_0$. We notice that there will be no gain resulting from the variation of the radio channel for users in Zone 0.

5.2.2.0.2 Zone 2: Users in this zone are those who do not get C_0 with probability equal to 0.95. Hence, from (5.2.4), r_2 is given by,

$$\begin{aligned}\mathbb{P}(R_{k,2}(r_2, t) \neq C_0) &= 0.95 \Rightarrow \\ \mathbb{P}\left(\left(\frac{r^*}{r_2}\right)^4 \cdot x_k \cdot K_2 < 1\right) &= 0.95 \Rightarrow \\ e^{-\left(\frac{r_2}{r^*}\right)^4 \cdot \frac{1}{K_2}} &= 0.05 \Rightarrow r_2 = (-\ln(0.05)K_2)^{1/4} r^*\end{aligned}$$

To obtain the value of r_2 , we need to determine the value of K_2 . For that, we need to evaluate the interference I_2 suffered by users in Zone 2. As mentioned earlier, the interference in a given zone is supposed to be constant, in particular, we consider the worse case where it is equal to the interference endured at the border of the zone. Hence, the interference in Zone z , namely I_z , is equal to $I(r_{z+1})$ given by (4.2.7) in chapter 4. We compute the following two relations (we take $r_3 = \mathfrak{R} = 2 \cdot r^*$ as larger values of \mathfrak{R} induce very small rates at the border of the cell):

- If $\eta \ll I \Rightarrow \frac{\eta+I_0}{\eta+I_2} \rightarrow \frac{I_0}{I_2} \approx \frac{I(r_1)}{I(\mathfrak{R})} \approx 0.31$.
- If $\eta \gg I \Rightarrow \frac{\eta+I_0}{\eta+I_2} \rightarrow 1$.

Due to the fact that $\frac{\eta+I_0}{\eta+I_2}$ is an increasing function in η , we have that $0.31 \leq \frac{\eta+I_0}{\eta+I_2} \leq 1$. Knowing that $\frac{\sigma_0}{\sigma_2} \approx 2.51$ [BBG⁺00], we deduce that $0.78 \leq K_2 \leq 2.51$.

The mean rate of a user k in Zone 2 is then $C_{k,2}(r) \approx C_0 \left(\frac{r^*}{r}\right)^4 K_2$ and the distribution of the feasible rates is approximately that of $C_{k,2}(r) \cdot x_k(t)$.

5.2.2.0.3 Zone 1: Users in this zone are consequently those who get their maximum peak rate C_0 with non-negligible probability. We assume that, for this intermediate zone, the distribution of the feasible rate is approximately the same for all users,

$$x'_k(t) \cdot C_{k,1} = \int_{r_1}^{r_2} C_0 \cdot \min\left[\left(\frac{r^*}{r}\right)^4 \cdot x_k(t) \cdot K_1, 1\right] \cdot \frac{2rdr}{r_2^2 - r_1^2}, \quad (5.2.6)$$

with x'_k being the unit mean random variable representing the variations, due to fading, around the mean rate $C_{k,1}$ of user k in Zone 1. This approximation is made in order to obtain homogeneous fading in this zone.

From (5.2.6), we get the following,

$$C_1 = \int_{r_1}^{r_2} \mathbb{E}[\min\left[\left(\frac{r^*}{r}\right)^4 K_1 \cdot x_k(t), 1\right]] \cdot \frac{2rdr}{r_2^2 - r_1^2}, \quad (5.2.7)$$

with $\mathbb{E}[\min\left[\left(\frac{r^*}{r}\right)^4 K_1 \cdot x_k(t), 1\right]] = \frac{1 - e^{-\left(\frac{r}{r^*}\right)^4 \frac{1}{K_1}}}{\left(\frac{r}{r^*}\right)^4 \frac{1}{K_1}}$.

To compute K_1 , we proceed as for Zone 2. We take $K_2 = 1.7$ and thus $r_2 \approx 1.5 \cdot r^*$. We compute the following two relations:

- If $\eta \ll I \Rightarrow \frac{\eta+I_0}{\eta+I_1} \rightarrow \frac{I_0}{I_1} \approx \frac{I(r_1)}{I(r_2)} \approx 0.71$.
- If $\eta \gg I \Rightarrow \frac{\eta+I_0}{\eta+I_1} \rightarrow 1$.

Knowing that $\frac{\eta+I_0}{\eta+I_1}$ is an increasing function in η , we deduce that $0.71 \leq \frac{\eta+I_0}{\eta+I_1} \leq 1$. Having $\frac{\sigma_0}{\sigma_1} \approx 1.3$ [BBG⁺00], we finally obtain $0.92 \leq K_1 \leq 1.3$.

We conclude that despite the heterogeneity of fading all over the cell, by dividing it into the three previous zones, we can fairly assume the homogeneity of fading within each zone, required to obtain a "fair" scheduling (applied among users of the same zone). Hence, *Assumption 1* holds in our proposed model. Besides, *Assumption 2* is valid in our model for Zones 0 and 2, and better approximated for Zone 1.

In summary, for user k in Zone z , we can write the feasible rate as $R_{k,z} = C_{k,z} \cdot x_{k,z}$ by defining $x_{k,z}$ as being the variations (of unit mean) due to fading around the mean rate $C_{k,z}$. More explicitly, we have the following:

- For Zone 0, $x_{k,0} = 1$.
- For Zone 1, $x_{k,1} = x'_k$, which is a function of x_k given in details in Appendix 5.8.2.
- For Zone 2, $x_{k,2} = x_k$.

Remark 5.1. : There exist different methods which enable the BS to localize users and hence to classify them into different zones [Zha02].

5.3 Analytical Study of PF vs. WPF

We know that, at time slot t , PF schedules the user with the highest feasible rate relative to its current average throughput, i.e.,

$$user\ k^* = arg\ max_k \left[\frac{R_k(t)}{T_k(t)} \right],$$

where $R_k(t)$ is the feasible rate of user k and $T_k(t)$ is the exponentially smoothed throughput given by formula (4.2.9) in chapter 4 when PF is run in an ideal environment with homogeneous fading.

Next, in subsection 5.3.1, we analyse the WPF scheduler. Since there is not an exhaustive study of PF with heterogeneous fading in the literature, we propose, in subsection 5.3.2, an approximate analysis for PF in a realistic environment. In subsection 5.3.3, we corroborate the validity of our results through simulation.

5.3.1 The WPF Scheduler

In our model, an independent PF scheduler is applied among users belonging to the same zone and thus experiencing homogeneous fading. Therefore, we can adopt for the exponentially smoothed throughput the result obtained in (4.2.9) for each zone. Namely, in Zone z , the exponentially smoothed throughput of user k is given by,

$$T_{k,\mathbf{z}} \rightarrow C_{k,\mathbf{z}} \cdot \frac{g_z(n_z)}{n_z}, \quad (5.3.1)$$

where n_z is the total number of active users in Zone z and $g_z(n_z) = \mathbb{E}[\max(x_{1,\mathbf{z}}, \dots, x_{n_z,\mathbf{z}})]$.

5.3.1.1 Average Rate

The average rate of a user k belonging to Zone z is then,

$$\chi_{k,\mathbf{z},WPF} = \frac{C_{k,\mathbf{z}}}{n_z} \cdot g_z(n_z) \cdot \mathbb{P}(\alpha_z), \quad (5.3.2)$$

with event $\alpha_z = \{\text{Zone } z \text{ is served}\}$.

Proof. The average rate of a user k in Zone z served according to WPF is,

$$\begin{aligned} & \mathbb{E}\left[R_{k,\mathbf{z}} \cdot \mathbf{1}\left\{\frac{R_{k,\mathbf{z}}}{T_{k,\mathbf{z}}} = \max_{l=1..n_z} \frac{R_{l,\mathbf{z}}}{T_{l,\mathbf{z}}}\right\} \cdot \mathbf{1}\{\alpha_z\}\right] \\ &= C_{k,\mathbf{z}} \cdot \mathbb{E}\left[x_{k,\mathbf{z}} \cdot \mathbf{1}\left\{\frac{x_{k,\mathbf{z}}}{\frac{g_z(n_z)}{n_z}} = \max_{l=1..n_z} \frac{x_{l,\mathbf{z}}}{\frac{g_z(n_z)}{n_z}}\right\}\right] \cdot \mathbb{P}(\alpha_z) \\ &= C_{k,\mathbf{z}} \cdot \mathbb{E}\left[x_{k,\mathbf{z}} \cdot \mathbf{1}\{x_{k,\mathbf{z}} = \max_{l=1..n_z} x_{l,\mathbf{z}}\}\right] \cdot \mathbb{P}(\alpha_z) \end{aligned}$$

Since the random variables $x_{k,\mathbf{z}}$ are i.i.d., we obtain the following,

$$\frac{C_{k,\mathbf{z}}}{n_z} \cdot \mathbb{E}[\max(x_{1,\mathbf{z}}, \dots, x_{n_z,\mathbf{z}})] \cdot \mathbb{P}(\alpha_z).$$

□

We denote by $G_z(n_z)$ the scheduling gain in Zone z , defined as the ratio of what the user receives as compared to a simple RR scheduling in this zone and given by,

$$G_z(n_z) = \frac{\chi_{k,\mathbf{z},WPF}}{\frac{C_{k,\mathbf{z}}}{n_z}} = g_z(n_z) \cdot \mathbb{P}(\alpha_z).$$

The average rate per user in Zone z is then,

$$\chi_{\mathbf{z},WPF} = \frac{C_z \cdot G_z(n_z)}{n_z},$$

where C_z is the mean rate perceived by a user in Zone z . Namely, C_0 in Zone 0, C_1 (from formula (5.2.7)) in Zone 1 and $C_2 = C_0 K_2 \cdot \int_{r_2}^{\mathbb{R}} \left(\frac{r^*}{r}\right)^4 \frac{2rdr}{\mathbb{R}^2 - r_2^2}$ in Zone 2.

5.3.2 The PF Scheduler

We analyse a model where PF selects a user among all users present in the cell while adopting for the exponentially smoothed throughput the value taken by formula (4.2.9). We make this approximation in order to obtain a tractable model by supposing that formula (4.2.9) remains valid for a user in a given Zone z under PF with heterogeneous fading. We verify the validity of this assumption through simulation in subsection 5.3.3.

5.3.2.1 Average Rate

The average rate of a user k belonging to Zone z is then,

$$\chi_{k,\mathbf{z},PF} = \frac{C_{k,\mathbf{z}}}{n_z} \cdot \mathbb{E}[Z_z \cdot \mathbf{1}\left\{\frac{Z_z \cdot n_z}{g_z(n_z)} > \frac{Z_j \cdot n_j}{g_j(n_j)}, \forall j \neq z\right\}], \quad (5.3.3)$$

with $Z_j = \max\{x_{1,j}, \dots, x_{n_j,j}\}$.

Proof. The average rate of a user k in Zone z served according to PF is,

$$\begin{aligned} & \mathbb{E}\left[R_{k,\mathbf{z}} \cdot \mathbf{1}\left\{\frac{R_{k,\mathbf{z}}}{T_{k,\mathbf{z}}} = \max_{j=0,1,2} \max_{l=1..n_j} \frac{R_{l,j}}{T_{l,j}}\right\}\right] \\ &= C_{k,\mathbf{z}} \cdot \mathbb{E}\left[x_{k,\mathbf{z}} \cdot \mathbf{1}\left\{\frac{x_{k,\mathbf{z}}}{g_z(n_z)} = \max_j \max_l \frac{x_{l,j}}{g_j(n_j)}\right\}\right] \\ &= C_{k,\mathbf{z}} \cdot \mathbb{E}\left[x_{k,\mathbf{z}} \cdot \mathbf{1}\left\{\frac{x_{k,\mathbf{z}}}{g_z(n_z)} > \frac{Z_j}{g_j(n_j)}, \forall j \neq z\right\} \cdot \mathbf{1}\left\{\frac{x_{k,\mathbf{z}}}{g_z(n_z)} = \frac{Z_z}{g_z(n_z)}\right\}\right] \\ &= C_{k,\mathbf{z}} \cdot \mathbb{P}(A) \cdot \mathbb{E}\left[x_{k,\mathbf{z}} \cdot \mathbf{1}\left\{\frac{x_{k,\mathbf{z}}}{g_z(n_z)} > \frac{Z_j}{g_j(n_j)}, \forall j \neq z\right\} | A\right], \end{aligned}$$

with event $A = \{x_{k,\mathbf{z}} = Z_z\}$. The random variables $x_{k,\mathbf{z}}$ being i.i.d., formula (5.3.3) follows. \square

We deduce from (5.3.3) the scheduling gain in Zone z denoted by $G_z(n_0, n_1, n_2)$ and defined as the ratio of what the user receives as compared to a simple RR scheduling,

$$G_z(n_0, n_1, n_2) = \frac{\chi_{k,\mathbf{z},PF}}{\frac{C_{k,\mathbf{z}}}{n_z}}.$$

The average rate per user in Zone z is then,

$$\chi_{\mathbf{z},PF} = \frac{C_z \cdot G_z(n_0, n_1, n_2)}{n_z}.$$

For clarity, the detailed formulae are found in Appendix 5.8.2.

5.3.2.2 Access Probability

To evaluate the impact of heterogeneous fading on the access probability when applying PF to the whole cell, we define the following probabilities (the detailed formulae are found in Appendix 5.8.3),

$$a = \mathbb{P}(Z_2 \cdot \frac{C_2}{T_2} > Z_1 \cdot \frac{C_1}{T_1}), b = \mathbb{P}(Z_2 \cdot \frac{C_2}{T_2} > \frac{C_0}{T_0}) \text{ and } c = \mathbb{P}(Z_1 \cdot \frac{C_1}{T_1} > \frac{C_0}{T_0}).$$

Therefore, the probability to serve a user in Zone 2 is $P_2 = \frac{a-b}{n_2}$, the probability to serve a user in Zone 1 is $P_1 = \frac{(1-a) \cdot c}{n_1}$ and the probability to serve a user in Zone 0 is $P_0 = \frac{(1-b) \cdot (1-c)}{n_0}$. If we had homogeneous fading all over the cell, the probability of a user k to be selected would be the same for all users in the cell and is given by formula (4.2.11) in chapter 4.

5.3.3 Numerical Results

We present in this section our numerical experiments performed to illustrate the previous results. We consider in this section the case of infinitely backlogged queues. The number of users in each zone is then fixed and equal to 10, with $n_0 = n_1 = n_2 = 10$ and thus $n = 30$. We take $C_0 = 1$, $r^* = 1$, $K_2 = 1.7$ and $K_1 = 1$. As a result, we get $r_1 \approx 0.5$ and $r_2 \approx 1.5$. Rayleigh Fading is considered corresponding to an exponential distribution of the process $x_k(t)$.

Users are served according to PF and according to our WPF that comprises three different scenarios:

- **WPF(1,1,1)** where slots are distributed fairly across zones ($\mathbb{P}(\alpha_0) = \mathbb{P}(\alpha_1) = \mathbb{P}(\alpha_2) = 1/3$).
- **WPF(1,1,4)** where, in order to favour far users who are penalized by their small rates, Zone 2 is given four more slots than Zone 1 and Zone 0 ($\mathbb{P}(\alpha_0) = \mathbb{P}(\alpha_1) = 1/6$ and $\mathbb{P}(\alpha_2) = 2/3$).
- **WPF(4,2,1)** where, in order to increase the total capacity, Zone 0 is given twice as many slots as Zone 1 and the latter is given twice as many slots as Zone 2 ($\mathbb{P}(\alpha_0) = 4/7$, $\mathbb{P}(\alpha_1) = 2/7$ and $\mathbb{P}(\alpha_2) = 1/7$).

In all experiments, we determine the average rate per user and display the results for users belonging to the same zone for PF and for WPF. We compare the results obtained by

simulation to those obtained numerically from $\chi_{\mathbf{z},PF}$ and $\chi_{\mathbf{z},WPF}$.

Results are shown in Table 5.1 and indicate that the analytical formulae provide highly accurate estimates of simulation results and thus our proposed approximation for PF is valid. As for performance, we see in WPF(1,1,1) that there is a conservation in the mean rate in Zone 0 and Zone 1 in comparison with PF, contrary to Zone 2 where a slight degradation is witnessed. This loss is compensated for by the increase in the probability to access the channel for users in Zone 2. Indeed, from subsection 5.3.2.2, P_0 and P_1 are roughly equal to $1/30$ (as in the homogeneous case from P given by (4.2.11)) while P_2 is approximately equal to 0.017 (whereas P gives $1/30$ for the homogeneous case). This means that with heterogeneous fading, the PF algorithm favours close users who are scheduled about twice as often as far users. Yet, in WPF, if the system wants to share resources fairly between users, it can give one time slot to each zone successively as it is done in WPF(1,1,1) where $\mathbb{P}(\alpha_z) = 1/3$. In other words, the probability to choose a user will be $1/3 \cdot 1/10$ (recall that users in the same Zone z have the same probability $\frac{1}{n_z}$ to be selected) exactly as in the ideal homogeneous system. Far users will then have the same chance to be scheduled as close users and hence the lost equity in the distribution of slots among users will be restored.

Furthermore, the system can now be entirely controlled as a significant flexibility in the allocation of resources is introduced:

- If the system seeks to realize a fair rate sharing, it can give more slots to far users who are disadvantaged as compared to nearer users due to their small feasible rates. For instance in WPF(1,1,4), far users in Zone 2 being given four times more slots than close users in Zones 0 and 1, perceive a gain of 50% in comparison with PF.
- However, if the system wants to maximize the overall throughput without causing the starvation of distant users (as it is done in the MaxRate scheduler), it can give more slots to close users than to far users. In particular, in WPF(4,2,1), users in Zone 0 perceive a gain of 76% as compared to PF leading to a gain in global rate of approximately 20%.

We graphed in Figure 5.1 the mean rate per Zone and the Total Mean capacity of the cell for PF and for WPF (from simulations results of Table 5.1). The variations of curves with the variation of scenarios highlight the mentioned trade-off between fairness and efficiency and clearly show how it is now fully controlled.

Zone 0	PF	WPF(1,1,1)	WPF(4,2,1)	WPF(1,1,4)
NUM	0.034	0.034	0.065	0.0167
SIM	0.033	0.033	0.061	0.0167
Zone 1	PF	WPF(1,1,1)	WPF(4,2,1)	WPF(1,1,4)
NUM	0.033	0.0297	0.026	0.0165
SIM	0.033	0.0315	0.0274	0.0160
Zone 2	PF	WPF(1,1,1)	WPF(4,2,1)	WPF(1,1,4)
NUM	0.013	0.010	0.0042	0.0195
SIM	0.012	0.011	0.0045	0.0208

Table 5.1: Average Rate per user

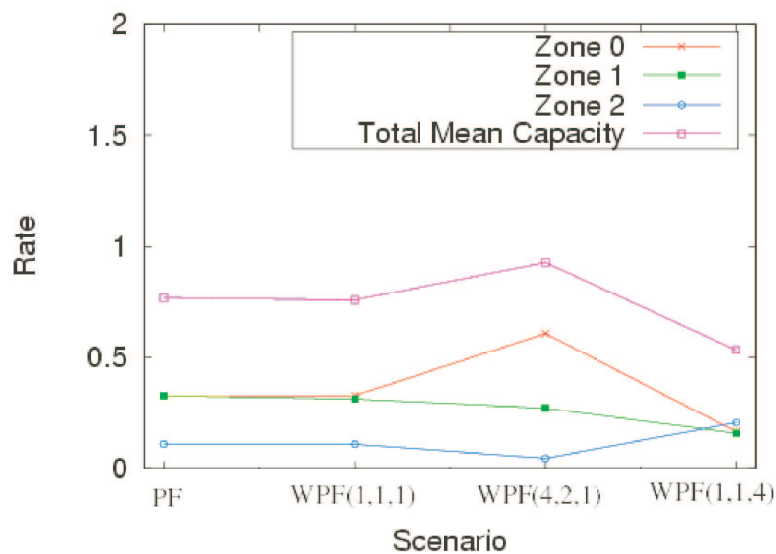


Figure 5.1: Mean Rate per Zone and Total Mean Capacity

5.4 Dynamic Model of WPF

With heterogeneous fading, the PF loses the symmetry properties of the Multi-class PS discipline [Coh78] because the rate at which users are served in Zone z is a function of the number of users in all zones according to (5.3.3). The three zones can be considered as a network of three nodes with no routing between nodes. We denote by $n = (n_0, n_1, n_2)$ the network state where n_z is the number of flows in node z . We know that the capacity of each node is equally shared between the active flows present in the node, as a consequence the present queueing network consists of three processor-sharing nodes with state-dependent capacities, that is the capacity of node z depends on the state $n = (n_0, n_1, n_2)$ of the network. Assuming the fact that arrivals at each node follow a Poisson process and the services required are exponential and i.i.d., the given network is a Whittle network [She95] if the so-called balance property is established.

Let e_y be the unit vector with 1 in component y and 0 elsewhere, for $y = 0, 1, 2$. The balance property is established if we have the following,

$$G_z(n - e_y) \cdot G_y(n) = G_y(n - e_z) \cdot G_z(n),$$

$\forall z, y \in 0, 1, 2$ and $\forall n$ such that $n_y > 0$ and $n_z > 0$.

Unfortunately, this formula does not apply in our case, therefore, we only studied the dynamic model for our proposed WPF scheduler.

We deduce from formula (5.3.2) that each zone, in our WPF system, behaves like a Multi-class PS queue whose service rate is $\frac{G_z(n_z)}{n_z}$. In particular, Zone 0 behaves like a simple PS system owing to the fact that $g_0(n_0) = 1$. Hence, our proposed model, contrary to PF, is fully tractable in the dynamic case.

We assume that data flows arrive as a Poisson process of intensity $\lambda \cdot ds$ in any area of surface ds . Flow sizes are i.i.d. and S is the corresponding random variable. We denote by $\rho = \lambda \cdot \mathbb{E}[S]$ the traffic load and by $d\rho(r) = \rho \cdot 2\pi r dr$ the traffic load generated by users whose distance to the BS ranges between r and $r + dr$. Such a system has the well-known insensitivity property which means that performance depends mainly on the load factor (and on the maximum number of users in presence of an admission control policy) and not on the distribution of flow size which is continually changing given the ever varying nature of data applications. Thus, our scheduling approach, in addition to making the system more flexible, simplifies dimensioning.

5.4.1 Analytical Model

From [Coh78], we obtain the stationary distribution of the number of users in Zone z ,

$$\pi_z(x) = \frac{\prod_{i=1}^x \frac{\rho_z}{G_z(i)}}{\sum_{k=0}^{n_z} \prod_{i=1}^k \frac{\rho_z}{G_z(i)}},$$

where ρ_z is the load in Zone z and n_z is the maximum number of admitted users in this zone.

More explicitly, we have the following:

- For Zone 0, $\rho_0 = \int_{r_0}^{r_1} \frac{d\rho(r)}{C_0} = \frac{\rho\pi r_1^2}{C_0}$.
- For Zone 1, $\rho_1 = \int_{r_1}^{r_2} \frac{d\rho(r)}{C_1} = \frac{\rho\pi(r_2^2 - r_1^2)}{C_1}$.
- For Zone 2, $\rho_2 = \int_{r_2}^{\mathfrak{R}} \frac{d\rho(r)}{C_0 \cdot (\frac{r^*}{r})^\beta} = \frac{\rho\pi(\mathfrak{R}^{\beta+2} - r_2^{\beta+2})}{C_0 \cdot (r^*)^\beta \cdot (\beta+2)}$.

Using Little's law, we find that the flow throughput $Th_{i,z}$ of user i in Zone z , defined as the ratio of the mean flow size $\mathbb{E}[S]$ to the mean flow duration, is given by,

$$Th_{i,z} = C_{i,z} \cdot \frac{\rho_z \cdot (1 - B_z)}{\mathbb{E}[n_z]}, \quad (5.4.1)$$

where $B_z = \pi_z(x = n_z)$ is the blocking probability and $\mathbb{E}[n_z] = \sum_{i=1}^{n_z} i \cdot \pi_z(i)$ is the mean number of active users in Zone z .

5.4.2 Simulation Results

We present here numerical experiments that we performed to illustrate the above results. We consider a system where users initiate file transfer requests as a Poisson process of intensity $\lambda\pi\mathcal{R}^2$ and traffic demand is uniformly distributed in the cell. Rayleigh Fading is considered. At most 10 users are admitted simultaneously in each zone to guarantee a minimum rate of $\frac{C(\mathcal{R})}{30}$. Guaranteeing a minimum rate is a QoS notion appropriate for non-real time users. New transfers generated in a zone where there are already 10 transfers in progress are blocked and lost. Flow sizes are i.i.d. and exponentially distributed with mean equal to 2500 Kbits (which means equal to 1 for $C_0 = 1$).

We determine the throughput per user and display the average throughput for users belonging to the same zone. Users are served according to our WPF(1,1,1). The simulation results obtained are compared to the normalized throughput $\frac{Th_{i,z}}{C_{i,z}}$ obtained in (5.4.1).

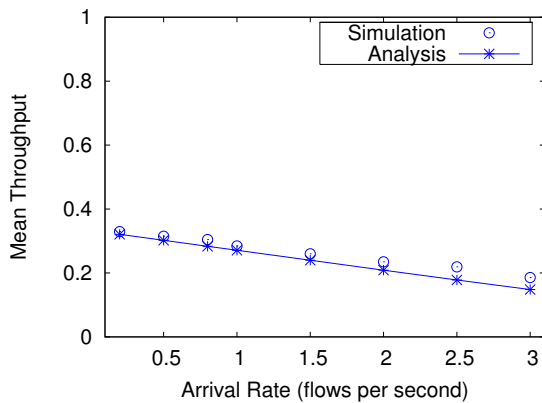


Figure 5.2: Average Throughput for Zone 0

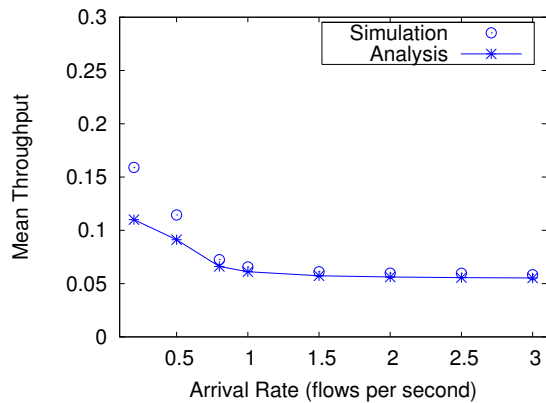


Figure 5.3: Average Throughput for Zone 1

Figures 5.2, 5.3 and 5.4 depict the mean throughput as a function of the file arrival rate respectively for Zone 0, Zone 1 and Zone 2. We can see how the analysis and simulation curves are nearly indistinguishable for Zone 0 and Zone 2 because both of these zones behave perfectly like a Multi-class PS system. Yet, for Zone 1, the analytical model gives less accurate predictions because the approximation made for this zone is not totally valid since it still experiences heterogeneous fading in a realistic environment: the closest

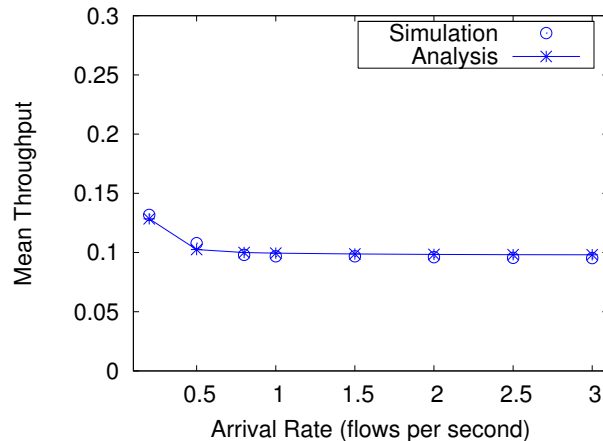


Figure 5.4: Average Throughput for Zone 2

users in Zone 1 have almost always fixed rates while the farthest users in the same zone have continuously varying rates. Nonetheless, we can fairly consider that the proposed analytical model approximates very well the behaviour of our WPF scheduler.

5.5 Intercell Scheduling

The proposed segmentation of the cell in three zones offers another possibility to favour a specific class of users through intercell interference management by adopting a simple power control scheme. We know that the BS transmits to only one user at a time at full power in order to get rid of intracell interference. However, we can tune the transmitted power depending on the served zone in order to reduce intercell interference for some users. For this purpose, we suggest in this section to serve users in Zone z at power $\varphi_z \cdot P$ with $0 < \varphi_z \leq 1$. We will show how this scheme will enable us once again, by alleviating intercell interference, to choose between favouring far users who suffer from inherently small rates and favouring close users to augment overall throughput.

We reconsider hexagonal networks where interference suffered by a user in a given cell is almost entirely generated by the 6 neighbouring BSs. As already mentioned, this assumption is fairly valid in an urban environment where the path loss is at least equal to 4. Thanks to the partitioning of the system we performed, a BS serves alternately Zone 0, Zone 1 and Zone 2. Hence, we can easily achieve the following: for each BS serving Zone $z \pmod{3}$, three of the BSs surrounding it serve Zone $(z + 1) \pmod{3}$ while the three others serve Zone $(z + 2) \pmod{3}$ according to the plan in Figure 5.5.

As a result, users in Zone 2, for instance, always endure intercell interference resulting from serving Zones 0 and Zone 1 at power $\varphi_0 \cdot P$ and $\varphi_1 \cdot P$ respectively.

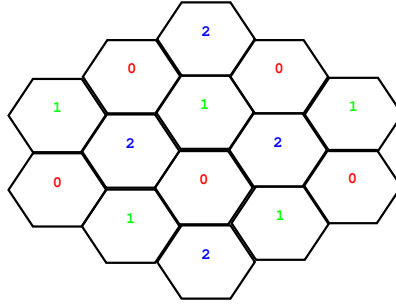


Figure 5.5: Intercell Scheduling

The rate obtained for user k in Zone z in this model is then,

$$R'_{k,\mathbf{z}} = \frac{W}{\sigma_z} \cdot \frac{\varphi_z \cdot P \cdot \gamma_k}{\eta + I(z+1) + I(z+2)},$$

where $I(z+1)$ is the intercell interference resulting from the surrounding BSs serving Zone $(z+1) \pmod{3}$ (I' in the original model) and $I(z+2)$ is the intercell interference resulting from the surrounding BSs serving Zone $(z+2) \pmod{3}$ (I'' in the original model).

The rate obtained for user k in Zone z without power control is,

$$R_{k,\mathbf{z}} = \frac{W}{\sigma_z} \cdot \frac{P \cdot \gamma_k}{(\eta + I' + I'')}.$$

To compare $R'_{k,\mathbf{z}}$ and $R_{k,\mathbf{z}}$, we compute the following ratio,

$$\psi_z = \frac{R'_{k,\mathbf{z}}}{R_{k,\mathbf{z}}} = \frac{\varphi_z \cdot (\eta + I' + I'')}{\eta + \varphi_{z+1} I' + \varphi_{z+2} I''}.$$

We assume that $I' \approx I''$ and η is negligible in comparison with intercell interference.

If we wish to improve the performance of far users, we can set $\varphi_2 = 1$ (thus the BS will serve users in Zone 2 at full power) and $\varphi_0 < \varphi_1 < 1$ (so that Zone 1 receives more power than Zone 0). Consequently, we obtain $\psi_2 = \frac{2}{\varphi_0 + \varphi_1} > 1$ and the less power we give close users, the more we increase the rate perceived by far users. While $\psi_0 = \frac{2\varphi_0}{1+\varphi_1} < \psi_1 = \frac{2\varphi_1}{1+\varphi_0} \leq 1$. If φ_0 and φ_1 satisfy the subsequent additional relation $1 + \varphi_0 = 2 \cdot \varphi_1$, we can preserve the performances in Zone 1 ($\psi_1 = 1$) and only reduce the rate in Zone 0, the latter will not be that disadvantaged because often users in Zone 0 receive excess power that goes to waste due to their proximity to the BS. For instance, for $\varphi_0 = 1/2$ and $\varphi_1 = 3/4$, we get $\psi_2 = 1.6$, $\psi_1 = 1$ and $\psi_0 \approx 0.6$.

As for increasing the global throughput, we can set $\varphi_1 = 1$ (as already mentioned, serving users in Zone 0 at full power could lead to resource wastage) and $\varphi_2 < \varphi_0 < 1$. Consequently, we obtain $\psi_1 = \frac{2}{\varphi_0 + \varphi_2} > 1$ and $\psi_2 = \frac{2\varphi_2}{1 + \varphi_0} < \psi_0 = \frac{2\varphi_0}{1 + \varphi_2} \leq 1$. Once again, if φ_0 and φ_2 verify the subsequent additional relation $1 + \varphi_2 = 2 \cdot \varphi_0$, we can preserve the performances in Zone 0 with $\psi_0 = 1$.

5.6 The WPF+CDMA Scheduler

The authors in [KK06a] showed that because the SNR does not scale linearly with the feasible rate for all users in the cell, scheduling one user at a time may not result in maximum channel utilization. Furthermore, for almost orthogonal channels and for high SNRs, regular CDMA offers higher average rate than the scheduled design. We deduce then that CDMA scheduling is more appropriate than TDMA scheduling for users in Zone 0 as they enjoy very good channel conditions. Additionally, as mentioned earlier, users in Zone 0 cannot take advantage from opportunistic scheduling because of their almost constant rates. Since we operated this segmentation of the cell, we have the freedom to treat each zone differently. Therefore, we will serve users in Zone 0 in a CDMA fashion while keeping on serving users in Zone 1 and Zone 2 according to the PF algorithm.

5.6.1 Average Rate per Slot

We consider the case where we serve simultaneously n_0 users in Zone 0, each user receiving a power of $P_k = \frac{P}{n_0}$. The average rate R_k of user k can be assumed to follow a logarithmic relation (which is a better approximation than the linear assumption obtained in formula (4.2.3) given in chapter 4),

$$R_k(\zeta_k(t), n_0) = W \log_2 \left(1 + \frac{\zeta_k(t)}{f \cdot \zeta_k(t) \cdot (n_0 - 1) + n_0} \right),$$

where $\zeta_k(t) = \frac{P \cdot (\frac{\epsilon}{r_0})^\beta \cdot g_k(t)}{\eta + I_0}$ is the SNR of user k in Zone 0, $g_k(t)$ the instantaneous channel gain (which is constant and equal to 1 in Zone 0) and f the orthogonality factor that represents the fraction of power transmitted by the BS that appears as interference to the user.

It is sensible to assume that $\zeta_k(t)$ is a stationary and ergodic stochastic process for every user. Thus, the asymptotic data rate, where $\zeta = \frac{P \cdot (\frac{\epsilon}{r_0})^\beta}{\eta + I_0}$, is given by,

$$\begin{aligned} \overline{R}_k &= \lim_{T \rightarrow \infty} \frac{1}{T} \int_0^T R_k(\zeta_k(t), n_0) dt \\ &= \int_0^\infty R_k(\zeta_k, n_0) \cdot \delta\left(\zeta_k - \frac{P \cdot (\frac{\epsilon}{r_0})^\beta}{\eta + I_0}\right) d\zeta_k = R_k(\zeta, n_0) \end{aligned} \tag{5.6.1}$$

The average rate obtained for user k while using the PF algorithm is then,

$$R_k(\zeta, n_0 = 1) \cdot \mathbb{P}(\text{serving user } k) = \frac{W}{n_0} \cdot \log_2(1 + \zeta). \quad (5.6.2)$$

To compare (5.6.1) and (5.6.2), we compute the following ratio ν ,

$$\nu(\zeta, f, n_0) = \frac{n_0 \cdot \log_2\left(+\frac{\zeta}{f \cdot \zeta \cdot (n_0 - 1) + n_0}\right)}{\log_2(1 + \zeta)}. \quad (5.6.3)$$

If the BS uses orthogonal codes to transmit to distinct users, the intracell interference is virtually eliminated, which corresponds to $f = 0$. However, when there is multi-path fading, this form of interference is only partially reduced which implies $f \in [0, 1]$. Using orthogonal codes in our case requires synchronisation of all users which is easily done for the downlink channel. In addition, the channel for users in Zone 0 is hardly experiencing any fading at all and the risk of receiving delayed copies which are not orthogonal any more is significantly minimized. Thus, considering that $f \rightarrow 0$ is a quite reasonable hypothesis. Knowing that the mean SNR for users in Zone 0 is at least equal to 9.5dB [BBG⁺00], we deduce that $\nu(\zeta \geq 9.5\text{dB}, f = 0, n_0 = 10) > 2.77$. Hence, we conclude that we profit considerably from applying the WPF+CDMA scheme.

5.7 Concluding Remarks

In this chapter, we propose a new scheduling approach for new generation cellular networks. The approach is based on the partitioning of the cell into zones in such a way that inside each zone the fading and SNR are quite homogenous. We propose a hierarchical scheduler – named WPF – which, at a first level, serves the zones in a WRR fashion and, at a second level, serves users within each zone with independent PF schedulers. We proved that our scheduler restored to the PF scheduler its celebrated fairness property. Indeed, the conditions necessary to obtain a *fair* PF are met for the first and the last zone and better approximated for the intermediate zone. Furthermore, we gave the system flexibility through the decoupling of the cell: on the one hand, we were able to control the proportion of slots given to each zone and on the other hand, we were able to choose the most appropriate way of serving each zone while taking into account its inherent characteristics. In fact, we found that it is efficient to apply the PF algorithm for Zones 1 and 2, and CDMA for Zone 0 because of its good channel condition and its incapacity to profit from multi-user diversity (with almost constant rates).

Our analytical and numerical studies show how our approach allows controlling the trade-off between global efficiency and fairness, a capability that PF lacks for. Moreover, we propose an analytical model for the PF algorithm under realistic heterogeneous fading

conditions that we validate by simulation. An analysis of WFP under dynamic traffic conditions is also provided.

Finally, our segmentation of the cell enabled us to control resources via another different and simple method based on Intercell scheduling.

5.8 Appendix

We define $u = \frac{1}{K_1} \cdot (\frac{r_1}{r^*})^4$, $v = \frac{1}{K_1} \cdot (\frac{r_2}{r^*})^4$, $K = \frac{C_0 K_1}{C_1}$ and $Z_j = \max\{x_{1,j}, \dots, x_{n_j,j}\}$.

5.8.1 Computing $g_z(n_z)$:

From (5.2.6), we know that $x_{k,1} = x'_k$ is a function of $x_{k,2} = x_k$. Hence, we obtain the following:

$$x'_k = f(x_k) = \begin{cases} \frac{K}{\sqrt{uv}} \cdot x_k & \text{if } x_k \leq u \\ \frac{K(2\sqrt{x_k} - \sqrt{u} - \frac{x_k}{\sqrt{v}})}{(\sqrt{v} - \sqrt{u})} & \text{if } u \leq x_k \leq v \\ K & \text{if } x_k \geq v \end{cases}$$

The random variables $x_{k,2}$ being exponentially distributed, we have that:

$$\begin{aligned} g_2(n_2) &= \mathbb{E}[\max(x_{1,2}, \dots, x_{n_2,2})] = \int_0^\infty \mathbb{P}(Z_2 > s) ds \\ &= \int_0^\infty 1 - (1 - e^{-s})^{n_2} ds = \sum_{i=1}^{n_2} \frac{1}{i} \end{aligned}$$

$$\begin{aligned} g_1(n_1) &= \mathbb{E}[\max(x_{1,1}, \dots, x_{n_1,1})] = \int_0^\infty \mathbb{P}(Z_1 > s) ds \\ &= \int_0^{f(v)} 1 - (1 - e^{-f^{-1}(s)})^{n_1} ds \end{aligned}$$

with

$$f^{-1}(s) = \begin{cases} \frac{\sqrt{uv}}{K} \cdot s & \text{if } 0 \leq s \leq f(u) \\ (\sqrt{v} - [v - (\sqrt{uv} + s \frac{\sqrt{v}(\sqrt{v} - \sqrt{u})}{K}]^{\frac{1}{2}})^2 & \text{if } f(u) \leq s \leq f(v) \end{cases}$$

And $g_0(n_0) = 1$ (because $x_{k,0} = 1$).

We denote by $h_2(z)$ and $h_1(z)$ the density functions of respectively Z_2 and Z_1 which are given by ($Z_0 = 1$):

$$\begin{aligned} h_2(z) &= n_2 e^{-z} (1 - e^{-z})^{n_2-1} \\ h_1(z) &= \frac{n_1 e^{-f^{-1}(z)} (1 - e^{-f^{-1}(z)})^{n_1-1}}{f' \circ f^{-1}(z)} \quad \text{if } 0 \leq z < f(v) \\ &= (1 - (1 - e^{-v})^{n_1}) \cdot \delta(z - f(v)) \quad \text{if } z \geq f(v) \end{aligned}$$

5.8.2 Computing the scheduling gains $G_z(n_0, n_1, n_2)$:

The gain in Zone 2 is $G_2(n_0, n_1, n_2) =$

$$\begin{aligned} & \mathbb{E}[Z_2 \cdot \mathbf{1}\{\frac{Z_2 n_2}{g_2(n_2)} \geq \frac{Z_1 n_1}{g_1(n_1)}\} \cdot \mathbf{1}\{\frac{Z_2 n_2}{g_2(n_2)} \geq n_0\}] = \\ & \mathbb{E}[Z_2 \cdot \mathbf{1}\{\frac{Z_2 n_2}{g_2(n_2)} \geq \frac{Z_1 n_1}{g_1(n_1)} \geq n_0\}] + \mathbb{E}[Z_2 \cdot \mathbf{1}\{\frac{Z_2 n_2}{g_2(n_2)} \geq n_0 \geq \frac{Z_1 n_1}{g_1(n_1)}\}] = \\ & \int_{\frac{g_1(n_1)n_0}{n_1}}^{\infty} h_1(z_1) \int_{\frac{g_2(n_2)n_1}{g_1(n_1)n_2}, z_1}^{\infty} z_2 h_2(z_2) dz_2 dz_1 + \mathbb{P}(Z_1 \leq \frac{g_1(n_1)n_0}{n_1}) \int_{\frac{g_2(n_2)n_0}{n_2}}^{\infty} z_2 h_2(z_2) dz_2 \end{aligned}$$

The gain in Zone 1 is $G_1(n_0, n_1, n_2) =$

$$\begin{aligned} & \mathbb{E}[Z_1 \cdot \mathbf{1}\{\frac{Z_1 n_1}{g_1(n_1)} \geq \frac{Z_2 n_2}{g_2(n_2)}\} \cdot \mathbf{1}\{\frac{Z_1 n_1}{g_1(n_1)} \geq n_0\}] = \\ & \mathbb{E}[Z_1 \cdot \mathbf{1}\{\frac{Z_1 n_1}{g_1(n_1)} \geq \frac{Z_2 n_2}{g_2(n_2)} \geq n_0\}] + \mathbb{E}[Z_1 \cdot \mathbf{1}\{\frac{Z_1 n_1}{g_1(n_1)} \geq n_0 \geq \frac{Z_2 n_2}{g_2(n_2)}\}] = \\ & \int_{\frac{g_2(n_2)n_0}{n_2}}^{\infty} h_2(z_2) \int_{\frac{g_1(n_1)n_2}{g_2(n_2)n_1}, z_2}^{\infty} z_1 h_1(z_1) dz_1 dz_2 + \mathbb{P}(Z_2 \leq \frac{g_2(n_2)n_0}{n_2}) \int_{\frac{g_1(n_1)n_0}{n_1}}^{\infty} z_1 h_1(z_1) dz_1 \end{aligned}$$

The gain in Zone 0 is $G_0(n_0, n_1, n_2) =$

$$\mathbb{E}[\mathbf{1}\{\frac{Z_1 n_1}{g_1(n_1)} \leq n_0\} \cdot \mathbf{1}\{\frac{Z_2 n_2}{g_2(n_2)} \leq n_0\}] = \mathbb{P}(Z_2 \leq \frac{g_2(n_2)n_0}{n_2}) \cdot \mathbb{P}(Z_1 \leq \frac{g_1(n_1)n_0}{n_1})$$

5.8.3 Computing the probabilities a , b & c :

$$\begin{aligned} a &= \mathbb{P}(\frac{Z_2 C_2}{T_2} > \frac{Z_1 C_1}{T_1}) = \mathbb{P}(Z_1 < Z_2 \frac{g_1(n_1)n_2}{g_2(n_2)n_1}) \\ &= \int_0^{\infty} \mathbb{P}(z_1 < s \cdot \frac{g_1(n_1)n_2}{g_2(n_2)n_1}) \cdot h_2(s) ds \\ &= \int_0^{\frac{g_2(n_2)n_1}{g_1(n_1)n_2} \cdot f(v)} (1 - e^{-f^{-1}(s \frac{g_1(n_1)n_2}{g_2(n_2)n_1})})^{n_1} h_2(s) ds + \int_{\frac{g_2(n_2)n_1}{g_1(n_1)n_2} \cdot f(v)}^{\infty} h_2(s) ds \end{aligned}$$

$$b = \mathbb{P}(\frac{Z_2 C_2}{T_2} > \frac{C_0}{T_0}) = \mathbb{P}(Z_2 > \frac{g_2(n_2)n_0}{n_2}) = \int_{\frac{g_2(n_2)n_0}{n_2}}^{\infty} h_2(s) ds$$

$$c = \mathbb{P}(\frac{Z_1 C_1}{T_1} > \frac{C_0}{T_0}) = \mathbb{P}(Z_1 > \frac{g_1(n_1)n_0}{n_1}) = \int_{\frac{g_1(n_1)n_0}{n_1}}^{\infty} h_1(s) ds$$

Chapter 6

A Hierarchical Proportional Fair Scheduler

In this chapter, we evaluate to what extent TDMA scheduling is really advantageous for HDR/HSDPA systems. We show that simultaneous transmission can outperform, for some users in the cell, one-by-one transmission when we adopt a realistic model where the SNR is logarithmic with the perceived rate. Therefore, being a TDMA-like scheduler, PF does not result in optimal performances for all users in the cell. More importantly, when the channel quality is not linear with the transmission rate (i.e. when we let go of Assumption 2 cited in chapter 4), PF fails to be fair and efficient. We propose in this chapter a hybrid PF/CDMA scheduler that will get round these drawbacks while increasing the total system throughput.

6.1 Introduction

In HSDPA/HDR systems, time is divided into very short intervals (1.67 ms for HDR and 0.67ms for HSDPA) and the BS transmits at full power to a single user per time slot aiming to get rid of intracell interference. This TDMA-like scheduling is adopted because of its proven optimality when the SNR scales linearly with the effective transmission rate [BBR99]. However, because the SNR does not scale linearly with the feasible rate for all users in the cell, scheduling one user at a time may not result in maximum channel utilization. We suggest, in this chapter, to divide the cell in two zones where slots will be distributed across the different zones in a WRR fashion: users in the first zone will be served according to regular CDMA while users in the second zone will be served one at a time according to the PF algorithm. We will show how this new hierarchical scheduler, termed HPF, will increase the total throughput of the cell.

The rest of the chapter is organized as follows. In section 6.2, we present the proposed HPF approach. In section 6.3, we analyse its performance; in particular, we obtain analytical results for the mean rate in Standard PF (SPF) and in HPF for a fixed number of users. We also show how our hierarchical scheduler improves the performance of the cell in terms of average rate. In section 6.4, we extend the model of our HPF algorithm to accommodate a dynamic user configuration and we corroborate the results obtained by simulations. Finally, in section 6.5, we give a brief conclusion.

6.2 A Hierarchical Scheduling Approach

The present chapter proposes to divide the cell into two zones where each zone is served at a time while users in a given zone are scheduled differently. We begin by giving, in section 6.2.1, the adopted radio model. We compare CDMA scheduling and TDMA scheduling in section 6.2.2 and then explain, in section 6.2.3, the reason behind this "logical" division.

6.2.1 The Radio Resource

In this section, we present the model of the radio resource and the way it is shared among users. We then compute the peak rate of each user accordingly.

6.2.1.1 The Propagation Model

Let P be the transmission power emitted by the BS and γ_k the free space path loss. The power received by user k is then,

$$P_k = P \cdot \gamma_k. \quad (6.2.1)$$

The adopted model for the free space path loss is,

$$\gamma_k = 1 \text{ if } r_k \leq \epsilon \text{ and } \gamma_k = \left(\frac{\epsilon}{r_k}\right)^\beta \text{ otherwise,}$$

where β is the path loss exponent, ϵ is the maximum distance at which the full power P is received and r_k the distance separating user k from the BS.

6.2.1.2 The Feasible Rate

For user k , the Signal-to-Noise Ratio SNR_k and the peak rate R_k , which is assumed to follow a logarithmic relation with the SNR according to Shannon's law, are respectively given by,

$$SNR_k = \frac{\phi_k \cdot P_k}{(\eta + I_{BS} + I_k)}, \quad R_k = W \cdot \log_2(1 + SNR_k), \quad (6.2.2)$$

where W is the cell bandwidth, P_k the power received by the user, η the background noise, ϕ_k the fraction of power transmitted to user k by its BS, I_{BS} the interference caused by other BSs to user k (intercell interference) and I_k the interference caused to user k by its own BS (intracell interference) and given by the following relation,

$$I_k = P_k \cdot (f_k(1 - \phi_k) + h_k\phi_k), \quad (6.2.3)$$

where f_k is the orthogonality factor and h_k is a self-noise coefficient. We assume that $h_k < 1$ which means that the interference experienced by a user from its own signal is not greater than the signal itself.

6.2.2 CDMA vs. TDMA

The authors in [BBR99] showed that it is better for a BS to transmit to only one user at a time rather than to transmit to several such users simultaneously for $h_k < 1$. Yet, we will show here that this is not necessarily true if the feasible rate does not scale linearly with the SNR.

For that, we consider a time interval during which the total power level P at the BS remains constant and we suppose that throughout the interval a proportion ϕ_k of the total power P is allocated to user k such that $\sum_k \phi_k = 1$.

From (6.2.2) and (6.2.3), the feasible rate of user k is,

$$R_{k,CDMA} = W \log_2 \left(1 + \frac{\phi_k P_k}{\eta + I_{BS} + P_k(f_k(1 - \phi_k) + h_k\phi_k)} \right).$$

Now we suppose that each user k is allocated the total power P but for a fraction ϕ_k of the interval. During the period that the BS transmits to user k , no power is allocated to other users in the cell, thus user k endures no interference from other users within the cell. Consequently, the feasible rate of user k during the whole interval is,

$$R_{k,TDMA} = \phi_k W \log_2 \left(1 + \frac{P_k}{\eta + I_{BS} + P_k h_k} \right).$$

The SNR of a user depends on the radio channel and varies with time due to user mobility and fading effects. We will only consider the impact of fast fading in our model by replacing SNR_k of user k by,

$$SNR_k(t) = SNR_k \cdot x_k(t), \quad (6.2.4)$$

where $x_k(t)$ are i.i.d. copies of some stationary process $x(t)$ with unit mean that represents the effect of fast fading. As we consider Rayleigh fading throughout the chapter, $x_k(t)$ follows an exponential distribution.

It follows that the asymptotic rate for every user k is,

$$\begin{aligned} R_k &= \lim_{T \rightarrow \infty} \frac{1}{T} \int_0^T R_k(SNR_k(t)) dt \\ &= \int_0^\infty R_k(SNR_k \cdot x_k) \cdot g(x_k) dx_k \end{aligned}$$

where $g(x_k) = e^{-x_k}$, $x_k \geq 0$.

To compare the two schemes, we compute the ratio, termed ς_k , of the rate obtained in a CDMA scheme over the rate obtained in a TDMA scheme,

$$\begin{aligned} \varsigma_k &= \frac{\lim_{T \rightarrow \infty} \frac{1}{T} \int_0^T R_{k,CDMA}(SNR_k(t)) dt}{\lim_{T \rightarrow \infty} \frac{1}{T} \int_0^T R_{k,TDMA}(SNR_k(t)) dt} \\ &= \frac{\int_0^\infty \log_2 \left(1 + \frac{\phi_k snr_k x_k}{1 + snr_k \cdot (f_k(1 - \phi_k) + h_k \phi_k)} \right) e^{-x_k} dx_k}{\phi_k \int_0^\infty \log_2 \left(1 + \frac{snr_k x_k}{1 + snr_k h_k} \right) e^{-x_k} dx_k} \end{aligned}$$

where

$$snr_k = \frac{\gamma_k P}{\eta + I_{BS}}. \quad (6.2.5)$$

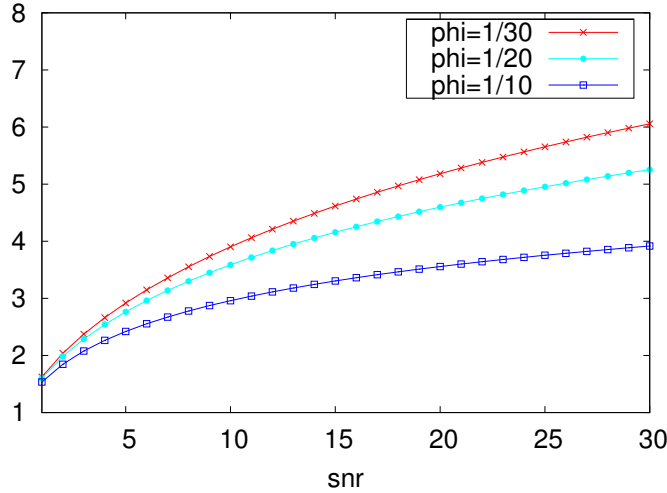
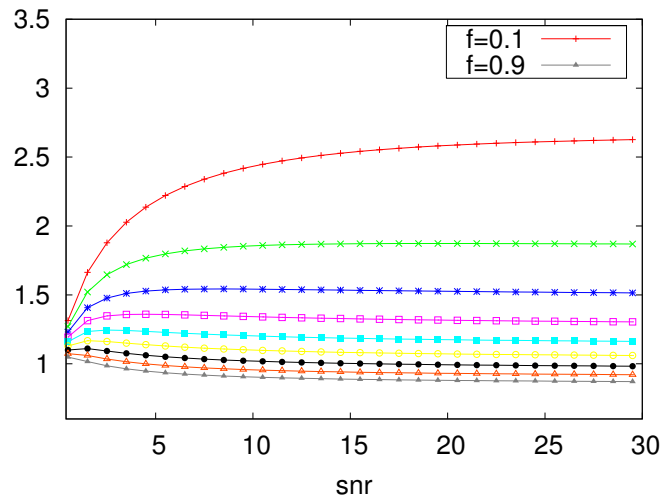
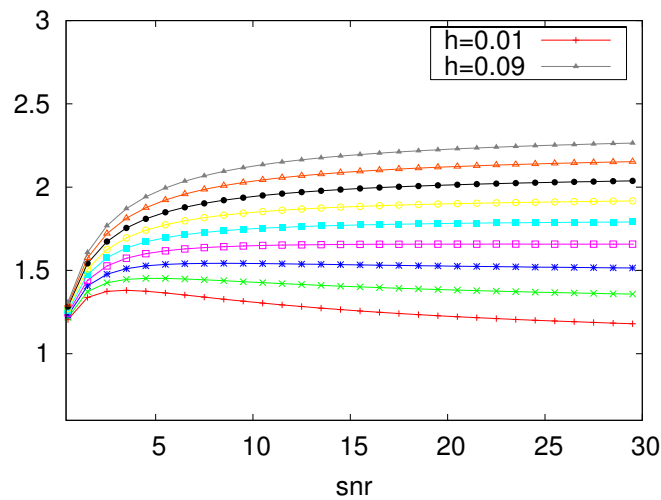


Figure 6.1: Ratio ς_k for $f=0$

To evaluate ς_k , we will plot it as a function of snr_k for different values of f_k , h_k and ϕ_k . In the special case where $f_k = 0$ and $\phi_k < 1$, we can see in Figure 6.1, where ς_k is plotted for different values of ϕ_k , that ς_k is strictly greater than 1. We deduce that in the case of perfect orthogonality, it is always more profitable to apply CDMA rather than TDMA especially for high values of snr_k . In Figure 6.2, ς_k is depicted for $\phi_k = 1/30$, for $0.1 \leq f_k \leq 0.9$ and for $h_k = 0.03$ (which is a reasonable value for h_k according to [Vit95, CB92]). We see that

Figure 6.2: Ratio ς_k for $h=0.03$ Figure 6.3: Ratio ς_k for $f=0.3$

for $f_k \leq 0.6$, it is better to apply CDMA rather than TDMA scheduling. In Figure 6.3, ς_k is depicted as a function of snr_k for $\phi_k = 1/30$, for $0.01 \leq h_k \leq 0.09$ and for $f_k = 0.3$. We see that for a moderate value of f_k , it is always better to apply CDMA rather than TDMA especially for high values of h_k .

6.2.3 Delimiting the Cell into Zones

We saw in the preceding section that omitting to adopt a simplifying model where the transmission rate received by users varies linearly in the SNR lead us to the conclusion that it is not always better to serve one user at a time. This conclusion has driven us to

divide the cell into two zones:

- In the first zone, termed **Zone 1**, the peak rate R is almost never proportional to the SNR and thus TDMA scheduling does not result in optimal performances.
- Contrary to the second zone, termed **Zone 2**, where this linearity is satisfied with non-negligible probability and therefore TDMA scheduling is appropriate. Our target is to define the previously introduced zones in such a way that the two assumptions become more realistic inside each zone.

We know that $\log_2(1+x) \approx x/\ln(2)$ is valid for very small values of x . Thus, we will adopt this approximation for $x \leq 0.05$ leading to a maximum deviation of 2.4% from the actual value at $x = 0.05$. As a result, we assume that the following approximation,

$$R_{k,TDMA}(t) \approx \phi_k W \cdot SNR_k(t) / \ln(2) \quad (6.2.6)$$

is valid for

$$SNR_k(t) = SNR_k \cdot x_k(t) \leq 0.05 \quad (6.2.7)$$

where

$$SNR_k = \frac{P_k}{\eta + I_{BS} + P_k h_k} \quad (6.2.8)$$

denotes the SNR user k would get in the absence of fast fading.

Accordingly, we will define the geographical region in the cell, termed **Zone 1**, where users do not profit fully from TDMA scheduling because they almost never (we can say with probability 99%) satisfy formula (6.2.7), i.e.

$$\mathbb{P}(SNR_k \cdot x_k(t) \geq 0.05) > 0.99. \quad (6.2.9)$$

To compute (6.2.9), we need to evaluate (6.2.8) beginning with I_{BS} . For that we adopt the approach in [KA05] where the intercell interference is caused by all BSs (working at maximum power P) in the network taken to be homogeneous with a density of stations ρ_{BS} per unit of surface. Therefore, we get the following,

$$I_{BS} = P \cdot \gamma(r) \cdot \frac{2\pi\rho_{BS}}{\beta-2} r^\beta [(2\Re - r)^{2-\beta} - (R_S - r)^{2-\beta}],$$

with \Re being the cell radius and R_S the network radius.

By defining $\eta = \alpha P$ and taking $\rho_{BS} = \frac{1}{\pi\Re^2}$, we get from the path loss model and (6.2.5),

$$\frac{1}{snr_k} = \alpha \cdot \max\left[\left(\frac{r_k}{\epsilon}\right)^\beta, 1\right] + \nu(r_k), \quad (6.2.10)$$

with $\nu(r_k) = \frac{2}{\beta-2} \cdot (\frac{r_k}{\mathfrak{R}})^2 [(2\frac{\mathfrak{R}}{r_k} - 1)^{2-\beta} - (\frac{R_S}{r_k} - 1)^{2-\beta}]$.

We obtain from (6.2.8) and (6.2.10),

$$\frac{1}{SNR_k} = \alpha \cdot \max[(\frac{r_k}{\epsilon})^\beta, 1] + \nu(r_k) + h_k. \quad (6.2.11)$$

Finally, from (6.2.9) and (6.2.11), and taking $\mathfrak{R} = 2.0 \cdot \epsilon$ (higher values of \mathfrak{R} induce very low rates at the border of the cell), we have the following,

$$e^{\frac{-0.05}{SNR_k}} > 0.99 \Rightarrow r < \nabla \approx 1.4 \cdot \epsilon, \quad (6.2.12)$$

obtained for $\beta = 4.0$ (urban environment), $R_S = 10\mathfrak{R}$ (quasi-infinite network [KA05]), $\alpha = 10^{-10}$, $h_k = 0.03$ (which are realistic parameters according to [CB92, Sce00]) and $f_k = 0.1$. Assumed values for the orthogonality factor are 0.4 for urban macro-cells and 0.06 for urban micro-cells according to [Sce00]. The size of **Zone 1** being close to a micro-cell (a micro-cell is approximately equal in size to half of a macro-cell), it is reasonable to assume that $f_k = 0.1$.

Therefore, users in **Zone 2** are those who are situated at a distance greater than ∇ and for whom formula (6.2.6) is valid with non-negligible probability.

Because TDMA scheduling is not appropriate for users in **Zone 1**, we suggest to serve them in a CDMA fashion (we prove in section 6.3 that this will result in a performance enhancement) while serving users in **Zone 2** in a TDMA fashion, more specifically according to the well-known PF algorithm. To carry out this hybrid scheduling, we suggest in this chapter an alternative scheduling approach to plain PF, termed HPF. At its first hierarchical level, HPF distributes the slots between the two zones in a WRR fashion (**Zone 1** will be served with probability $\mathbb{P}(A_1)$ and **Zone 2** with probability $\mathbb{P}(A_2)$). At its second hierarchical level, HPF serves users inside **Zone 1** in a CDMA fashion and users inside **Zone 2** according to the PF algorithm. We show next that HPF augments the overall mean capacity of the cell.

6.3 Analytical Study of HPF vs. Standard PF

The total number of users present in **Zone 1** is n_1 and in **Zone 2** is n_2 . Traffic demand is uniformly distributed in the cell.

6.3.1 The Average Peak Rate in HPF

Theorem 6.1. The average peak rate obtained in **Zone 1** is given by,

$$R_{HPF,1} = W\mathbb{P}(A_1) \int_0^\infty e^{-x_k} dx_k \left[\log_2(1 + SNR(\epsilon) \cdot x_k) \frac{\epsilon^2}{\nabla^2} + \int_\epsilon^\nabla \log_2(1 + SNR(r_k) \cdot x_k) \frac{2r_k dr_k}{\nabla^2} \right],$$

with event $A_1 = \{\mathbf{Zone 1} \text{ is being served}\}$, $SNR(r_k) = \frac{\phi_k \cdot snr(r_k)}{1 + snr(r_k) \cdot (f_k(1 - \phi_k) + h_k \phi_k)}$ and $\phi_k = \frac{1}{n_1}$.

Proof. The average peak rate of a user k belonging to **Zone 1** served according to HPF (CDMA scheduling) is,

$$R_{HPF,k,1} = W\mathbb{P}(A_1) \int_0^\infty \log_2(1 + SNR(r_k) \cdot x_k) e^{-x_k} dx_k. \quad (6.3.1)$$

The probability that user k is located between r_k and $r_k + dr_k$ in **Zone 1** being $\frac{2\pi r_k dr_k}{\pi \nabla^2}$, we obtain $R_{HPF,1}$. \square

Theorem 6.2. The average peak rate obtained in **Zone 2** is given by,

$$R_{HPF,2} = W\mathbb{P}(A_2) \int_0^\infty f_{n_2}(x_k) dx_k \left[\int_\nabla^{\mathfrak{R}} \log_2(1 + SNR(r_k) \cdot x_k) \frac{2r_k dr_k}{\mathfrak{R}^2 - \nabla^2} \right],$$

with event $A_2 = \{\mathbf{Zone 2} \text{ is being served}\}$, $SNR(r_k) = \frac{snr(r_k)}{1 + snr(r_k) \cdot h_k}$ and $f_{n_2}(x_k) = e^{-x_k} (1 - e^{-x_k})^{n_2 - 1}$.

Proof. In **Zone 2**, users are served according to the PF algorithm and we know that the latter schedules, at time slot t , the user with the highest SNR relative to its current average SNR, i.e. user k^* such as,

$$k^* = \arg \max_k \frac{SNR_k(t)}{T_k(t)},$$

with $SNR_k(t) = SNR(r_k) \cdot x_k(t)$ and T_k being the exponentially smoothed SNR, given by,

$$T_k(t+1) = \left(1 - \frac{1}{\tau}\right) \cdot T_k(t) + \frac{1}{\tau} \cdot SNR_k(t) \cdot \mathbf{1}_{user(t)=k},$$

with $\mathbf{1}_{user(t)=k}$ being the indicator function which equals 1 if user k was chosen at time slot t and 0 otherwise. τ is a time constant that captures the time-scales of the PF scheduler. The random variables representing the fading being i.i.d., we have that $T_k = SNR(r_k) \cdot U_k$, where U_k are identically distributed random variables (but not independent). Moreover, if $\frac{1}{\tau} \rightarrow 0$, then,

$$T_k \rightarrow SNR(r_k) \cdot V, \quad (6.3.2)$$

where V is a constant. In practice, τ has large values and thus, we adopt formula (6.3.2) in our analysis.

Therefore, the average rate of a user k belonging to **Zone 2** served according to the standard PF is:

$$\begin{aligned} R_{HPF,k,2} &= W \cdot \mathbb{E}[\log_2(1 + SNR_k(t)) \cdot \mathbf{1}\{A_2\} \cdot \mathbf{1}\{\frac{SNR_k(t)}{V \cdot SNR(r_k)} = \max_{l=1..n_2} \frac{SNR_l(t)}{V \cdot SNR(r_l)}\}] \\ &= W\mathbb{P}(A_2) \cdot \mathbb{E}[\log_2(1 + x_k SNR(r_k)) \cdot \mathbf{1}\{x_k = \max_{l=1..n_2} x_l\}] \\ &= W\mathbb{P}(A_2) \cdot \mathbb{E}[\log_2(1 + SNR(r_k)x_k) | B_{n_2}] \mathbb{P}(B_{n_2}) \end{aligned}$$

with $B_{n_2} = \{x_k = \max(x_1, \dots, x_{n_2})\}$.

Knowing that $\mathbb{P}(B_{n_2}) = \frac{1}{n_2}$ because the random variables $x_k(t)$ are i.i.d., we obtain,

$$R_{HPF,k,2} = W\mathbb{P}(A_2) \int_0^\infty \log_2(1 + SNR(r_k) \cdot x_k) f_{n_2}(x_k) dx_k, \quad (6.3.3)$$

with $f_{n_2}(x_k) = e^{-x_k}(1 - e^{-x_k})^{n_2-1}$.

The probability that user k is located between r_k and $r_k + dr_k$ in **Zone 2** being $\frac{2\pi r_k dr_k}{\pi(\mathfrak{R}^2 - \nabla^2)}$, we get $R_{HPF,2}$. \square

6.3.2 The Average Peak Rate in Standard PF

The analysis is identical to the one done in **Zone 2** except that $\mathbb{P}(A_2) = 1$ because the cell is considered as a whole. Thus, we get from (6.3.3) the average peak rate of a user k ,

$$R_{PF,k} = W \int_0^\infty \log_2(1 + SNR(r_k) \cdot x_k) f_n(x_k) dx_k, \quad (6.3.4)$$

where $SNR(r_k) = \frac{snr(r_k)}{1 + snr(r_k) \cdot h_k}$ and $f_n(x_k) = e^{-x_k}(1 - e^{-x_k})^{n-1}$.

Hence, the average peak rate of the cell in Standard PF is,

$$R_{PF} = W \int_0^\infty f_n(x_k) dx_k \left[\log_2(1 + SNR(\epsilon) \cdot x_k) \frac{\epsilon^2}{\mathfrak{R}^2} + \int_\epsilon^{\mathfrak{R}} \log_2(1 + SNR(r_k) \cdot x_k) \frac{2r_k dr_k}{\mathfrak{R}^2} \right].$$

We define the following two mean peak rates to evaluate the impact of HPF on both categories of users,

$$\begin{aligned} R_{PF,1} &= W \int_0^\infty f_n(x_k) dx_k \left[\log_2(1 + SNR(\epsilon) \cdot x_k) \frac{\epsilon^2}{\nabla^2} + \int_\epsilon^\nabla \log_2(1 + SNR(r_k) \cdot x_k) \frac{2r_k dr_k}{\nabla^2} \right], \\ R_{PF,2} &= W \int_0^\infty f_n(x_k) dx_k \left[\int_\nabla^{\mathfrak{R}} \log_2(1 + SNR(r_k) \cdot x_k) \frac{2r_k dr_k}{\mathfrak{R}^2 - \nabla^2} \right] \end{aligned}$$

6.3.3 Average Gain

6.3.3.1 Numerical Results

We begin by computing the ratio of the mean peak rate obtained by applying CDMA divided by the mean peak rate obtained by applying the PF algorithm,

$$\psi_k = \frac{\int_0^\infty \log_2\left(1 + \frac{snr_k x_k}{n + snr_k \cdot (f_k(n-1) + h_k)}\right) e^{-x_k} dx_k}{\int_0^\infty \log_2\left(1 + \frac{snr_k x_k}{1 + snr_k h_k}\right) (1 - e^{-x_k})^{n-1} e^{-x_k} dx_k}.$$

We plot, in Figure 6.4, ψ_k as a function of snr_k , for $h_k = 0.03$, $f_k = 0.1$ and $n = 30$. We can see that it is better to apply CDMA when serving users until snr_k goes approximately below 5.0, which means for $r_k \geq 1.5 \cdot \epsilon$ where it is preferable to switch to the PF scheduling. This highlights the validity and sensibility of the idea behind our hierarchical scheduler.

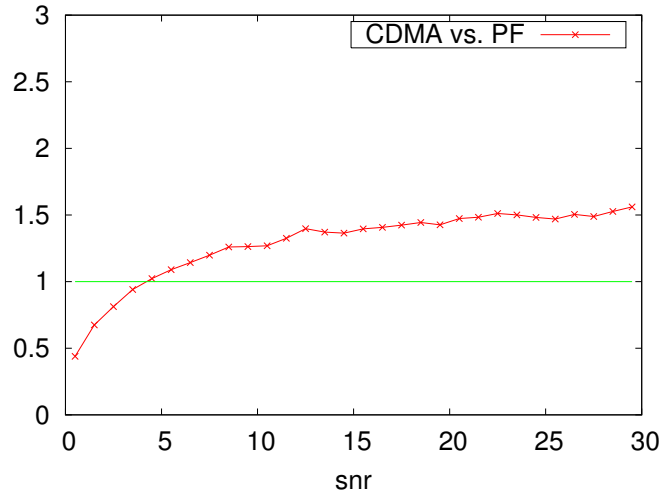


Figure 6.4: Ratio ψ_k for $f=0.1$, $h=0.03$

To evaluate the average gain in the total average peak rate of the cell, we compute the following ratios,

$$\psi = \frac{R_{HPF,1} + R_{HPF,2}}{R_{PF}}, \quad \psi_1 = \frac{R_{HPF,1}}{R_{PF,1}} \quad \text{and} \quad \psi_2 = \frac{R_{PF,2}}{R_{HPF,2}}.$$

Following the assumption that users are uniformly distributed in the cell, it is reasonable to suppose that $n_1 = n \cdot \frac{\nabla^2}{\mathfrak{R}^2}$ and $n_2 = n \cdot \frac{\mathfrak{R}^2 - \nabla^2}{\mathfrak{R}^2}$. To compute the cited ratios, we still have to set the values taken by $\mathbb{P}(A_1)$ and $\mathbb{P}(A_2)$. We begin by setting the value of $\mathbb{P}(A_2)$ such that users in **Zone 2**, in our HPF, have the same chance to access the channel as users in Standard PF situated in the same geographical area, for that reason we take $\mathbb{P}(A_2) = \frac{\mathfrak{R}^2 - \nabla^2}{\mathfrak{R}^2}$ and thus $\mathbb{P}(A_1) = 1 - \mathbb{P}(A_2) = \frac{\nabla^2}{\mathfrak{R}^2}$.

We obtain for $n = 30$: $\psi_1 \approx 1.31$, $\psi_2 \approx 1.1$ and $\psi \approx 1.16$ which means that our HPF will

Zone 1	SPF	HPF	ψ_1
NUM	0.187	0.246	1.31
SIM	0.189	0.251	1.33
Zone 2	SPF	HPF	ψ_2
NUM	0.112	0.102	1.10
SIM	0.12	0.110	1.04

Table 6.1: Total Average Peak Rate

lead to a total gain of 16% in the average peak capacity of the cell without significantly affecting users with low *snr* situated in **Zone 2**.

Nevertheless, if we want to realize more gain in the total peak rate of the cell, we increase $\mathbb{P}(A_1)$ at the expense of lowering the rates realized by users in **Zone 2**. For instance, if we serve **Zone 1** twice as often as **Zone 2**; in other words, if we set $\mathbb{P}(A_1) = 2/3$ and $\mathbb{P}(A_2) = 1/3$, we obtain $\psi \approx 1.39$ leading to a gain of 39%.

6.3.3.2 Simulation Results

We present in this section simulations performed to illustrate the previous results. Users are served according to the Standard PF (SPF) and according to our HPF where slots are distributed such that $\mathbb{P}(A_1) = \frac{\nabla^2}{\mathfrak{R}^2}$ and $\mathbb{P}(A_2) = \frac{\mathfrak{R}^2 - \nabla^2}{\mathfrak{R}^2}$. The number of users in each zone is fixed and equal to 15. We take $W = 1.0$, $h_k = 0.03$, $f_k = 0.1$ and $\epsilon = 1.0$. In all experiments, we determine the average rate per user and display the results for users belonging to the same zone. We plot the average rate realized by users occupying a ring of internal radius r and external radius $r + dr$ such that $dr = 0.01$ and compare results with what we obtain using formulae (6.3.1) and (6.3.3) respectively for **Zone 1** and **Zone 2** in HPF, and formula (6.3.4) in SPF for a given user situated at distance r from the BS. In Figure 6.6, we notice a slight degradation in the average rate in our model in comparison with SPF as predicted. However, in Figure 6.5, we can see how close users benefit from being served in a CDMA fashion rather than in a TDMA fashion as it is done in the PF scheduler. Furthermore, we can see how the analytical results give very precise estimations of the simulation results as the two curves are indistinguishable.

In table 6.1, we compute the mean rate obtained in each zone by simulation and we compared it to the mean rate obtained numerically from $R_{HPF,1}$ and $R_{HPF,2}$ for HPF and from $R_{PF,1}$ and $R_{PF,2}$ for SPF, respectively for **Zone 1** and **Zone 2**. We can see that the two sets of values are very close. Finally, we obtain $\psi = 1.17$ by simulation and $\psi = 1.16$ numerically.

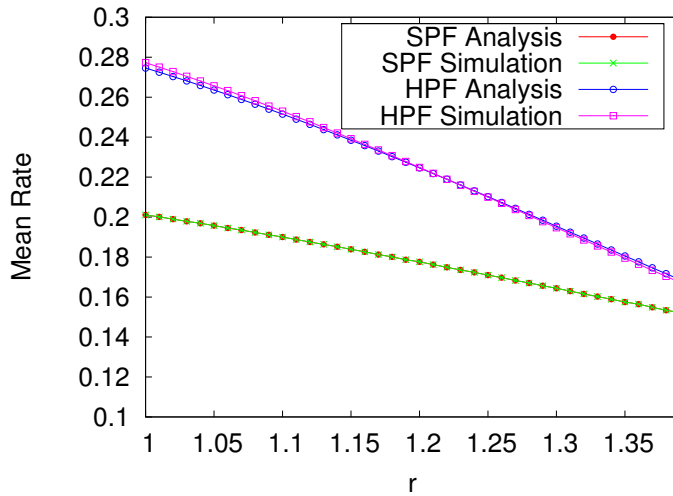


Figure 6.5: Average Rate for Zone 1

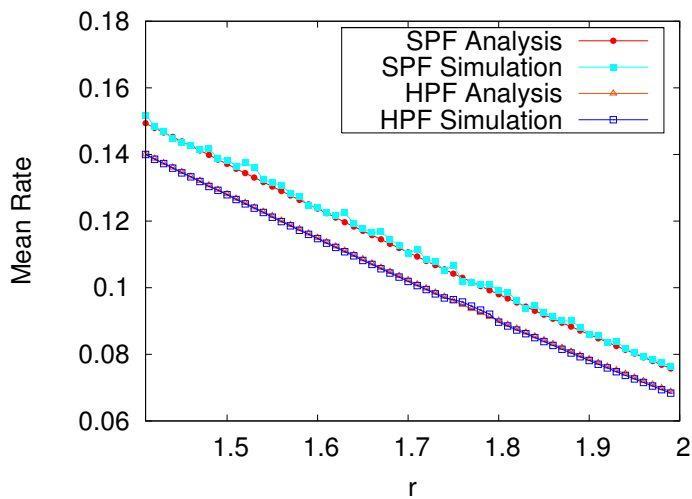


Figure 6.6: Average Rate for Zone 2

6.4 Dynamic Model of HPF

In order for **Zone x** to behave like a Multi-class PS system [Coh78], its service rate must only depend on the total number of users occupying it.

In **Zone 1**, the SNR of user k is,

$$SNR_{k,1} = \frac{\phi_k}{\alpha/\gamma_k + \nu_k + f \cdot (1 - \phi_k) + h \cdot \phi_k}. \quad (6.4.1)$$

In order for **Zone 1** to behave like a Multi-class PS system, we need to adopt the following two assumptions in our analytical model:

6.4.0.2.1 Hypothesis I: We compute the SNR at an "average location" within **Zone 1** by replacing, in (6.4.1), γ_k and ν_k by their sample averages γ_I and ν_I for r_k ranging from ϵ to ∇ . In practical radio network dimensioning, it is not possible to use the parameters of each user but average values of the individual parameters among users ([HT02, SH00]) which makes this first assumption fairly plausible. Besides, considering two ranges of r by considering two zones will give us much more precise values for these parameters than those obtained by considering the cell as a whole. The average parameters are obtained according to the following,

$$\alpha/\gamma_I + \nu_I = \int_{\epsilon}^{\nabla} \frac{\alpha(\frac{r_k}{\epsilon})^{\beta} + \nu(r_k)}{\nabla^2} 2r_k dr_k + (\frac{\epsilon}{\nabla})^2 \cdot (\alpha + \nu(\epsilon)). \quad (6.4.2)$$

6.4.0.2.2 Hypothesis II: Due to the fact that we are considering an average value of the SNR, the impact of fading will not be taken into consideration in the analysis. That is once again a reasonable assumption in a CDMA system where the fading of the channel will be combated through the various available techniques [Sys05] (space time coding, adaptive modulation, dynamic frequency selection, etc.) and where the high rates available in **Zone 1** will further minimize the effect of fading.

In section 6.4.2, we will corroborate the validity of these two hypothesizes through simulation by showing that the discrepancy between the values obtained by making these two assumptions in the analytical model, from those obtained by simulation, where these assumptions are omitted, is negligible. Finally, we have the following, for $\phi_k = \frac{1}{n_1}$,

$$SNR_I(n_1) = (n_1 \cdot (\alpha/\gamma_I + \nu_I + f) + h - f)^{-1}.$$

As a consequence, each user will get the following rate when the BS divides its transmission power P equally between active users,

$$R_1 = W \log_2(1 + SNR_I(n_1)) \mathbb{P}(A_1).$$

In **Zone 2**, we know from (6.3.3) that the rate of user k is,

$$R_{HPF,k,2} = W \mathbb{P}(A_2) \int_0^{\infty} e^{-x_k} (1 - e^{-x_k})^{n_2-1} \cdot \log_2(1 + x_k \cdot SNR_{k,2}) dx_k,$$

with $SNR_{k,2} = (\alpha/\gamma_k + \nu_k + h)^{-1}$.

We define the following,

$$F_{k,2}(n_2) = \frac{R_{HPF,k,2}}{W \mathbb{P}(A_2) \cdot \log_2(1 + SNR_{k,2})}. \quad (6.4.3)$$

By plotting $F_{k,2}(n_2)$ as a function of $\nabla \leq r \leq \Re$ for different values of n_2 , we can see in Figure 6.7 that it varies slightly and can be well approximated by a constant for every value of n_2 .

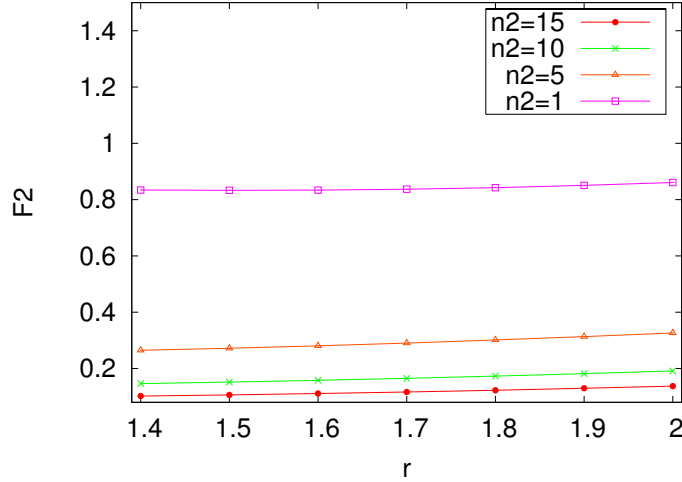


Figure 6.7: $F_{k,2}(n_2)$ as function of r

Thus, we define $F_2(n_2)$ that consists in replacing γ_k and ν_k by their average values γ_{II} and ν_{II} in (6.4.3). The average parameters are obtained according to,

$$\alpha/\gamma_{II} + \nu_{II} = \int_{\nabla}^{\Re} \frac{\alpha(\frac{r_k}{\epsilon})^\beta + \nu(r_k)}{\Re^2 - \nabla^2} 2r_k dr_k. \quad (6.4.4)$$

We adopt the subsequent approximation $F_{k,2}(n_2) \approx F_2(n_2)$ necessary for **Zone 2** to behave like a Multi-class PS system. We compute the following standard deviation $\frac{|F_{k,2}(n_2) - F_2(n_2)|}{F_{k,2}(n_2)}$ for $\nabla \leq r \leq \Re$ and $1 \leq n_2 \leq 15$ realizing that the maximum deviation from the real value is approximately equal to 0.15 at $n_2 = 15$ and $r = \Re$. We will further validate this approximation through simulation.

6.4.1 The Processor Sharing Model

Users arrive as a Poisson process of intensity $\lambda \cdot ds$ in any area of surface ds . Flow sizes are i.i.d. and σ is the corresponding random variable. We denote by $\rho = \lambda \cdot \mathbb{E}[\sigma]$ the traffic density and by $d\rho(r) = \rho \cdot 2\pi r dr$ the traffic intensity generated by users whose distance to the BS ranges between r and $r + dr$. The maximum number of simultaneously admitted users in **Zone x** will be limited to $n_{Max,x}$ in order to guarantee a minimum rate. New transfers generated in a zone where they are already $n_{Max,x}$ transfers in progress are blocked and lost. Based on the above analysis, we see that, in every zone, each user k is served at a fraction $F_x(n_x)$ of some constant $c_{k,x}$ whenever there are n_x active users in its

zone:

In **Zone 1**

$$F_1(n_1) = \log_2(1 + SNR_I(n_1)) \quad (6.4.5)$$

$$c_{k,1} = W \cdot \mathbb{P}(A_1)$$

In **Zone 2**

$$F_2(n_2) = \frac{\int_0^\infty e^{-x_k} (1 - e^{-x_k})^{n_2-1} \log_2(1 + x_k \cdot SNR_{II}) dx_k}{\log_2(1 + SNR_{II})} \quad (6.4.6)$$

$$c_{k,2} = W \cdot \mathbb{P}(A_2) \log_2(1 + SNR_k)$$

with $SNR_{II} = (\alpha/\gamma_{II} + \nu_{II} + h)^{-1}$

We see from (6.4.5) and (6.4.6) that $F_x(\cdot)$ is an arbitrary positive function satisfying the subsequent constraints for $n_x \leq n_{Max,x}$:

$$0 \leq F_x(n_x) \leq \infty \quad (\text{I})$$

$$\text{and } n_x \cdot F_x(n_x) \leq \infty \quad (\text{II})$$

Thus, every zone behaves like a PS system with equal but time varying service allocation as users randomly enter and leave the system. As a consequence, we can directly apply the formulae in [Coh78] regarding the stationary state distributions of our system with the assumption that users arrive according to a Poisson process. As already mentioned, such a system has the well-known insensitivity property. Hence, our scheduling approach, in addition to increasing the overall throughput of the cell, relieves it from dimensioning issues.

The stationary distribution of the number of active users in **Zone x** is,

$$\pi_x(n) = \frac{\frac{\rho_x^n}{\psi_x(n) \cdot n!}}{\sum_{k=0}^{n_{Max,x}} \frac{\rho_x^k}{\psi_x(k) \cdot k!}},$$

where $\psi_x(n) = \prod_{i=1}^n F_x(i)$ and ρ_x is the load in **Zone x**:

- $\rho_1 = \int_\epsilon^\nabla \frac{d\rho(r_k)}{c_{k,1}} = \frac{\rho\pi(\nabla^2 - \epsilon^2)}{W\mathbb{P}(A_1)}$.
- $\rho_2 = \int_\nabla^\Re \frac{d\rho(r_k)}{c_{k,2}} = \frac{\rho\pi}{W\mathbb{P}(A_2)} \int_\nabla^\Re \frac{2r_k dr_k}{\log_2(1 + SNR_{k,2})}$.

Using Little's law, we find that the flow throughput $Th_{k,x}$ of user k in **Zone x**, defined as

the ratio of the mean flow size $\mathbb{E}[\sigma]$ to the mean flow duration, is given by,

$$Th_{x,k} = c_{x,k} \cdot \frac{\rho_x (1 - B_x)}{\mathbb{E}[n_{MAX,x}]},$$

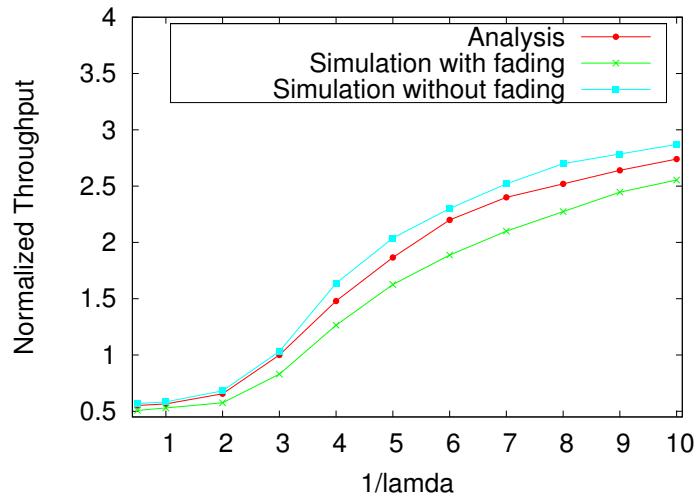
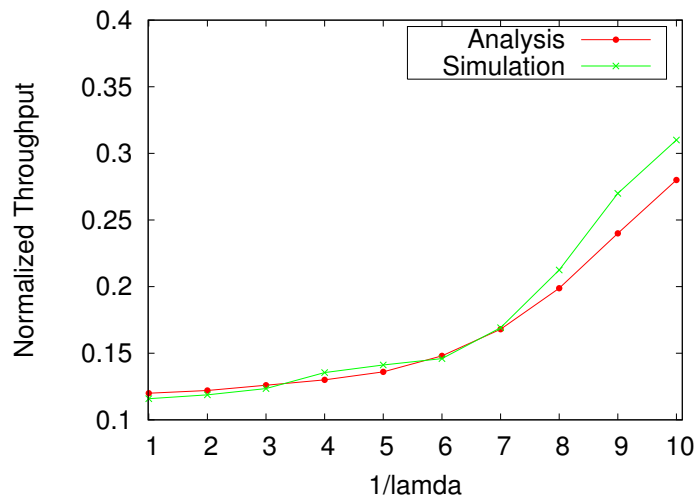
where, in **Zone** \mathbf{x} , $B_x = \pi_x (n = n_{Max,x})$ is the blocking probability and $\mathbb{E}[n_{Max,x}] = \sum_{i=1}^{n_{Max,x}} i \cdot \pi_x(i)$ is the mean number of active users.

6.4.2 Simulation Results

We present here our simulations performed to illustrate the above results. We consider a system where users initiate file transfer requests as a Poisson process of intensity $\lambda_T = \lambda\pi\mathfrak{R}^2$ and traffic demand is uniformly distributed in the cell. At most 15 users are admitted simultaneously in each zone ($n_{Max,x} = 15$). The system operates in a time-slotted fashion with a slot duration equal to 2ms. We take $W = 1.0$, $h = 0.03$, $f = 0.1$ and $\epsilon = 1.0$. Flow sizes are independent and exponentially distributed with normalized mean equal to 20. Users are served according to our hierarchical approach of PF where each zone is served at a time ($\mathbb{P}(A_1) = \mathbb{P}(A_2) = 1/2$). We obtain respectively from (6.4.2) and (6.4.4), $\alpha/\gamma_I + \nu_I \approx 0.05$ and $\alpha/\gamma_{II} + \nu_{II} \approx 0.5$. The divergence in the preceding two values show the difficulty to give fitting mean values for the parameters γ_k and ν_k when we consider the entire cell. This explains why we failed to find an appropriate analytical model for the Standard PF as it covers the whole cell.

We determine the normalized throughput per user $T_{x,k}/c_{x,k}$ and display the average normalized throughput for users belonging to the same zone as a function of $\frac{1}{\lambda_T}$. The simulation results obtained are compared to the analytical results of subsection 6.4.1. For **Zone 1**, we run two sets of simulations to show that the proposed Multi-class PS model is still valid in spite of the two restrictive hypotheses considered in section 6.4.1: in the first set of simulations, fading is omitted, while in the second set, we consider a Rayleigh fading channel. However, in the two sets of experiments, the parameters γ_I and ν_I are not taken as constants as in the analytical model but vary with distance. Similar to **Zone 1**, in simulations we run for **Zone 2**, the parameters γ_{II} and ν_{II} are not taken as constants as in the analytical model but vary with distance. Figures 6.8 and 6.9 depict the average normalized throughput as a function of $\frac{1}{\lambda_T}$.

In Figure 6.8, we can see how analytical results are very close to simulation results when fading is omitted. Nevertheless, when fading is taken into consideration, simulation results follow the same trend as analytical results and are reasonably close. In Figure 6.9, we can see how analytical formulae provide highly accurate estimates of simulation results especially at moderate to high loads. Therefore, we can fairly consider that the proposed analytical model approximates very well the behaviour of our HPF.

Figure 6.8: Throughput as a function of $\frac{1}{\lambda_T}$ in **Zone 1**Figure 6.9: Throughput as a function of $\frac{1}{\lambda_T}$ in **Zone 2**

6.5 Concluding Remarks

This work suggested decoupling the cell into two zones and serving each zone in a WRR fashion using an appropriate scheduler. We chose to apply the PF algorithm for **Zone 2** because the feasible rate of users belonging to this zone is almost proportional to their SNR and because of their moderate to bad channel conditions which require serving one user at a time to cancel intracell interference. Whereas for **Zone 1**, we chose to serve its users in a CDMA fashion because of the logarithmic relation between their SNR and their feasible rate and because of the good channel conditions they experience. We proved that

our scheduler globally increased performances in terms of average rates besides the fact that the model resulting from our proposed scheduler is completely tractable which frees the system from dimensioning issues.

Chapter 7

Flow Size-Aware Proportional Fair Schedulers

In this chapter, we address and solve the third drawback of PF, relative to Assumption 3 given in chapter 4, i.e. its lack of efficiency when serving short-lived flows. We show through simulations that PF fails to treat short flows fairly which can be critical as they represent the majority of data flows. In this chapter, we propose three enhanced size-aware opportunistic schedulers that significantly reduce the transfer time of short flows without imposing a significant degradation on the performances of long flows.

7.1 Introduction

The PF scheduler is the most widely adopted opportunistic scheduler in 3G wireless networks. Unfortunately, it is biased against short-lived flows because the algorithm behind the scheduler cannot converge when it comes to serving a flow that only lasts a few time slots. This is critical because, as it has been shown by various Internet traffic analyses [CB97], data traffic consists of a small number of long-lived flows while the largest number of flows are short-lived. Furthermore, opportunistic schedulers rely on elastic traffic delay tolerance to schedule flows only when their channel quality is relatively high. But how long a short flow is willing to wait for good channel conditions when its performance goal is to minimize transfer latency, contrary to long flows whose performance goal is to maximize throughput. Hence, there always exists a compromise between two conflicting objectives when opportunistic schedulers serve elastic traffic: guaranteeing efficiency for long flows and providing short-term temporal fairness for short flows. Therefore, devising opportunistic scheduling policies which provide a prompt service to short flows while only incurring a slight penalty to long flows in terms of realized throughput is of paramount importance.

In addition, short flows suffer from other issues mainly related to the TCP protocol. Indeed, current TCP congestion control mechanisms focus on network feedback. This approach is too conservative for short flows which take often less than one round-trip time to communicate and results in underutilization of available network bandwidth. In wireline networks, the problem of protecting short flows from the adverse impact of TCP has been well studied. In [Kle76], a Least Attained Service (LAS) scheduling scheme is presented where short flows are favoured. More recently, the authors in [AABN03] (see also the references therein) developed a two level priority Processor Sharing scheme that exploit the file size information to favour short-lived flows. Other interesting approaches are found in [Alt03, PAAD03]. In the wireless domain, the issues related to the TCP protocol are further exacerbated because of the highly variable nature of the radio resource. Therefore, to help protect short-lived flows while allocating efficiently the scarce wireless resources, we propose in this chapter three flow size-aware opportunistic schedulers where file size information is integrated in the PF algorithm to reduce the Sojourn Time experienced by short flows. The proposed schemes provide a notable enhancement to short-lived flows performances, without a significant degradation in the QoS supplied to long-lived flows. We note that the interaction between the TCP protocol and our proposed models are not investigated in the present chapter but in the following one.

The rest of the chapter is organized as follows. In section 7.2, we present the radio propagation model and our traffic hypotheses. In section 7.3, we show how the PF scheduler is biased against short-lived flows. In sections 7.4 to 7.6, we present our three flow size-aware opportunistic scheduling mechanisms along with analytical study and simulations to assess performances. We give conclusions in section 7.7.

7.2 Radio Model and Traffic Characteristics

The radio model used in this chapter is mainly that of section 4.2.1 in chapter 4: the propagation model of subsection 4.2.1.1 remains the same, however, the mean feasible rate in formula 4.2.6 of subsection 4.2.1.2 is modified as background noise is neglected. Hence, we obtain the following for the feasible rate of user k ,

$$R_k(r, t) = C_k(r) \cdot x_k(t), \quad (7.2.1)$$

where the mean feasible rate $C_k(r)$ of user k is given by,

$$C_k(r) = \frac{W}{\sigma} \cdot h\left(\frac{\mathfrak{R}}{r}\right), \quad (7.2.2)$$

and $h^{-1}\left(\frac{\mathfrak{R}}{r}\right) = (2\frac{\mathfrak{R}}{r}-1)^{-\beta} + 2 \cdot \left(\left(\frac{\mathfrak{R}}{r}-1\right)^2 + 3\left(\frac{\mathfrak{R}}{r}\right)^2\right)^{-\frac{\beta}{2}} + (2\frac{\mathfrak{R}}{r}+1)^{-\beta} + 2 \cdot \left(\left(\frac{\mathfrak{R}}{r}+1\right)^2 + 3\left(\frac{\mathfrak{R}}{r}\right)^2\right)^{-\frac{\beta}{2}}$

Note that we did not add to the model the refinements of chapters 5 and 6 to investigate only the impact of *Assumption 3* on PF. Therefore, the feasible rate $R_k(r, t)$ varies linearly with the i.i.d. fast fading fluctuations $x_k(t)$ for all users in this model. As we consider Rayleigh fading, x_k follows an exponential distribution.

7.2.1 Traffic Characteristics

We assume traffic demand is uniformly distributed in the cell. Data flows arrive as a Poisson process of intensity $\lambda \cdot ds$ in any area of surface ds . Flow size σ follows the Bounded Pareto (BP) distribution which is commonly used in analysis because it can exhibit the high variance property as observed in the Internet traffic and also because the maximum flow size can be set to mimic the largest Internet flow size. We denote the BP distribution by $BP(p, q, \alpha)$ where p and q are respectively the minimum and maximum flow size and α is the exponent of the power law. The probability density function of the BP distribution is,

$$f(x) = \frac{\alpha \cdot \left(\frac{p}{C}\right)^\alpha}{1 - \left(\frac{p}{q}\right)^\alpha} \cdot x^{-\alpha-1}, \quad p \leq x \leq q, 0 \leq \alpha \leq 2,$$

where C is the mean rate of the flow.

We will consider the following realistic scenario:

- 80% of flows are short flows and their size follows the following Bounded Pareto distribution $BP(1\text{kbytes}, 10\text{kbytes}, 1.16)$ of mean $\mathbb{E}[\sigma_S] = 2.4\text{kbytes}$.
- 20% of flows are long flows and their size follows the following Bounded Pareto distribution $BP(10\text{kbytes}, 5000\text{kbytes}, 1.16)$ of mean $\mathbb{E}[\sigma_L] = 45.7\text{kbytes}$.

Thus, the load of short flows is approximately 17.5% of total load while the load of long flows is approximately 82.5% of total load. Hence, we have two classes of flows and we denote by $d\rho_S = 2\pi r dr \cdot \lambda_S \mathbb{E}[\sigma_S]$ and by $d\rho_L = 2\pi r dr \cdot \lambda_L \mathbb{E}[\sigma_L]$ the traffic intensity respectively generated by short flows and long flows whose distance to the BS is between r and $r + dr$, where $\rho_S = 0.8 \cdot \rho$ and $\rho_L = 0.2 \cdot \rho$.

7.3 Proportional Fair Algorithm

We know that in the PF algorithm, at time slot t , the scheduled user is the one with the highest feasible rate relative to its current average throughput, i.e. user k^* such as,

$$k^* = \arg \max_k \frac{R_k(r_k, t)}{T_k(r_k, t)},$$

where $T_k(r_k, t)$ is the exponentially smoothed throughput given by formula (4.2.9) in chapter 4.

As explained in chapter 4, when the PF algorithm reaches convergence, it behaves like a Multi-class PS system treating all users fairly while taking advantage from the channel variations. However, PF is not quite fair and efficient when serving short-lived flows which is a real issue considering that these flows represent the majority of elastic traffic. To highlight this fact, we give in the following section the analysis of the dynamic model of PF; in particular, we give the analytical expressions for the mean sojourn time of short flows and the mean throughput of long flows and underline the discrepancy, at high loads, between the mathematical model and simulation results for short flows.

7.3.1 The Analytical Study of PF

When convergence is reached, PF behaves like a Multi-class PS system, thus we can compute the mean transfer delay for short flows and mean throughput for long flows according to [Coh78].

The stationary distribution of the number of active flows is,

$$\pi(x) = \frac{\prod_{i=1}^x \frac{\rho}{G(i)}}{\sum_{k=0}^n \prod_{i=1}^k \frac{\rho}{G(i)}},$$

where $\rho = \int_{\epsilon}^{\mathfrak{R}} \frac{d\rho(r)}{C(r)}$ is the load in the cell with $d\rho(r) = d\rho_S(r) + d\rho_L(r)$ and n is the maximum number of admitted flows. $C(r)$ follows from (7.2.2).

Using Little's law, the mean transfer delay experienced by a short flow k is,

$$\mathbb{E}[S_{S,k}] = \frac{\mathbb{E}[\sigma_S] \cdot \mathbb{E}[n]}{C_k(r) \cdot \rho \cdot (1 - B)}, \quad (7.3.1)$$

where $B = \pi(x = n)$ is the blocking probability and $\mathbb{E}[n] = \sum_{i=1}^n i \cdot \pi(i)$ is the mean number of active flows.

The throughput of a long flow k , defined as the ratio of the mean long flow size $\mathbb{E}[\sigma_L]$ to the mean long flow duration, is,

$$Th_{L,k} = \frac{\rho \cdot (1 - B) \cdot C_k(r)}{\mathbb{E}[n]}. \quad (7.3.2)$$

7.3.2 Numerical Experiments

We present in this subsection our numerical experiments that illustrate the previous analytical results. We consider a system where users initiate file transfer requests as a

Poisson process of intensity $\lambda\pi\mathfrak{R}^2$. Flow sizes are independent and follow the composite heavy-tailed distribution presented in section 7.2.1. Users are served according to the PF algorithm and at most $n = 40$ users are admitted in the system to guarantee a minimum rate of $C_{min} = \frac{C(\mathfrak{R})}{40}$. New transfers generated when the maximum number of users is already in progress are blocked and lost. We take $\frac{W}{\sigma} = 5.0$. We determine the normalized mean sojourn time for short flows $\mathbb{E}[S_{S,k}] \cdot C_k(r)$, obtained from (7.3.1), depicted in Figure 7.1. We also determine the normalized mean throughput $\frac{Th_{L,k}}{C_k(r)}$ for long flows, obtained from (7.3.2), depicted in Figure 7.2.

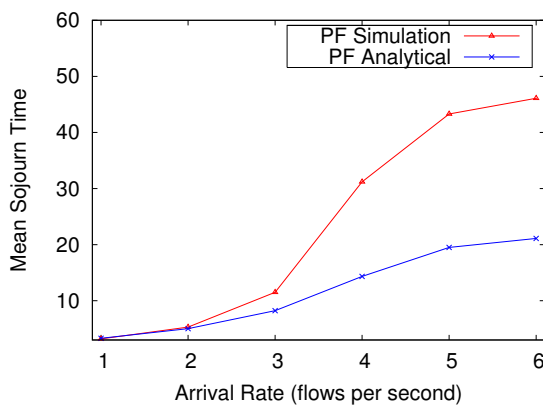


Figure 7.1: Mean Sojourn Time of short flows

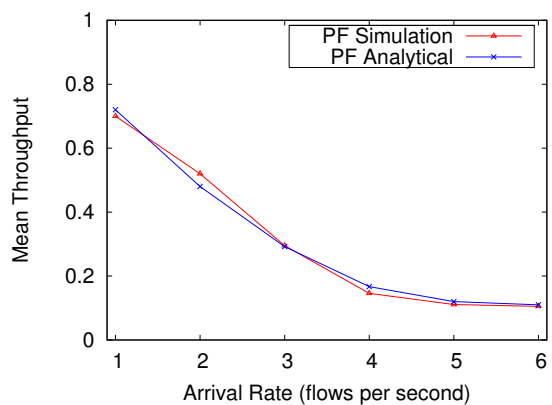


Figure 7.2: Mean Throughput of long flows

We can see in Figure 7.2 that the analytical formulae provide highly accurate estimates of results obtained by simulation for long flows which is not the case when $\lambda \geq 3.0$ ($\rho_S \geq 0.45$) for short flows as graphed in Figure 7.1. Indeed, in PF, it is impractical to guarantee the same probability of accessing the channel for all flows over short time scales; yet, over longer time scales, as channel conditions vary, lagging flows can "catch up" which is not possible for short flows. This situation is, of course, further aggravated at high loads when the cell is crowded because short flows have to wait longer for their turn which can have a severe impact on their sojourn time. This problem is more emphasized by the large value taken by τ , the time constant of the PF smoothing filter, in formula (1.2.4) of chapter 1. However, reducing the value of τ is not an appropriate solution because it deprives us from better exploiting multi-user diversity. A better solution could be to augment gradually τ with the size of the flow. Another possible solution would be to give the exponentially smoothed throughput a very small initial value $T(r_k, t = 0)$ in order to favour short flows, but then the latter will take slots even with very poor current rates which is contrary to the PF target.

To overcome this inherent drawback of PF, we propose in this chapter three modified versions of PF where short flows are given preferential treatment. We suggest in the first

algorithm – termed Size-Based Hierarchical PF (SB-HPF) – to isolate short flows from long flows, in order to protect the former. Slots are first distributed among the two classes of flows and inside each class, flows are served according to the PF algorithm. In the second algorithm – termed Size Based Adapted PF (SB-APF) – we tweak the PF algorithm in a way to augment the probability of short flows to access the channel. The last algorithm – termed PF-LAS – is a combined version of both PF and the LAS (Least Attained Service) algorithm [RUK03], which is known to favour short flows to the few largest flows.

7.4 The SB-HPF Scheduler

Our hierarchical scheduler serves alternately short flows (with a weight w_S) and long flows (with a weight w_L) that are separated logically into two classes and applies independent PF to each class.

7.4.1 The Analytical Study of SB-HPF

Because the two classes of flows, served by means of PF, behave like a Multi-class PS system, we can compute the average transfer delay for short flows and the average realized throughput for long flows. The stationary distribution of the number of active flows in class Z is,

$$\pi_Z(x) = \frac{\prod_{i=1}^x \frac{\rho_Z}{G(i)}}{\sum_{k=0}^{n_Z} \prod_{i=1}^k \frac{\rho_Z}{G(i)}},$$

where $\rho_Z = \int_{\epsilon}^{\mathcal{R}} \frac{d\rho_Z(r)}{C(r) \cdot w_Z}$ is the load in class Z and n_Z is the maximum number of admitted flows in that class.

From Little's law, the mean transfer delay experienced by a short flow k is,

$$\mathbb{E}[S_{S,k}] = \frac{\mathbb{E}[\sigma_S] \cdot \mathbb{E}[n_S]}{C_k(r) \cdot w_S \cdot \rho_S \cdot (1 - B_S)}, \quad (7.4.1)$$

where $B_S = \pi_S(x = n_S)$ is the blocking probability for short flows and $\mathbb{E}[n_S] = \sum_{i=1}^{n_S} i \cdot \pi_S(i)$ is the mean number of active short flows.

The throughput $Th_{L,k}$ of a long flow k – defined as the ratio of the mean long flow size $\mathbb{E}[\sigma_L]$ to the mean long flow duration – is,

$$Th_{L,k} = \frac{\rho_L \cdot (1 - B_L) \cdot C_k(r) \cdot w_L}{\mathbb{E}[n_L]}, \quad (7.4.2)$$

where $B_L = \pi_L(x = n_L)$ is the blocking probability for long flows and $\mathbb{E}[n_L] = \sum_{i=1}^{n_L} i \cdot \pi_L(i)$ is the mean number of active long flows.

The allocation of slots being dynamic, the proposed scheduler will guarantee a minimum

throughput $Th_{L,k}$ and a maximum sojourn time $\mathbb{E}[S_{S,k}]$ for each flow k .

7.4.1.1 Numerical Experiments

We present in this section our numerical experiments performed with the same parameters as those presented in section 7.3.2. Users are served according to PF ($n = 40$) and according to SB-HPF that comprises 2 different scenarios:

- SB-HPF(2,1) where short flows receive 2 times more slots than long flows, i.e. $w_S = 2/3$ and $w_L = 1/3$. To obtain the same minimum rate as in PF ($C_{min} = \frac{C(\mathfrak{R})}{40}$), at most 26 short flows ($C_{min} = \frac{C(\mathfrak{R})}{26} \cdot \frac{2}{3}$) and 14 long flows ($C_{min} = \frac{C(\mathfrak{R})}{14} \cdot \frac{1}{3}$) are admitted simultaneously.
- SB-HPF(1,2) where long flows receive 2 times more slots than short flows, i.e. $w_L = 2/3$ and $w_S = 1/3$. To obtain the same minimum rate as in PF, at most 26 long flows ($C_{min} = \frac{C(\mathfrak{R})}{26} \cdot \frac{2}{3}$) and 14 short flows ($C_{min} = \frac{C(\mathfrak{R})}{14} \cdot \frac{1}{3}$) are admitted simultaneously.
- SB-HPF(1,1) where each category of flows is served one at a time, i.e. $w_L = 1/2$ and $w_S = 1/2$. To obtain the same minimum rate as in PF, at most 20 long flows and 20 short flows ($C_{min} = \frac{C(\mathfrak{R})}{20} \cdot \frac{1}{2}$) are admitted simultaneously.

In all experiments, we determine the normalized average sojourn time for short flows $\mathbb{E}[S_{S,k}] \cdot C_k(r)$ from (7.4.1) and the normalized average throughput for long flows $\frac{Th_{L,k}}{C_k(r)}$ from (7.4.2).

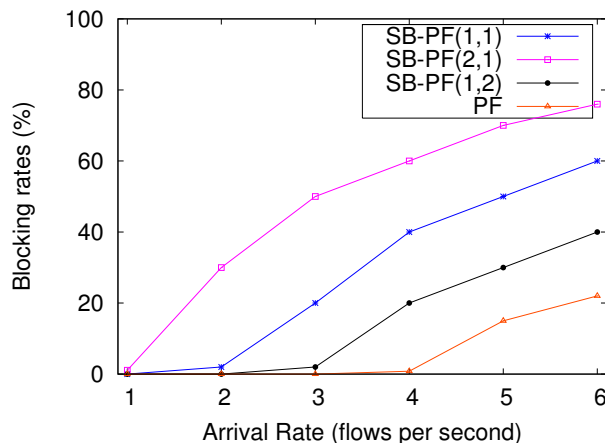


Figure 7.3: Blocking Rates for long flows

Figures 7.4, 7.6 and 7.8 illustrate the mean sojourn time for short flows as a function of arrival rate and indicate that the analytical formulae provide a highly accurate estimate for SB-HPF. However, a slight divergence is noticed in SB-HPF(1,2) for $\lambda < 3.0$ because

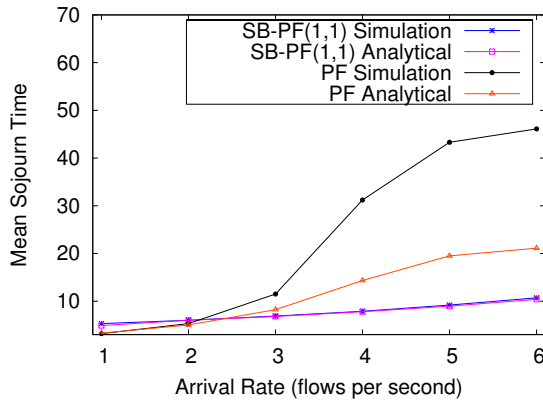


Figure 7.4: Mean Sojourn Time of short flows for SB-HPF(1,1)

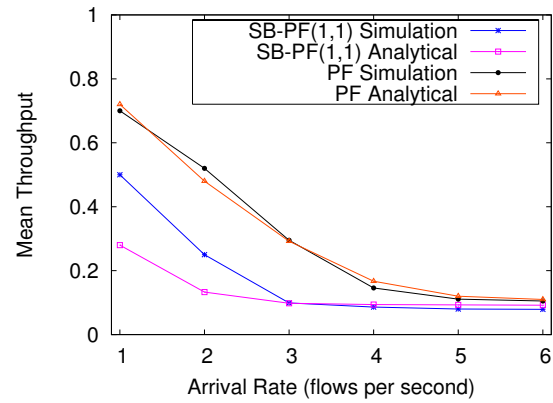


Figure 7.5: Mean Throughput of long flows for SB-HPF(1,1)

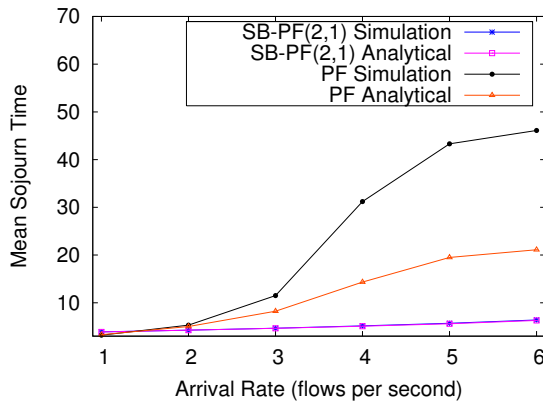


Figure 7.6: Mean Sojourn Time of short flows for SB-HPF(2,1)

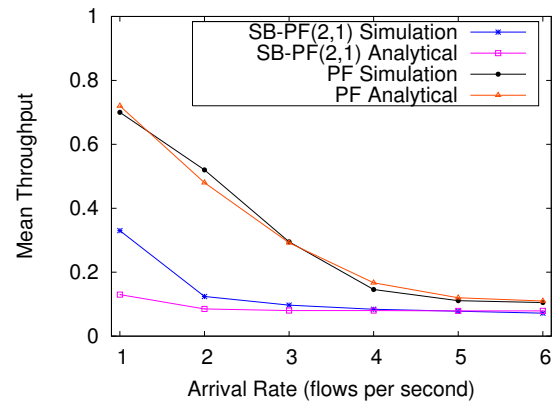


Figure 7.7: Mean Throughput of long flows for SB-HPF(2,1)

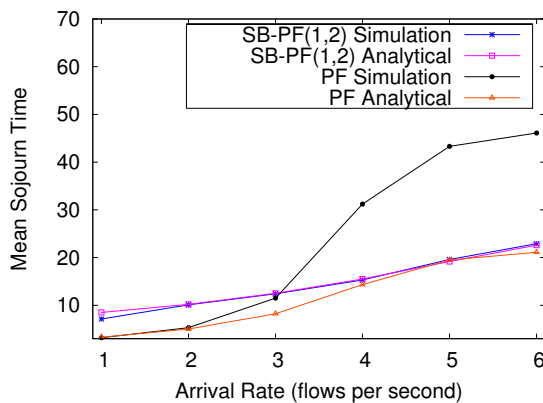


Figure 7.8: Mean Sojourn Time of short flows for SB-HPF(1,2)

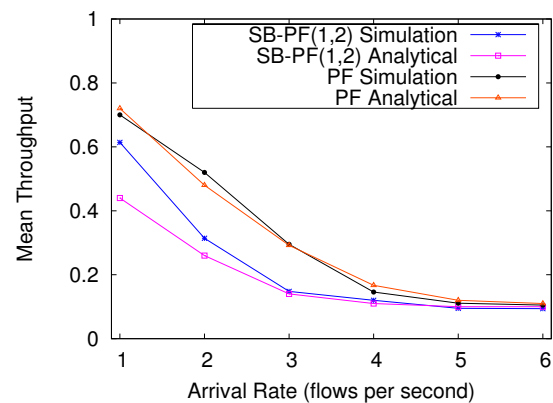


Figure 7.9: Mean Throughput of long flows for SB-HPF(1,2)

short flows profit from the excess of slots reserved to long flows, the latter being served twice more often but arriving in the system four times less frequent than short flows. Yet,

at moderate to high load, mathematical results and simulation results are indistinguishable which proves that the PF algorithm converges well for short flows when they are separated from long flows.

Figures 7.5, 7.7 and 7.9 illustrate the mean throughput for long flows as a function of arrival rate and indicate that the analytical formulae give a lower bound on simulation results at low load, while at high load, the two sets of values coincide as predicted.

As for results, we can see from Figure 7.4 that short flows profit largely from being isolated from long flows for $\lambda > 2.0$. For smaller values of λ , the mean number of short flows is strictly smaller than 1 in SB-HPF which means that there are rarely more than two flows present simultaneously in the system and consequently short-lived flows do not profit from the gain resulting from multi-user diversity. For the same values of λ , there are more flows in the system served according to the original PF and thus short flows profit from the benefits of opportunistic scheduling without its mentioned adverse effects in a crowded cell. The gain obtained for short flows at high load comes at the expense of long flows who will see a degradation in their performances in terms of mean throughput. Nevertheless, the degradation is not severe at low load because long flows profit from the surplus of slots reserved to short flows. As for high load, although this deterioration in performances is limited by admission control, it comes at the cost of relatively high blocking rates as depicted in Figure 7.3. However, in SB-HPF(1,2), long flows perceive only a slight degradation in terms of mean throughput at a cost of acceptable blocking rates at high load in comparison with the original PF. As for short flows, we can see in Figure 7.8 that for $\lambda \geq 3.0$, they realize much lower transfer delays in comparison with PF. We conclude that SB-HPF(1,2) is beneficial at high loads, exactly when the PF algorithm falls short from treating fairly short flows, while still preserving the performances of long flows.

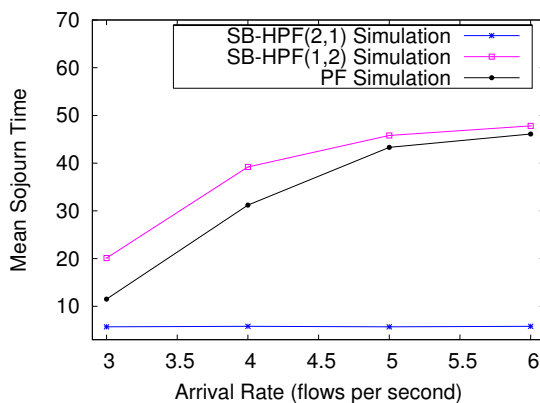


Figure 7.10: Mean Sojourn Time of short flows

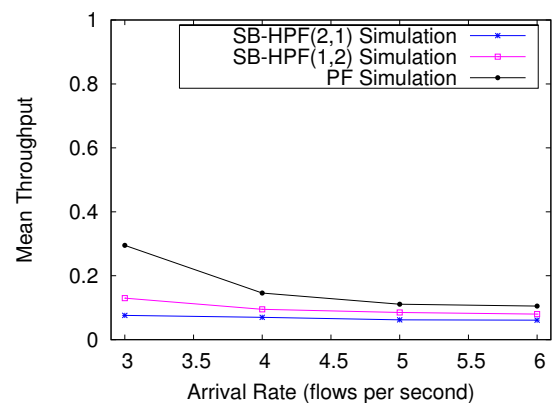


Figure 7.11: Mean Throughput of long flows

In what preceded, we supposed that we had an ideal knowledge of the size of each flow, yet, this is not the case in practice. Since the majority of data flows are short flows, we will run another set of experiments where we will start off optimistically by considering that every new flow is a short flow. If a flow turns out to be a long flow (the number of packets received for this flow goes beyond a certain threshold (10Kbytes)), then the system switches it to the class of long flows. We will present the results obtained for SB-HPF(1,2) and SB-HPF(2,1), depicting short flow performances in Figure 7.10 and long flows performances in Figure 7.11. As we can see from Figure 7.10, short flows suffer from increasing transfer delays in SB-HPF(1,2) as compared with PF. This was expected as the main benefit of the proposed algorithm vanishes when long and short flows are initially mixed. The bias of PF against short flows reappears because they are no longer isolated from long flows. However, in SB-HPF(2,1), short flows are served frequently enough so that the PF algorithm converges even when they are served along with long flows. Their transfer delays are notably lower than what they obtain in plain PF. As for long flows, we can see in Figure 7.11 that the degradation in term of mean throughput is acceptable in comparison with PF, but more importantly, these performances are obtained for blocking rates that are comparable with those of PF. We conclude that when the size of flows is not known a priori, the SB-HPF(2,1) scenario lowers remarkably the mean sojourn time of short-lived flows without too much penalizing long-lived flows. Nevertheless, we can still remedy this slight degradation in performance for long flows through Measurement-Based Admission Control (MBAC).

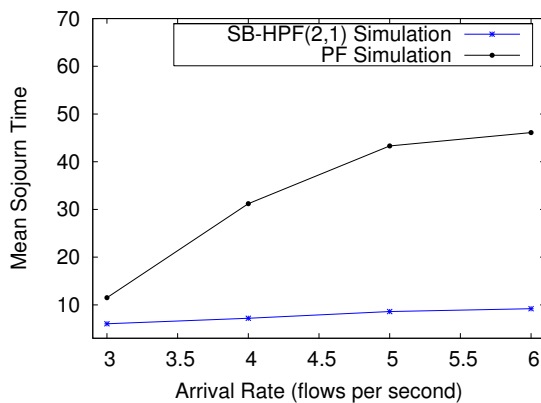


Figure 7.12: Mean Sojourn Time of short flows (with MBAC)

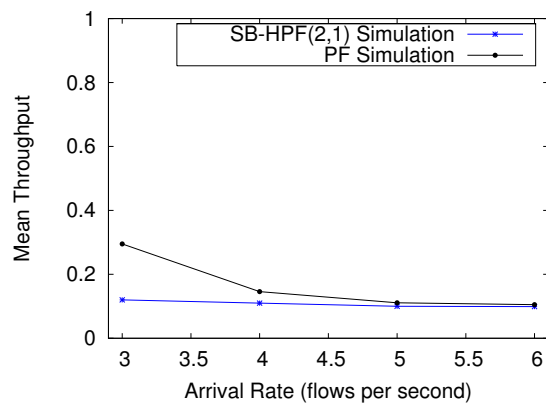


Figure 7.13: Mean Throughput of long flows (with MBAC)

In MBAC, it is the performance of long flows that will trigger the blocking of new arrivals because of the discrimination performed against these flows. Since the number of ongoing flows is limited, the system will easily compute the throughput realized by each long flow without facing scalability issues, and whenever any of these throughputs goes below a

predefined minimal value, Th_{min} , all new arrivals are blocked. New flows are admitted back in the system if all throughputs realized by long flows go beyond another predefined value ($\delta \cdot Th_{min}$ with $\delta > 1$). For each λ , Th_{min} will be set equal to the throughput obtained for long flows by the analytical formulae for SB-HPF(2,1). The improvement obtained for long flows comes at the price of a slight increase in blocking rates. We have thus significantly favoured short flows without penalizing long flows.

7.5 The SB-APF Scheduler

We know that the PF scheduler serves the user with the highest feasible rate relative to its current average throughput (this ratio is commonly called RICQ – Relative Instantaneous Channel Quality –) and so in order to favour short flows, we propose to increase their RICQ in comparison with long flows (or equivalently reduce the RICQ of long flows) thus increasing their chance to be selected by the scheduler. In order to do that, two methods are put forward: the first one is termed SB-APF-a and the second SB-APF-b.

7.5.1 The SB-APF-a Scheduler

Aiming to increase the RICQ of short flows in comparison with long flows, we chose in this algorithm to divide the RICQ of long flows by a constant A greater than 1. Therefore, short flows will have precedence in accessing resources over long flows. The value of A must be chosen carefully in order not to deprive long flows from accessing the channel, and simulations were run for different values of A .

7.5.1.1 Analytical Study

Long flows will be indexed by L and short flows by S . We know that the exponentially smoothed throughput of a long flow i is $T_{L,i} = \frac{A \cdot g(n_L)}{n_L} \cdot C_{L,i}$ and of a short flow i is $T_{S,i} = \frac{g(n_S)}{n_S} \cdot C_{S,i}$. The number of long and short flows are respectively n_L and n_S .

The average rate of a long flow i is,

$$\chi_{L,i} = \frac{C_{L,i}}{n_L} \cdot \mathbb{E}[Z_L \cdot \mathbf{1}\{Z_L \geq \frac{A \cdot n_S \cdot g(n_L)}{g(n_S) \cdot n_L} \cdot Z_S\}], \quad (7.5.1)$$

with $Z_k = \max(x_{k,1}, \dots, x_{k,n_k})$, where $k = \{S, L\}$.

Proof. The average rate of a long flow i is:

$$\begin{aligned}
\chi_{L,i} &= \mathbb{E}[R_{L,i} \cdot \mathbf{1}\{\frac{R_{L,i}}{T_{L,i}} = \max_{k=\{S\},\{L\}} \max_{l=1,\dots,n_k} \frac{R_{k,l}}{T_{k,l}}\}] \\
&= C_{L,i} \cdot \mathbb{E}[x_{L,i} \cdot \mathbf{1}\{\frac{x_{L,i}}{A \cdot \frac{g(n_L)}{n_L}} \geq \frac{n_S}{g(n_S)} \cdot Z_S\} \cdot \mathbf{1}\{\frac{x_{L,i}}{A \cdot \frac{g(n_L)}{n_L}} = \frac{Z_L}{A \cdot \frac{g(n_L)}{n_L}}\}] \\
&= C_{L,i} \cdot \mathbb{E}[x_{L,i} \cdot \mathbf{1}\{x_{L,i} \geq \frac{A \cdot g(n_L)n_S}{g(n_S)n_L} \cdot Z_S\} \cdot \mathbf{1}\{x_{L,i} = Z_L\}] \\
&= C_{L,i} \cdot \mathbb{E}[x_{L,i} \cdot \mathbf{1}\{x_{L,i} \geq \frac{A \cdot g(n_L)n_S}{g(n_S)n_L} \cdot Z_S\} | \{x_{L,i} = Z_L\}] \cdot \mathbb{P}\{x_{L,i} = Z_L\}
\end{aligned}$$

The random variables $x_{L,i}$ being i.i.d., formula (7.5.1) follows. \square

We denote by $f_k(z)$ the density function of Z_k . The random variables x_k having an exponential distribution of unit mean, we get $f_k(z) = n_k \cdot e^{-z} \cdot (1 - e^{-z})^{n_k-1}$. Hence, we obtain from (7.5.1) the following,

$$\chi_{L,i} = \frac{C_{L,i}}{n_L} \cdot \int_0^\infty f_S(x) \int_{\frac{A \cdot g(n_L)n_S}{g(n_S)n_L} \cdot x}^\infty y \cdot f_L(y) dy dx. \quad (7.5.2)$$

Another value of interest to our algorithm is the probability of short flows to access the channel because increasing this probability comes down to reducing the mean sojourn time of short flows. The conditional probability that a short flow i has a relatively better channel than a long flow j is,

$$\mathbb{P}\left(\frac{R_{L,j}}{T_{L,j}} \leq \frac{R_{S,i}}{T_{S,i}} | R_{S,i}\right) = 1 - e^{-A \frac{g(n_L)n_S}{g(n_S)n_L} \cdot x}.$$

The resulting asymptotic time fraction assignment $P_{S,i}$ for a short flow i is given by,

$$P_{S,i} = \sum_{u=0}^{n_L} \sum_{v=0}^{n_S-1} C_k^{n_L} C_l^{n_S-1} (-1)^{u+v} (1 + v + uA \frac{g(n_L)n_S}{g(n_S)n_L})^{-1}. \quad (7.5.3)$$

Proof.

$$\begin{aligned}
P_{S,i} &= \int_0^\infty (\mathbb{P}(\frac{R_{L,j}}{T_{L,j}} \leq \frac{R_{S,i}}{T_{S,i}} | R_{S,i}))^{n_L} \cdot (\mathbb{P}(\frac{R_{S,k}}{T_{S,k}} \leq \frac{R_{S,i}}{T_{S,i}} | R_{S,i}))^{n_S-1} \cdot e^{-x} dx \\
&= \int_0^\infty (1 - e^{-A \frac{g(n_L)n_S}{g(n_S)n_L} \cdot x})^{n_L} \cdot (1 - e^{-x})^{n_S-1} \cdot e^{-x} dx \\
&= \int_0^\infty \left(\sum_{u=0}^{n_L} C_u^{n_L} (-1)^u e^{-uA \frac{g(n_L)n_S}{g(n_S)n_L} \cdot x} \right) \cdot \left(\sum_{v=0}^{n_S-1} C_v^{n_S-1} (-1)^v \cdot e^{-vx} \right) \cdot e^{-x} dx \\
&= \sum_{u=0}^{n_L} \sum_{v=0}^{n_S-1} C_u^{n_L} C_v^{n_S-1} (-1)^{u+v} (1 + v + uA \frac{g(n_L)n_S}{g(n_S)n_L})^{-1}
\end{aligned}$$

□

For $A = 1.0$, $n_L = n_S$ and $n = n_L + n_L$, we get $P_{S,i} = \frac{1}{n}$ and thus we have the original PF. However, for $A > 1.0$, $P_{S,i} > \frac{1}{n}$ while the asymptotic time fraction assignment for a long flow j , $P_{L,j}$, is smaller than $\frac{1}{n}$. We conclude that SB-APF-a increases the chance of short flows to access resources and hence reduces their transfer times.

7.5.1.2 Numerical Experiments

We present in this section our numerical experiments performed to illustrate the previous analytical results. We set $n_0 = n_1 = 20$ in SB-APF-a and $n = n_0 + n_1 = 40$ in PF. Users are served according to PF and according to our SB-APF-a that is run for different values of A , ranging from 1.1 to 2.5. We determine in the first set of experiments the probability to access the channel for short flows and compare it to $P_{S,i}$, obtained from (7.5.3). We determine in the second set of experiments the normalized average rate for long flows and compare it to $\frac{\chi_{L,i}}{C_{L,i}}$, obtained from (7.5.2).

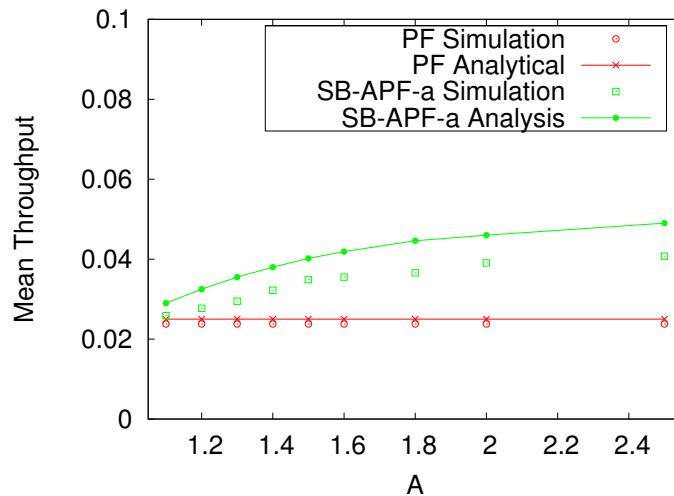


Figure 7.14: Mean Sojourn Time of short flows

The results as graphed in Figures 7.14 and 7.15 show that the analytical formulae give pretty exact estimates of the values obtained by simulation. However, the formulae in SB-APF-a consistently overestimate the access probability for short flows and underestimate the mean throughput for long flows. This is once again due to the fact that the PF algorithm performance is biased against short flows as explained in section 7.3. For that reason, it is better to separate short flows and long flows as we did in SB-HPF so that short flows profit fully from the preferential treatment they are given. As for performance,

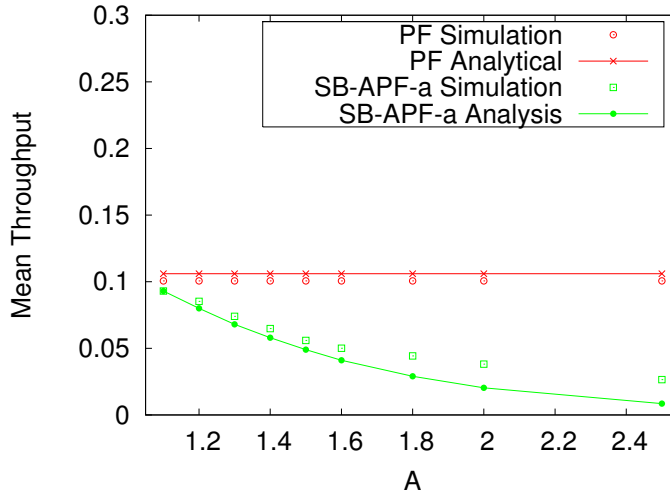


Figure 7.15: Mean Throughput of long flows

we see that we have an increase in the access probability for short flows at the expense of a decrease in throughput for long flows.

7.5.2 The SB-APF-b Scheduler

For this algorithm, aiming to increase the RICQ for short flows, we reduce the value of their exponentially smoothed throughput by omitting to update it every time we serve a short-lived flow according to formula (1.2.4) given in chapter 1 but once every Y times. We hide from the PF algorithm the fact that these flows are being served as frequently as they really are, consequently, short flows will be served promptly and receive additional time slots.

7.5.2.1 Numerical Analysis

We now give a brief proof to show that updating the average throughput T_s of user s every $\frac{1}{Y}$ times will increase its probability to be served in comparison with a user l that is treated in a regular fashion according to the PF scheduling politic. Omitting to update T_s every time user s is served leads us to replace it by $T_s - a$ with $a < T_s$, the value of a increasing with the value of Y . For a fading Rayleigh channel, the conditional probability that user s has a relatively better channel than user l is,

$$\mathbb{P}\left(\frac{R_l}{T_l} \leq \frac{R_s}{(T_s - a)} \mid R_s\right) = \mathbb{P}\left(x_l \leq \frac{T_s}{(T_s - a)} \cdot x_s \mid R_s\right) = 1 - e^{-x_s \cdot \frac{T_s}{(T_s - a)}}.$$

The resulting asymptotic time fraction assignment P_s of user s is given by the following,

$$P_s = \int_0^{\infty} (1 - e^{-x_s \cdot \frac{T_s}{(T_s - a)}}) \cdot e^{-x_s} dx_s = \frac{T_s}{(2T_s - a)}. \quad (7.5.4)$$

From (7.5.4), we deduce that the asymptotic time fraction assignment P_l of user l is equal to $P_l = 1 - P_s = \frac{(T_s - a)}{(2T_s - a)}$. Given that $T_s > a$, it is obvious that $P_s > P_l$, and the greater the value taken by Y , the greater will be the value taken by a and consequently, the more P_s is greater than P_l . We have proved then that SB-APF-b increases the chance of short flows to be served and thus reduces their transfer time. Unfortunately, a more elaborated analysis is not possible because we do not know what value will be taken by a for a given value of Y . Thus, we restricted to simulation results to evaluate the performances of SB-APF-b in comparison with PF.

7.5.2.2 Numerical Experiments

We present in this section our numerical experiments. Users are served according to the PF algorithm and according to our SB-APF-b that is run successively for three values of Y : 3,5 and 7. At most 20 short flows and 20 long flows are admitted in the system for PF and for SB-APF-b. In all experiments, we determine the normalized average sojourn time for short flows and the normalized average throughput for long flows.

The gain obtained in terms of mean sojourn time for short flows, as graphed in Figure 7.16, is rather small; and the decrease in the average throughput for long flows, as plotted in Figure 7.17, is acceptable. However, the overall performances are modest, most probably because of the bias of the PF algorithm against short flows. In fact, short-lived flows are unable, once again, to fully profit from the privileged treatment they are given unless they are separated from long flows.

7.6 The PF-LAS Scheduler

The third algorithm is a modified version of the flow size-aware scheduler LAS [RUK03, Kle76]. LAS favours short flows without prior knowledge of flow sizes. To this end, LAS gives service to the flow that has received the least service. LAS scheduling is optimal with respect to the average time in the system among all work-conserving disciplines that do not take advantage of precise knowledge of the flow length, when the service time distribution has a Decreasing Hazard Rate (DHR) (which is the case for Internet traffic).

We calculate the mean response time $\bar{T}(\frac{S}{C})$ for flows with size S and average data rate C in LAS. Let $F(\frac{S}{C})$ be the distribution function of the flow service time. Let m_s^n be the n^{th}

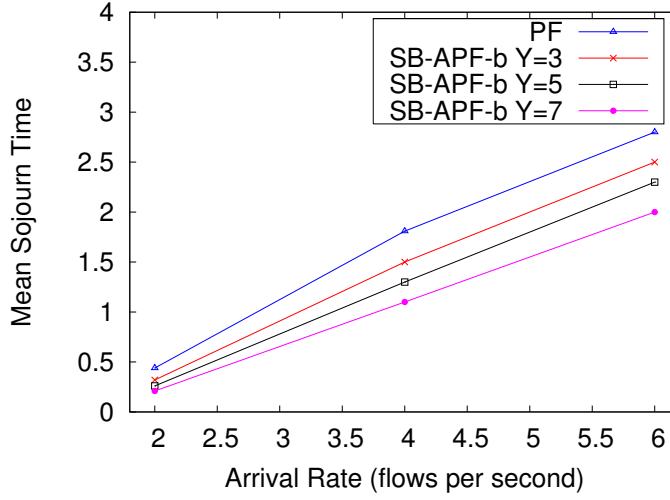


Figure 7.16: Mean Sojourn Time of short flows

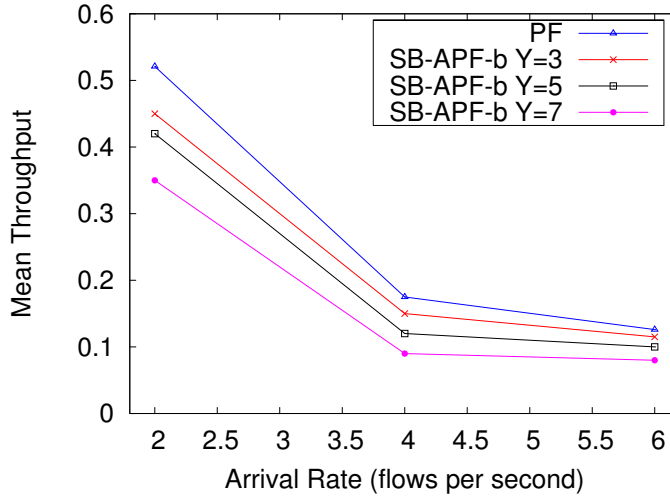


Figure 7.17: Mean Throughput of long flows

moment of the truncated distribution at S . Namely,

$$m_{S,C}^n = \int_{\frac{p}{C}}^{\frac{S}{C}} y^n dF(y) + \left(\frac{S}{C}\right)^n \cdot (1 - F(\frac{S}{C})).$$

The utilization factor for the truncated distribution is $\rho_{S,C} = \lambda \cdot m_{S,C}^1$ where λ is the intensity of arrivals at the cell (taken to follow a Poisson process).

The average response time of user i with service time S_i is,

$$\bar{T}_i(\frac{S_i}{C_i}) = (\bar{W}(S_i, C_i) + \frac{S_i}{C_i}) \cdot (1 - \rho_{S_i, C_i})^{-1}, \quad (7.6.1)$$

with $\bar{W}(S_i, C_i) = \frac{\lambda}{2} \cdot m_{S_i, C_i}^2 \cdot (1 - \rho_{S_i, C_i})^{-1}$.

7.6.1 The Wireless LAS Scheduler

We run the LAS algorithm in the previous wireless environment with Rayleigh fading. We approximate the average sojourn time of user i with service time S_i from (7.6.1) (recall that the average rate C_i is equal to $\mathbb{E}[R_i]$). Accordingly, the scheduler picks, at time slot t , user i^* such as,

$$i^* = \arg \max_i \frac{\mathbb{E}[R_i]}{S_i(t)}.$$

7.6.2 The PF-LAS Scheduler

This algorithm seeks to improve the performance of wireless LAS by taking into account the instantaneous variations of the channel condition. Therefore, the scheduler picks, at time slot t , user i^* such as,

$$i^* = \arg \max_i \left(\frac{\mathbb{E}[R_i]}{S_i(t)} \cdot \frac{R_i(t)}{T_i(t)} \right),$$

where $T_i(t)$ is the exponentially smoothed throughput.

We know that,

$$\frac{R_i(t)}{T_i(t)} = \frac{C_i \cdot x_i(t)}{C_i \cdot U_i(t)} = \frac{x_i(t)}{U_i(t)},$$

and to get the average response time for user i , we replace in (7.6.1) S_i by $S_i \cdot \frac{U_i}{x_i}$. But as we modified the PF algorithm, the exponentially smoothed throughput does not converge to what we obtained in formula (4.2.9) of chapter 4 and consequently $U_i \neq \frac{g(n)}{n}$ where n is the number of active users. We compute then a lower bound on the average response time experienced by flows. A lower bound for a flow i is obtained when the latter realizes always the highest rate among the n possible rates (n being the mean number of users present in the system) and when U_i keeps its initial value U_0 ,

$$\bar{T}_{max} \left(\frac{S_{i,max}}{C_i} \right) = (\bar{W}(S_{i,max}, C_i) + \frac{S_{i,max}}{C_i}) (1 - \rho_{S_{i,max}, C_i})^{-1},$$

with $S_{i,max} = \frac{S_i \cdot U_0}{\mathbb{E}[x_1, \dots, x_n]}$.

7.6.3 Numerical Experiments

We consider a system where users initiate file transfer requests as a Poisson process of intensity $\lambda \pi \mathfrak{R}^2$ (traffic demand is uniformly distributed in the cell). Flow sizes are independent following the Bounded Pareto distribution $BP(1kbytes, 1000kbytes, 1.16)$. Users

are served according to the Wireless LAS termed WLAS and according to our PF-LAS. In all experiments, we determine the average sojourn time for short flows and the average throughput for long flows. We take $U_0 = 0.5$.

Figures 7.19 and 7.18 display the mean sojourn time as a function of flow size for short flows (whose size goes up to 40 Kbytes) for $\lambda = 20$ and 15 respectively, indicating that the analytical formulae provide an exact estimate for WLAS and that the Lower Bound (LB) computed for the sojourn time in PF-LAS is tight enough that it can be fairly considered as an estimation of this sojourn time. As for results, the gain obtained in PF-LAS in terms of mean transfer delay is considerable. Figure 7.20 displays the mean throughput of long flows for $\lambda=20$ and 15 and shows that long flows profit greatly in PF-LAS and realize notably higher throughputs in comparison with WLAS. This was expected as, in a wireless environment, an opportunistic scheduler always outperforms a blind scheduler that does not account for channel state.

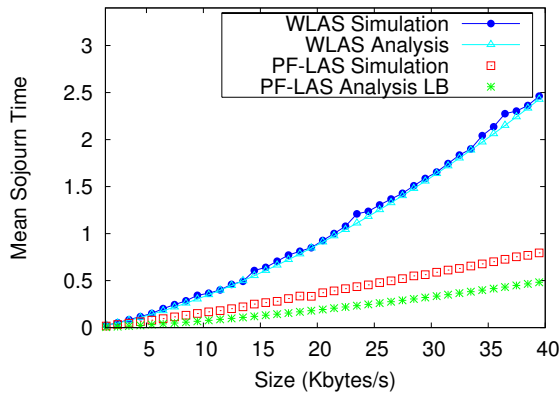


Figure 7.18: Mean Sojourn Time for $\lambda = 20.0$

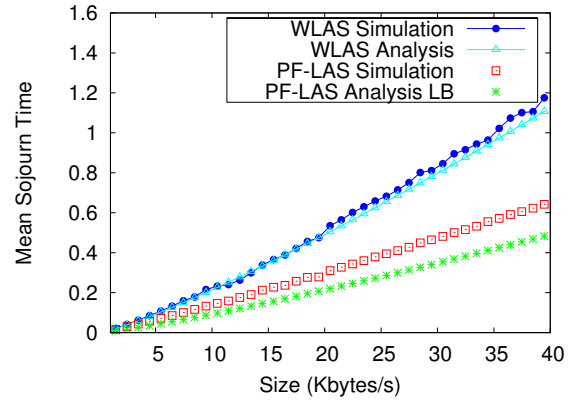
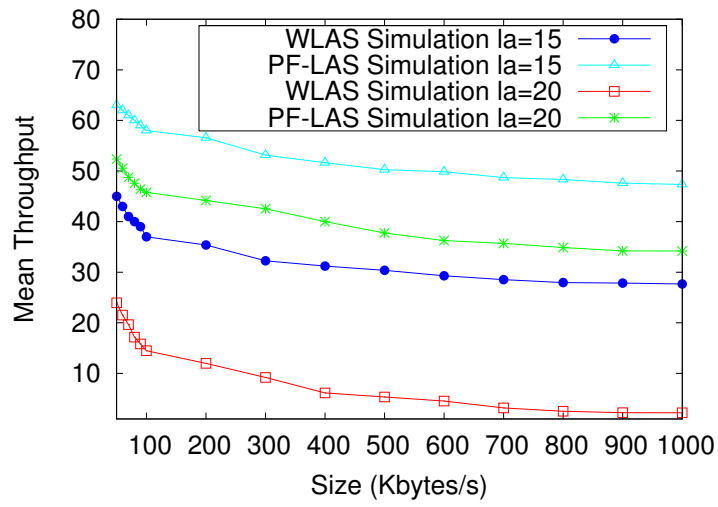


Figure 7.19: Mean Sojourn Time for $\lambda = 15.0$

7.7 Concluding Remarks

This chapter has put forward three opportunistic scheduling approaches where flow size information is taken into account by the scheduling policy. The proposed opportunistic size-aware schedulers reduce the latency for short flows without significantly disturbing the performances of long flows. While the SB-APF algorithm has given relatively modest performances, the MBAC version of SB-HPF, has remarkably improved latency of short flows in comparison with PF while preserving the performances of long flows. Further, the third algorithm termed PF-LAS, which is a modified version of the LAS scheduling, did not only significantly reduce the response time of short flows but also increased the throughput of long flows as compared to LAS which is known to be optimal with respect to the average time in the system among all work-conserving disciplines that do not take

Figure 7.20: Mean Throughput for $\lambda = 15.0$ and $\lambda = 20.0$

advantage of the precise knowledge of flow size.

Chapter 8

The impact of TCP on Flow Size-Aware Proportional Fair Scheduling

In this chapter, we evaluate the performance of the three enhanced size-aware opportunistic schedulers, proposed in the preceding chapter, in a realistic environment accounting for both fast and slow fading, users' mobility, but more importantly, the impact of the TCP/IP protocol. In fact, in addition to the bias of the PF algorithm against short-lived flows, the lack of coordination between PF (and opportunistic scheduling in general) and the congestion control mechanism of TCP induce very poor performance especially for short flows. We show through simulations that our proposed schedulers significantly reduce the transfer time of short flows without a significant degradation of the QoS provided to long flows (which are much less sensitive to response time).

8.1 Introduction

Despite the notable benefit resulting from opportunistic scheduling in HDR/HSDPA based mobile networks ([BBG⁺00, LGNJ01]), the conservative congestion control mechanism of TCP and the lack of coordination between the latter and opportunistic scheduling, have an adverse impact on short flows performance [KLZ04]. In the cited paper, the authors propose an enhancement to PF to deal with this issue when transmitting long TCP flows. Nevertheless, the proposed approach does not help in enhancing the QoS provided to short flows which are the most adversely impacted by the mentioned lack of coordination while they require the shortest response time. This is critical since short flows represent the large majority of elastic traffic as it has been shown by various Internet traffic analyses [CB97]. Current TCP congestion control mechanisms focus on network feedback which is

too conservative for short flows [AA02]. It usually results in underutilization of available network bandwidth due to the following slow start mechanisms:

- In TCP, a packet loss is detected by either the expiration of a retransmission timer or the arrival of a sequence of duplicate acknowledgements. Usually, retransmission after a timeout severely degrades the transmission rate. For short flows, since most of the time the congestion window has a relatively small value, the duplicate ACK mechanism is not triggered and thus packet loss always requires a timeout to be detected.
- TCP relies on its own packet samples to estimate an appropriate retransmission timeout (RTO) value. For the first data packets, since no sampling data is available, TCP has to use a conservatively estimated initial timeout (ITO) value as RTO. Losing these packets can have a disastrous effect on short flows performance owing to the large timeout period.
- In wireless networks, the mobility at the end hosts, the variations in the quality of the wireless channel and the usage of opportunistic schedulers can cause packet losses and delays for reasons other than network congestion. TCP reacts to such conditions by resetting its retransmission timer and initiating congestion control mechanisms. Thus, for short flows, TCP restarts unnecessarily its slow start phase resulting in even more reduced throughput and prolonged sojourn time.

Furthermore, the PF algorithm is biased against short-lived flows because it can not converge when the flow lasts a few time slots resulting in suboptimal performances especially at high loads as shown in chapter 7. In the chapter in question, in order to improve short flows performance, we proposed three flow size-aware opportunistic schedulers where file size information is integrated in the PF algorithm to reduce the sojourn time experienced by short flows. We evaluated the performances of the proposed schedulers with simplistic hypotheses where users are immobile and only endure Rayleigh fading. More importantly, our previous analysis did not account for the impact of TCP on the proposed schedulers. In this chapter, we assess the performances of our schedulers in a more realistic environment taking into consideration fast and slow fading as well as mobility of active users. Simulations were run in ns-2 to comprise the impact of TCP. We show that the proposed scheduling policies considerably reduce the transfer time of short-lived flows without causing a significant degradation in the QoS provided to long flows.

The rest of the chapter is organized as follows. In section 8.2, we present the radio propagation model and our traffic hypotheses. In section 8.3, we show how long-lived flows outperform short-lived flows in terms of mean throughput when they are served by

the PF scheduler. In sections 8.4 to 8.6, we present simulation results carried out to assess performances of our scheduling mechanisms. We conclude in section 8.7.

8.2 Radio Propagation and Traffic Models

In this section, we present the model of the radio resource and the way this resource is shared among users. We then describe our adopted hypotheses relative to the offered traffic.

8.2.1 System Model

We consider a UMTS cell with a BS at its centre and simple omni-directional antennas are used by the BS and mobiles. We only consider the performances of the downlink channel. A TDMA-like strategy where the BS transmits at full power to only one user in each time slot is adopted. Opportunistic scheduling is used with a combination of link adaptation and HARQ to provide high spectral efficiency:

- Link adaptation refers to the adaptation of a user's transmission data rate to its radio conditions based on DRC signals sent back by the user to the BS.
- With HARQ, erroneous transmissions of the same information block is combined with subsequent retransmission before decoding.

8.2.1.1 Propagation Model

Let P be the transmission power of the BS, GT the BS antenna gain, L_k the free space path loss and x_k the fading for user k . The power received in dB by user k situated at distance r_k from the BS is then given by,

$$P_k(r_k, t) = P + GT + L_k + x_k. \quad (8.2.1)$$

The adopted model for the free space path loss is,

$$L_k = L_{init}(d_0) + \beta \cdot 10 \log_{10}\left(\frac{r_k}{d_0}\right), \quad (8.2.2)$$

where β is the path loss exponent (taking values between 2 and 5) and L_{init} (in dB) is the path loss at distance d_0 from the BS.

The fading $x_k = X_{\sigma,k} + 10 \log_{10} F_k$ is the sum of slow fading $X_{\sigma,k}$ (in dB) and fast fading F_k . The shadow (slow) fading is caused by obstacles in the propagation path between the BS and the user and is modelled as a zero-mean stationary Gaussian process X_σ with

Parameter	Value
Cell radius	1000m
Propagation environment	Single Rayleigh Channel
Wavelength of the signal	0.15m
Distance r_k from BS	300m
User velocity v_k	3km/h
Standard deviation in shadow fading σ_0	8dB

Table 8.1: Simulation parameters

standard deviation σ_0 . Fast fading is caused by multi-path propagation and simulated Rayleigh fading is generated by the Jakes model [Jak93].

For user k , the signal-to-noise ratio and energy-per-bit to noise density ratio [Vit95] are respectively equal to,

$$SNR_k = \frac{P_k}{\eta + I}, \frac{E_b}{N_0} = \frac{W}{R_k} \cdot SNR_k, \quad (8.2.3)$$

where W is the cell bandwidth, P_k the power received by user k , η the background noise and I the interference due to other BSs.

For a given target error probability, $\frac{E_b}{N_0}$ must be greater than a given threshold δ (taken as a constant as it is done in the majority of references), the feasible data rate of user k is then,

$$R_k(r_k, t) = \frac{W}{\delta} \cdot SNR_k(r_k, t). \quad (8.2.4)$$

A given user k moves in a circle of radius r_k and with velocity v_k . All users will be situated at the same distance from the BS to only assess the impact of flow size on the scheduler performances. The mean rate perceived by flows at distance $r_k = 300m$ is $\mathbb{E}[R_k(r_k = 300m), t] = 200Kbytes/s$. All active mobile users initiate FTP downloads over TCP connections where the TCP packet is set to $1Kbyte$. The system operates in a time-slotted fashion with a slot duration equal to 2ms. At most 30 users are admitted in the system. New transfers generated when the maximum number of users is already in progress are blocked and lost. The simulation parameters and their values are summarized in Table 8.1.

8.2.2 Traffic Characteristics

Data flows arrive as a Poisson process of intensity λ . Short flows size σ_S is uniformly distributed between a minimum flow size a and a maximum flow size b . As for long flows, their size σ_L follows the Pareto distribution of probability density function,

$$f(x) = \frac{\alpha \cdot p^\alpha}{x^{\alpha+1}}, \quad p \leq x, 0 \leq \alpha \leq 2,$$

where p is the minimum long flow size and α is the exponent of the power law.

Since TCP flow sizes are heavy tailed, even though short flows represent a significant number of TCP flows, they will account for a small proportion of the total load. Therefore, we will consider the following scenario that mimics the characteristics of Internet data traffic [CB97]:

- 80% of flows are short flows uniformly distributed between $a = 1Kbyte$ and $b = 4Kbytes$, and of mean $\mathbb{E}[\sigma_S] = 2.5Kbytes$.
- While 20% of flows are long flows whose size follows the Pareto distribution with $\alpha = 1.16$ and of mean $\mathbb{E}[\sigma_L] = 45.5Kbytes$ (i.e. $p \approx 6Kbytes$).

Thus the load of short flows is approximately 18% of total load and the load of long flows is approximately 82% of total load.

8.3 Simulation results of the PF scheduler

To highlight the bias of PF against short-lived flows, we present simulation results with parameters presented in the previous section, and highlight the discrepancy between the mean throughput (in $Kbytes/s$) of long flows and of short flows. For that, we consider a system where users initiate file transfer requests as a Poisson process of intensity λ . Flow sizes are independent and follow the mixed heavy-tailed distribution presented in section 8.2.2. We determine the throughput per flow which is the ratio of flow size to flow sojourn time and plot the mean throughput for short and long flows as a function of load in Figure 8.1.

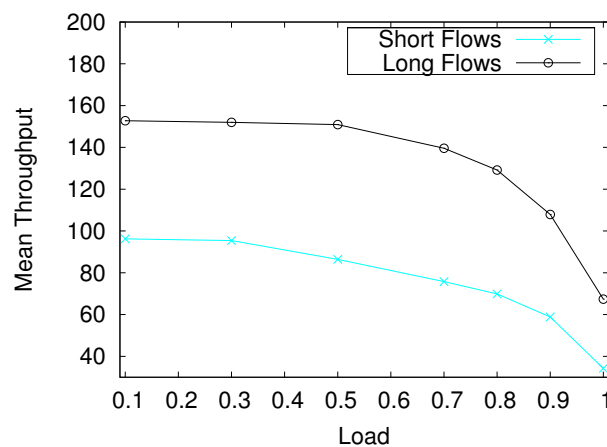


Figure 8.1: Mean Throughput of long and short flows in PF

We can see in Figure 8.1 that long flows realize notably higher throughputs in comparison with short flows. Indeed, the divergence between the mean throughput of short flows and long flows varies between approximately 30% at low load to 50% at high load. To overcome this inherent drawback of PF, we proposed in the previous chapter three modified versions of PF where short flows are given preferential treatment. We will evaluate in the following sections the performances of our devised scheduling policies in the real environment described in section 8.2.

8.4 Simulation results of the SB-HPF scheduler

We present in this section three numerical experiments performed with the same parameters as those presented in section 8.2, in which users are served respectively according to:

- The PF algorithm.
- The SB-HPF(2,1) algorithm, where by definition, short flows receive two times more slots than long flows.
- The SB-HPF(4,1) algorithm, where by definition, short flows receive four times more slots than long flows.

In the three cases, the number of admitted long and short flows is limited by admission control. The blocking probabilities are evaluated. The performance goal for short flows and long flows is different: for the former the goal is to minimize the average transfer latency while for the latter, it is to maximize throughput. For that reason, in all experiments, we determine the average sojourn time (in seconds) for short flows and the average throughput for long flows (in *Kbytes/s*). Figure 8.2 illustrates the mean sojourn time for short flows as a function of load for PF, SB-HPF(2,1) and SB-HPF(4,1), while Figure 8.3 illustrates the mean throughput for long flows as a function of load for the same scenarios.

We can see from Figure 8.2 that short flows profit largely, at high load, from having a minimum guaranteed allocated bandwidth. However, at low load, the improvement in terms of mean sojourn time is modest because of two reasons. First, as load decreases, the number of short flows present simultaneously in the system is gradually reduced and consequently short-lived flows profit less from multi-user diversity. Second, the bias of PF against short flows is less severe at low load. Therefore, at low load, there are more flows in the system served according to the original PF than according to SB-HPF (where short flows and long flows are divided in two classes) and thus short flows profit from the benefits of opportunistic scheduling without its mentioned adverse effects in a crowded

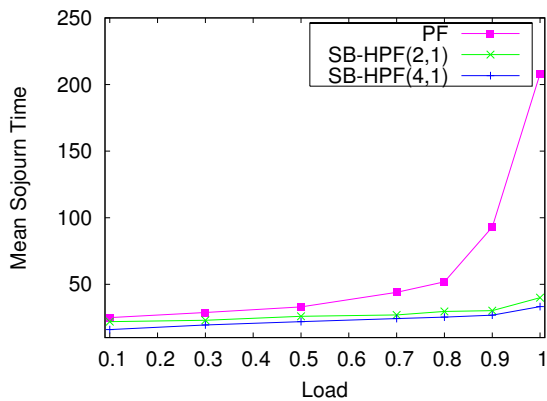


Figure 8.2: Mean Sojourn Time of short flows

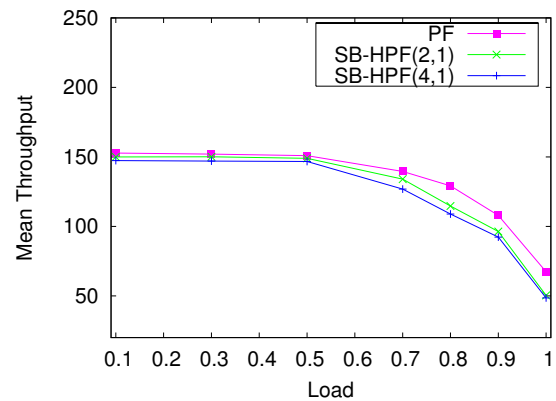


Figure 8.3: Mean Throughput of long flows

cell. The gain achieved for short flows at high load is obtained at the cost of only a slight degradation in terms of mean throughput for long flows as we can see from Figure 8.3, while blocking probabilities are equivalent in both algorithms.

As to comparing the SB-HPF(2,1) and the SB-HPF(4,1) scenarios, we can see from Figures 8.2 and 8.3 that it suffices to serve short flows twice more frequently than long flows. In fact, giving more resources to short flows barely altered the obtained performances and resulted in only a slight decrease in terms of mean sojourn time for short-lived flows at the expense of a slight decrease in terms of mean throughput for long-lived flows.

In what preceded, we supposed that we know a priori whether a flow is long or short. Unfortunately, most of the time, this information is not available at the scheduler. Since the majority of data flows are short flows, we will study an alternative version of the SB-HPF scheduler where every new flow is considered as a short flow and therefore included in the corresponding class. If a flow turns out to be a long flow, meaning that if the number of packets received for this flow goes beyond a certain threshold (*4Kbytes* in our numerical analysis), then the system considers the present flow as a long one and moves it to the corresponding class. We term this new approach SB-HPF-u for unknown size. We present hereafter the results obtained for SB-HPF-u(2,1) and for SB-HPF-u(4,1). Figures 8.4 and 8.6 illustrate the mean sojourn time for short flows as a function of load for PF, SB-HPF(2,1), SB-HPF-u(2,1) and for PF, SB-HPF(4,1), SB-HPF-u(4,1) respectively. Figures 8.5 and 8.7 illustrate the mean throughput for long flows as a function of load for PF, SB-HPF(2,1), SB-HPF-u(2,1) and for PF, SB-HPF(4,1), SB-HPF-u(4,1) respectively.

We can see from Figure 8.4 that short flows suffer from a little increase in transfer delay in SB-HPF-u(2,1) as compared to SB-HPF(2,1). However, the gain in terms of mean sojourn time in SB-HPF-u(2,1) in comparison with PF is still noteworthy, especially at high load.

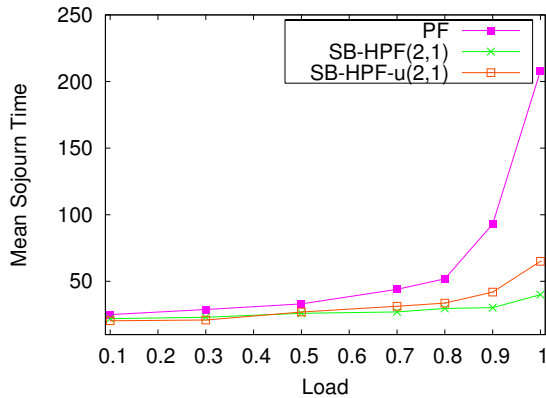


Figure 8.4: Mean Sojourn Time of short flows for SB-HPF(2,1)

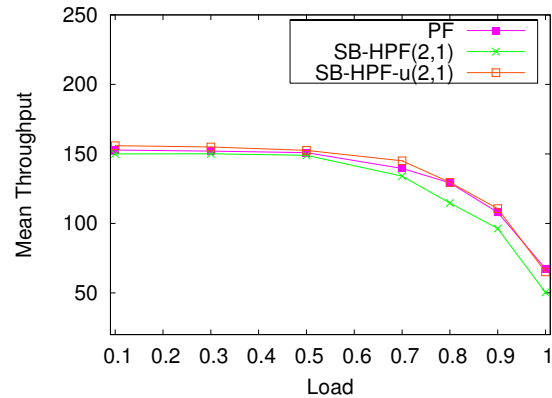


Figure 8.5: Mean Throughput of long flows for SB-HPF(2,1)

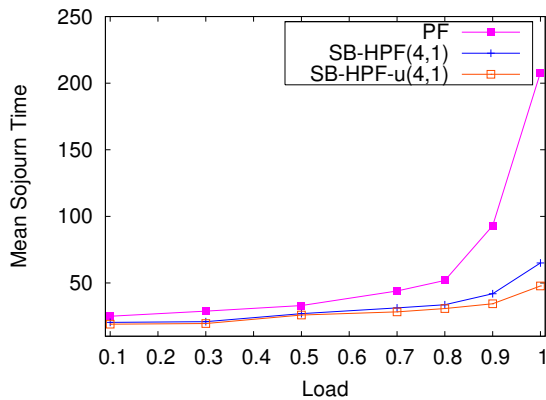


Figure 8.6: Mean Sojourn Time of short flows for SB-HPF(4,1)

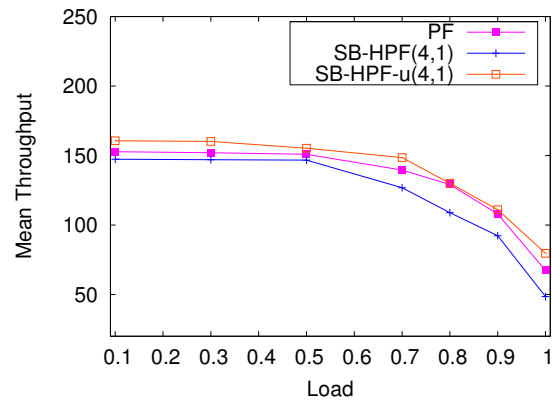


Figure 8.7: Mean Throughput of long flows for SB-HPF(4,1)

As for long flows in SB-HPF-u(2,1), we can see in Figure 8.5 that they profit from the "privileged" treatment they receive when they enter the system since they obtain mean throughputs equivalent to those perceived in PF.

The performances are even better for the SB-HPF-u(4,1) scenario. Indeed, We can see from Figure 8.6 that short flows perceive only a minor increase in terms of mean transfer delay in comparison with SB-HPF(1,4). As for long flows, we can see in Figure 8.7 that they realize in SB-HPF-u(4,1) and PF equivalent performances. We conclude that the SB-HPF-u(4,1) scenario lowers remarkably the mean sojourn time of short-lived flows without penalizing long-lived flows.

8.5 Simulation results of the SB-APF scheduler

We present in this section numerical experiments performed with the same parameters as those presented in section 8.2 to assess the performances of the SB-APF scheduler. Users

are served according to the PF algorithm and according to our SB-APF algorithm. We determine the average sojourn time for short flows depicted in Figure 8.8 as a function of load and the average throughput for long flows illustrated in Figure 8.9 as a function of load. We take $A = 2$.

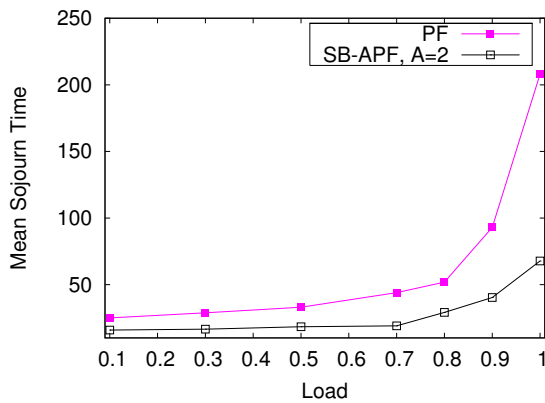


Figure 8.8: Mean Sojourn Time of short flows

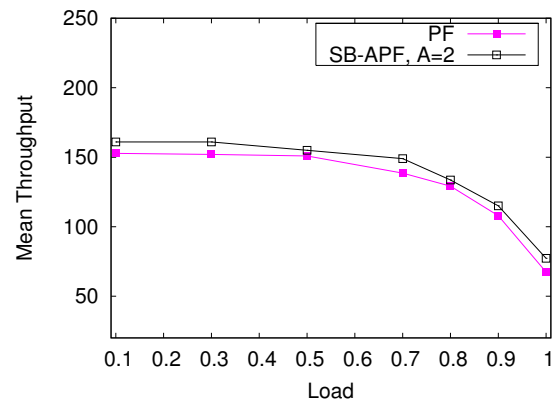


Figure 8.9: Mean Throughput of long flows

We can see from Figure 8.8 that short flows profit largely from the SB-APF mechanism especially at high to moderate load. As for long flows, we can see from Figure 8.9 that they realize in SB-APF slightly better performances in terms of mean throughput as compared to PF. Nevertheless, these good performances are obtained at the cost of relatively high blocking probabilities in comparison with PF. Indeed, SB-APF has a blocking probability 30% higher than PF at low load and 50% higher at high load. Lower values of A (equal to 2 in our numerical experiments), reduce the blocking rates but also the gain obtained for short-lived flows.

8.6 Simulation results of the PF-LAS scheduler

We present in this section the numerical experiments we performed with the same parameters as those presented in section 8.2 to assess the performances of the PF-LAS scheduler. Users are served according to the PF algorithm and according to the proposed PF-LAS. We determine the average sojourn time for short flows depicted in Figure 8.10 as a function of load and the average throughput for long flows illustrated in Figure 8.11 as a function of load.

We can see from Figure 8.10 that short flows realize notably lower sojourn times in PF-LAS in comparison with PF, especially at moderate to high load. As for long flows, we can see from Figure 8.11 that they realize higher mean throughputs in PF-LAS as compared to

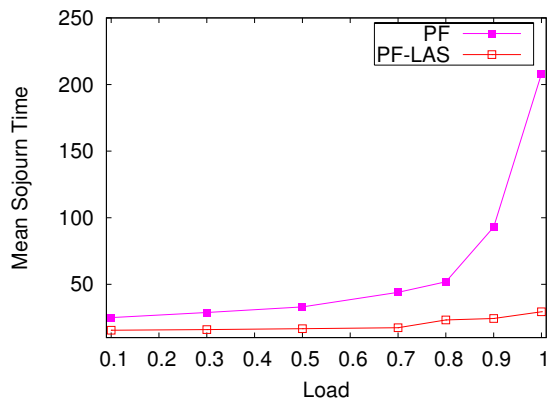


Figure 8.10: Mean Sojourn Time of short flows

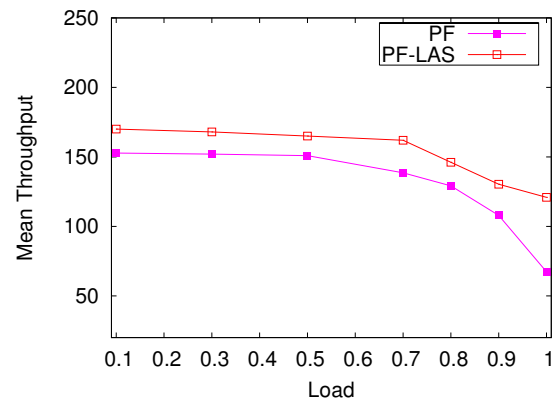


Figure 8.11: Mean Throughput of long flows

PF. However, here again, these performances are obtained at the cost of higher blocking probabilities in comparison with PF. In PF-LAS, the blocking probability increases by 30% to 60% at low to high load in comparison with PF.

8.7 Conclusion

Despite all the benefits resulting from opportunistic scheduling in the context of radio access, it has been shown that the lack of coordination between the latter and the congestion control mechanism of TCP induce poor performances. In chapter 7, we proposed three new schedulers designed to deal with the QoS requirements of long and short TCP controlled flows. The performance of the proposed schedulers are evaluated in the present chapter by simulation in a realistic radio environment. We conclude that the devised size-aware opportunistic schedulers reduce the latency for short flows while exploiting user diversity, thus allowing the wireless channel to be utilised efficiently, without significantly disturbing the performances of long flows. The simulation results provided for the proposed mechanisms show the large benefits that can be obtained by implementing them.

Chapter 9

General Conclusion

This chapter presents the general conclusion of the different studies described in this manuscript. We summarize the main contributions of our work and give the future research directions that stem from it.

9.1 Summary of Contribution

Over the few past decades, a tremendous growth of both the wireless technology and the Internet have been witnessed. Therefore, it was not surprising to see the convergence of the two branches. The resulting mobile Internet requires efficient radio resource management in order to meet the growing demand for high-data-rate wireless communications. However, designing efficient radio resource management schemes is a daunting task as the wireless channel is not only scarce but unreliable, subject to frequent, bursty and location-dependent errors. Channel-aware scheduling in general and Opportunistic scheduling in particular are key tools to achieve satisfactory user performance coupled with efficient utilization of the wireless channel. To improve spectrum efficiency, channel-aware schedulers exploit the channel state information and allocate resources accordingly. In this thesis, we investigated the two main approaches adopted to devise efficient channel-aware policies for elastic traffic: **Wireless Fair Queueing** and **Opportunistic Scheduling**. Wireless fair queueing makes use of channel state information to avoid allocating resources to users that cannot emit as they are in rather bad channel state, evading resource wastage. Furthermore, they strive to guarantee fairness in respect to the GPS model. Opportunistic scheduling goes a step further and makes use of channel state information to give priority to users experiencing relatively better channel quality and thus increases system efficiency. In our thesis, we proposed an opportunistic wireless fair queueing scheduler for 802.16 systems that remarkably improves overall performances thanks to multi-user diversity while granting users fairness according to the GPS model. We proposed also in the scope of our

thesis various enhanced opportunistic schedulers based on the well-known Proportional Fair scheduler that overcame its drawbacks.

9.1.1 Wireless Fair Queueing

Wireless fair queueing schedulers proposed so far mainly emulate wireline fair queueing. They make the assumption that the channel capacity is constant and propose a compensation mechanism more or less efficient to face the problem of disrupted communications due to erroneous sessions. In this thesis, instead of falsely assuming that the channel is constant and to hide its variations from contending flows, we make use of these variations to schedule HOL packets opportunistically. In fact, we propose, in [KK06c], a modified WFQ algorithm that integrates channel fluctuations instead of using a wireline fair queueing algorithm based on a flawed on-off channel model.

9.1.2 Opportunistic Scheduling: The Proportional Fair Scheduler

Many opportunistic schedulers were proposed for HDR/HSDPA systems with a full array of fairness criteria and multi-rate channel models. Notable among them is the Proportional Fair scheduler because it strikes a good balance between two conflicting objectives: temporal fairness and efficiency. Yet, PF is unable to control the allocation of resources by letting the system choose between temporal fairness and efficiency. Furthermore, PF lacks the ability to provide utilitarian fairness which is a real issue. Indeed, in wireline networks, when a certain amount of resource is assigned to a user, it is equivalent to granting the user a certain amount of throughput/performance value. However, the situation is different in wireless networks where the amount of resource and the performance value are not directly related. For instance, providing temporal fairness among users in a cell does not result in providing them with comparable throughputs as users close to the BS will typically obtain higher throughputs than users far from the BS. Therefore, guaranteeing temporal fairness in a wireless environment is far from guaranteeing utilitarian fairness. More importantly, PF results in an impaired temporal fairness and in suboptimal performances in realistic environments. In our work, we proposed three sets of schedulers to overcome the three main drawbacks of PF. The downsides of PF arise when we omit to adopt the aforementioned three false assumptions necessary so that PF behaves like a multi-class Processor Sharing system.

9.1.2.1 Weighted Proportional Fair Scheduler

Through the WPF scheduler proposed in [KKA06, Kha06], we were able to obtain, in a realistic environment impacted by heterogeneous fading, the performances that PF provides only in an idealistic environment with homogeneous fading: we were thus capable of

providing perfect temporal fairness to users. Furthermore, our WPF, contrary to PF, enjoys flexibility in sharing resources. Indeed, we were able to let the system choose between realizing utilitarian fairness, by favouring users far from the BS as they suffer from intrinsically small feasible rates, and achieving efficiency by favouring users close to the BS and thus realizing increased overall throughput. In addition, we controlled system resources by combining PF scheduling and a power-allocation mechanism for intercell interference alleviation. Here again, by reducing interference suffered by close users, we increased overall throughput (efficiency); and by reducing interference suffered by far users, we increased their individual realized throughput (utilitarian fairness). Moreover, our WPF permitted us to schedule different categories of users differently, using the most adapted scheduling scheme to each category and hence increasing global throughput.

9.1.2.2 Hierarchical Proportional Fair Scheduler

In HDR/HSDPA systems, scheduling one user at a time is recommended because of its optimality when the SNR scales linearly with the effective transmission rate. However, because the SNR does not scale linearly with the feasible rate for all users, absolute TDMA scheduling may not result in maximum channel utilization. Indeed, when we adopt a realistic channel model where the feasible rate is logarithmic with the SNR, this assumed linearity is only valid for users with small SNRs typically situated far from the BS. Therefore, we propose a hybrid scheduler in [KK06a], termed HPF, that alternates CDMA and TDMA scheduling. In fact, in HPF, far users are served according to PF because their feasible rate is almost proportional to their SNR and because of their moderate to bad channel conditions which require TDMA scheduling to cancel intracell interference. However, close users are served in a CDMA fashion because of the logarithmic relation between their SNR and their feasible rate and because of the good channel condition they experience. We proved that our scheduler globally increased the performance in terms of average rates.

9.1.2.3 Flow Size-Aware Proportional Fair Scheduler

Finally, we address and solve the third drawback of PF which is its lack of efficiency when serving short-lived flows. Indeed, we showed, in [KK06b], through simulations that the PF algorithm is biased against short flows as it fails to treat them fairly. This is a real issue as short flows represent the large majority of elastic traffic. Therefore, we proposed in [KK06b] three enhanced scheduling approaches that couple Size-aware scheduling and PF opportunistic scheduling. The developed schedulers significantly reduce the transfer time of short flows without really penalizing long flows. The performances of the proposed schedulers were also assessed in a realistic environment accounting for the impact of the TCP protocol.

9.2 Future Directions

The ongoing evolution towards the generalization of wireless access to multi-service networks stresses the need for optimizing the control of radio resources and in particular, for designing efficient scheduling approaches. Channel-aware scheduling is essential for providing high-rate data to users under the QoS constraints imposed by multi-service networks. In fact, channel-aware schedulers profit from the delay tolerance of elastic traffic to provide means for optimally sharing the limited and time-varying wireless resources. Our work restricted to studying opportunistic scheduling of elastic traffic and a possible research direction would be to study opportunistic scheduling for a mixture of real-time and non real-time traffic. The future framework of our investigations would be the novel and promising 3G LTE (3G Long Term Evolution) network. While in 3G, HSDPA offers theoretical downlink rates up to 14.4Mbps, the effective rate offered to users is assumed to be around 800Kbps. In 3G LTE, an IP optimized and simple network architecture promises a cell capacity up to 100Mbps. Furthermore, the advent of 3G LTE offers, for the first time, cellular VoIP (Voice over IP) with acceptable user performances. Efficient VoIP could provide mobile operators the ability to integrate voice and multimedia services. Therefore, thanks to the high rates and reduced latency it promises, 3G LTE offers the opportunity to devise high-performance opportunistic schedulers granting services with increased QoS to both elastic and streaming flows.

Hereafter some interesting issues resulting from our work that still need to be addressed: Both the WPF scheduler and HPF scheduler are based on a hierarchical allotment of resources between different categories (zones) of users and further investigation is still required to devise an optimal distribution of slots across the different categories. We also need to put focus on proposing a proper admission control scheme. Thanks to the segmentation of the cell into different categories, mainly defined by a category of users *close to the BS* and a category of users *far from the BS*, we can choose to fix differently the admission control threshold of each category: limiting the maximal number of active users for the entire cell will probably block new arrivals destined to the category of users *close to the BS* because of a concentration of users in the category of users *far from the BS*. In fact, active users are mostly located at the cell edges in steady state. This is due to the inherent elasticity of data transfers: users located far from the BS usually receive a smaller instantaneous rate than near users and therefore stay longer in the system. Fixing the maximal number of users per category frees us from this pathological and frequent situation, and enables us to set this maximal limit while taking into account the nature of each category (for instance, for the category of users *far from the BS*, besides its low rates, it is subject to intercell arrivals – handovers – which cannot be neglected while determining this threshold).

Finally, the schemes proposed in this thesis have been evaluated with rather simple radio channel and traffic models. To fully assess the performances of these scheduling policies, full evaluation with more realistic models would be needed, such as a radio model that accounts for both slow and fast fading, for bursty traffic, for mobility, etc.

Bibliography

- [AA02] K. Avrachenkov and U. Ayesta, *The effect of the initial window size and limited transmit algorithm on the transient behavior of tcp transfers*, 15th ITC Specialist Seminar on Internet Traffic Engineering and Traffic Management (2002). [8.1](#)
- [AABN03] K. Avrachenkov, U. Ayesta, P. Brown, and E. Nyberg, *Differentiation between short and long tcp flows: predictability of the response time*, INRIA Res. Report (2003). [7.1](#)
- [Alt03] E. Altman, *A stateless approach for improving tcp performance using diffserv*, Proceedings of the 18th International Teletraffic Congress (2003). [7.1](#)
- [BBG⁺00] P. Bender, P. Black, M. Grob, R. Padovani, and A. Viterbi, *Cdma/hdr: A bandwidth-efficient high-speed wireless data service for nomadic users*, IEEE Communications Magazine (2000). [\(document\)](#), [2](#), [2.1.2](#), [5.2.1.1](#), [5.2.2.0.2](#), [5.2.2.0.3](#), [5.6.1](#), [8.1](#)
- [BBR99] A. Bedekar, S. Borst, and K. Ramanan, *Downlink scheduling in cdma data networks*, Proceedings of IEEE Globecom (1999). [1.1.2](#), [1.2.3](#), [6.1](#), [6.2.2](#)
- [BG87] D. Bertsekas and R. G. Gallager, *Data networks*. [1.2.0.0.1](#), [1.2.2](#)
- [BGT93] C. Berrou, A. Glavieux, and P. Thitimajshima, *Near shannon limit errorcorrecting coding and decoding: Turbo codes*, In Proceedings of 1993 IEEE International Conference on Communications (1993). [\(document\)](#), [1.1](#)
- [BH00] A. Boukalov and S. Haggman, *System aspects of smart-antenna technology in cellular wireless communications-an overview*, IEEE Transactions on Microwave Theory and Techniques **48(6)** (2000), 919–929. [\(document\)](#), [1.1](#)
- [BKT96] P. Bhagwat, A. Krishna, and S. Tripathi, *Enhancing throughput over wireless lanss using channel state dependent packet scheduling*, in Proceedings of INFOCOM96 (1996), 1133–1140. [1.2.1](#), [1.2.1.1](#)

- [BLN99] V. Bharghavan, S. Lu, and T. Nandagopal, *Fair queueing in wireless networks: Issues and approaches.*, IEEE Personal Communications Magazine **February** (1999). [3.1](#)
- [Bon04] T. Bonald, *A score-based opportunistic scheduler for fading radio channels*, In Proceedings of European Wireless (2004). [1.2.2.2.3](#), [4.2.3.2](#)
- [Bor03] S. C. Borst, *User-level performance of channel-aware scheduling algorithms in wireless data networks*, In Proceedings of IEEE Infocom (2003). [1.2.2.3](#)
- [BP03] T. Bonald and A. Proutière, *Wireless downlink data channels: User performance and cell dimensioning*, MobiCom'03 (2003). ([document](#)), [1.2.2.3](#), [4.2.1.2](#), [5.2.2](#)
- [BW01] S. C. Borst and P. A. Whiting, *Dynamic rate control algorithm for hdr throughput optimization*, In Proceedings of IEEE Infocom (2001). [1.2.2.2.2](#)
- [CB92] I. Crohn and E. Bonek, *Modeling intersymbol-interference in a rayleigh fast fading channel with typical delay power profiles*, IEEE Transaction on Vehicular Technology **41(4)** (1992), 438–447. [6.2.2](#), [6.2.3](#)
- [CB97] M. Crovella and A. Bestavros, *Self-similarity in world wide web traffic: Evidence and possible causes*, IEEE/ACM Transactions on Networking (1997), 835–846. ([document](#)), [1.1.1.2](#), [3](#), [7.1](#), [8.1](#), [8.2.2](#)
- [CBHT02] E.F. Chaponniere, P.J. Black, J.M. Holtzman, and D.N.C. Tse, *Transmitter directed code division multiple access system using path diversity to equitably maximize throughput*, US Patent 6 (2002). [1.2.2](#), [4.1](#)
- [Coh78] J.W. Cohen, *The multiple phase service network with generalized processor sharing*, Acta Informatica **12** (1978), 245–284. [4.2](#), [4.2.2](#), [5.4](#), [5.4.1](#), [6.4](#), [6.4.1](#), [7.3.1](#)
- [DKS89] A. Demers, S. Keshav, and S. Shenker, *Analysis and simulation of a fair queueing model*, In Proceedings of ACM Sigcomm (1989). ([document](#)), [1.1.1.1](#), [1.2.1](#)
- [ENSZ98] T. S. Eugene Ng, I. Stoica, and H. Zhang, *Packet fair queueing algorithms for wireless networks with location-dependent errors*, In Proceedings of IEEE Infocom'98 (1998). [1.2.1](#), [1.2.1.3](#)
- [FJ95] S. Floyd and V. Jacobson, *Link-sharing and resource management models for packet networks*, IEEE/ACM Trans. Networking **3** (1995), 365–386. [1.2.1.1](#)
- [Fos96] G. J. Foschini, *Layered space-time architecture for wireless communication in a fading environment when using multi-element antennas*, Bell Labs Technical Journal (1996), 41–59. ([document](#)), [1.1](#)

- [FSS98] C. Fragouli, V. Sivaraman, and M. Srivastava, *Controlled multimedia wireless link sharing via enhanced class-based queuing with channel-state dependent packet scheduling*, in Proceedings of INFOCOM'98 **2** (1998), 572–580. [1.2.1.1](#)
- [Gol94] S. Golestani, *A self-clocked fair queueing scheme for broadband applications*, Proceedings of the IEEE INFOCOM '94 (1994), 636–646. ([document](#)), [1.2.1](#), [3.3](#)
- [Gos05] A. Gosh, *Broadband wireless access with wimax/802.16: current performance benchmarks and future potential*, IEEE Communications Magazine **43**(2) (2005), 129–136. [2](#), [3.1](#)
- [GVC97] P. Goyal, H. Vim, and H. Chen, *Start-time fair queuing: A scheduling algorithm for integrated services packet switching networks*, IEEE/ACM Trans. on Networking **5** (1997), no. 3, 690–704. ([document](#)), [1.2.1](#)
- [Hol00] J. Holtzman, *Cdma forward link waterfilling power control*, Proceedings of IEEE VTC Spring (2000). [1.2.2](#), [4.1](#)
- [Hol01] J. Holtzman, *Asymptotic analysis of proportional fair algorithm*, Proceedings of IEEE (2001). ([document](#)), [1.2.0.0.1](#), [1.2.2](#), [1.2.2.1](#), [4.1](#), [1](#), [5.1](#)
- [Hos02] P. Hosein, *Qos control for wcdma high speed data*, 4th International Workshop on Mobile and Wireless Communications Network (2002), 169–173. [1.2.2.1](#)
- [HR98] J. M. Holtzman and S. Ramakrishna, *A scheme for throughput maximization in a dual-class cdma system*, IEEE J. Sel. Areas Commun. **40** (1998), 830–844. [1.1.2](#), [1.2.3](#)
- [HT02] H. Holma and A. Toskala, *Wcdma for umts: Radio access for third generation mobile communications*, John Wiley & Sons, 2002. [6.4.0.2.1](#)
- [Jak93] W. C. Jakes, *Microwave mobile communications*, Piscataway, NJ: IEEE Press, 1993. [8.2.1.1](#)
- [JMA01] M. Jeong, H. Morikawa, and T. Aoyama, *A fair scheduling algorithm for wireless packet networks*, IEICE Trans. Fundamental **84** (2001), 1624–1635. [1.2.1.3](#)
- [KA05] J-M. Kelif and E. Altman, *Downlink fluid model of cdma networks*, VTC 2005 Spring (2005). [6.2.3](#), [6.2.3](#)
- [Kel97] F. P. Kelly, *Charging and rate control for elastic traffic*, European Trans. Telecommun. **8** (1997), 33–37. ([document](#)), [1.2.0.0.1](#), [1.2.2](#), [1.2.2.1](#), [1.2.2.2.1](#)
- [KH95] R. Knopp and P. Humblet, *Information capacity and power control in single-cell multi-user communications*, In Proceedings of IEEE ICC (1995). [1.2.0.0.1](#)

- [Kha06] K. Khawam, *Modified proportional fair scheduler*, PIMRC 2006 (2006). (document), 9.1.2.1
- [KK06a] K. Khawam and J-M. Kelif, *A hierarchical proportional fair scheduler*, NGI 2006 (2006). (document), 5.6, 9.1.2.2
- [KK06b] K. Khawam and D. Kofman, *Flow size-aware proportional fair scheduler*, NGI 2006 (2006). (document), 9.1.2.3
- [KK06c] K. Khawam and D. Kofman, *Opportunistic weighted fair queueing*, VTC fall 2006 (2006). (document), 9.1.1
- [KKA06] K. Khawam, D. Kofman, and E. Altman, *Weighted proportional fair scheduler*, QShine 2006 (2006). (document), 9.1.2.1
- [Kle76] L. Kleinrock, *Queueing systems, volume ii: Computer applications*, Wiley Interscience, 1976. 7.1, 7.6
- [KLZ04] T. Klein, K. Leung, and H. Zheng, *Improved tcp performance in wireless ip networks through enhanced opportunistic scheduling algorithms*, Globecom04 (2004). 8.1
- [KMT98] F. P. Kelly, A. Maulloo, and D. Tan, *Rate control for communication networks: shadow prices, proportional fairness and stability*, Journal of the Operational Research Society **49** (1998). 1.2.2
- [Kus04] H.J. Kushner, *Convergence of proportional-fair sharing algorithms under general conditions*, IEEE Transactions on Wireless Communications **3**(4) (2004). 1.2.2, 4.1, 4.2.3, 4.2.3, 4.2.3
- [LAN97] D. A. Levine, I. F. Akyildiz, and M. Naghshineh, *A resource estimation and call admission algorithms for wireless multimedia networks using the shadow cluster concept*, IEEE/ACM Transactions on Networking **5**(1) (1997), 1–13. 1.1.4
- [LB99] S. Lu and V. Bharghavan, *Fair scheduling in wireless packet networks*, IEEE/ACM Trans. Networking **7**(4) (1999), 473–489. 1.2.1, 1.2.1.2
- [LB00] J-Y. Le Boudec, *Rate adaptation, congestion control and fairness: A tutorial*. 1.2.2.1
- [LCS03] X. Liu, E. K. P. Chong, and N.B. Shroff, *A framework for opportunistic scheduling in wireless networks*, Computer Networking **41** (2003), 451–474. 1.2.2.2.1

- [LGNJ01] R. Love, A. Gosh, R. Nikides, and L. Jalloul, *High-speed downlink packet access performance*, Proceedings of IEEE VTC Spring (2001). (document), 2, 2.1.2, 8.1
- [LP99] P. Lehne and M. Petterson, *An overview of smart antenna technology for mobile communications systems*, IEEE Communications Surveys **2(4)** (1999), 2–13. (document), 1.1
- [MMD91] R. Mazumdar, L.G. Mason, and C. Dougligeris, *Fairness in network optimal flow control: Optimality of product forms*, IEEE Trans. Communications **39(5)** (1991), 775–782. 1.2.2
- [Nas50] J.F. Nash, *The bargaining problem*, Econometrics **18** (1950), 155–162. 1.2.2
- [NBK00] S. Nanda, K. Balachandran, and S. Kumar, *Adaptation techniques in wireless packet data services*, IEEE Communications Magazine (2000). (document), 1.1
- [PAAD03] B.J. Prabhu, E. Altman, and J. Abadia Dominguez, *A simulation study of tcp performance over umts*, IEEE VTC2003-fall (2003). 7.1
- [PG93] A. Parekh and G. Gallager, *A generalized processor sharing approach to flow control in integrated services networks: the multiple node case*, IEEE/ACM Trans. on Networking **1** (1993), no. 3, 344–357. (document), 1.1.1.1, 1.2.0.0.1, 1.2.1, 3.1
- [Pot95] J.G. Pottie, *System design choices in personal communications*, IEEE Personal Communications (1995), 50–67. 1.1.2
- [Rap96] T. Rappaport, *Wireless communications: Principles and practice*, Prentice Hall, 1996. 1.3
- [RUK03] I. Rai and G. Urvoy-Keller, *Analysis of las scheduling for job size distributions with high variance*, SIGMETRICS03 (2003). (document), 7.3.2, 7.6
- [Sce00] RF System Scenarios, *Technical specification group (tsg) ran wg4*, no. TR 25.942. 6.2.3
- [SH00] K. Sipila and Z. Honkasalo, *Estimation of capacity and required transmission power of wcdma downlink based on a downlink pole equation*, VTC Spring 2000 (2000). 6.4.0.2.1
- [She95] S. Shenker, *Fundamental design issues for the future internet*, IEEE JSAC **13** (1995), 1176–1188. 1.2.2.1, 5.4
- [Sys05] Orthogon Systems, *Os wp space time coding us*, White Paper (2005). 6.4.0.2.2

- [TG03] V. Tsibonis and L. Georgiadis, *Optimal downlink scheduling policies for slotted wireless time-varying channels*, IEEE Transactions on Wireless Communications (2003). [1.2.2](#), [4.1](#)
- [Tse] D. N. C. Tse, *Multi-user diversity and proportionally fair scheduling*, US Patent 6449490. [1.2.2](#), [4.1](#)
- [Ver98] S. Verdu, *Multiuser detection*, Cambridge University Press, 1998. ([document](#)), [1.1](#)
- [Vit95] A.J. Viterbi, *Cdma: Principles of spread spectrum communication*, Addison-Wesley, 1995. [4.2.1.2](#), [6.2.2](#), [8.2.1.1](#)
- [xxE] Qualcomm Inc. 1xEV: 1x EVolution, *Is-856 tia/eia standard*. [2.1.2](#)
- [Yat95] R. Yates, *A framework for uplink power control in cellular radio systems*, IEEE Journal on Selected Areas in Communications **43(7)** (1995), 1341–1347. ([document](#)), [1.1](#), [1.1.3](#)
- [Zha02] Y. Zhao, *Standardization of mobile phone positioning for 3g systems*, IEEE Communications Magazine **40(7)** (2002), 108–116. [5.1](#)